

**Environmental controls on carbon sequestration in a saline, boreal, peat-forming
wetland in the Athabasca Oil Sands Region**

by

Olena Volik

A thesis

presented to the University of Waterloo

in fulfilment of the

thesis requirements for degree of

Doctor of Philosophy

in

Geography

Waterloo, Ontario, Canada, 2018

© Olena Volik 2018

Examining Committee Membership

The following served on the Examining Committee for this thesis. The decision of the Examining Committee is by majority vote.

External Examiner

Nigel Roulet
Professor

Supervisor(s)

Richard Petrone
Professor

Internal Member

Jonathan Price
Professor

Internal-external Member

Roland Hall
Professor

Other Member

Merrin Macrae
Associate Professor

Author's Declaration

This thesis consists of materials all of which I authored or co-authored: see Statement of Contributions included in the thesis. This is a true copy of the thesis, including any required final revisions, as accepted by my examiners.

I understand that my thesis may be made electronically available to the public.

Statement of Contributions

This thesis is written in a manuscript format.

Chapter two is published as:

Volik O, Petrone RM, Hall RI, Macrae ML, Wells CM, Elmes M, Price JS (2017) Long-term precipitation-driven salinity change in a saline, peat-forming wetland in the Athabasca Oil Sands Region, Canada: a diatom-based paleolimnological study. *J Paleolim* 58:533–550. DOI: 10.1007/s10933-017-9989-4

O. Volik completed all data collection and analysis, and writing this manuscript. Dr. Petrone, Dr. Hall, Dr. Macrae and Dr. Price provided important comments and suggestions with respect to data analyses and interpretation, and editorial revisions. Section “Salinity fluctuation and precipitation change” was completed with contribution from C. Wells. Core dating was done by Dr. Wiklund at WATER Lab (Department of Biology, University of Waterloo) and water chemistry analyses were done by Vito Lam. All figures and tables were produced by O.Volik. The final editing of the manuscript was provided by the co-authors, Dr. Whitmore, Dr. Reavie and anonymous reviewers of the publication.

Chapter three is accepted as:

Volik O, Petrone RM, Hall RI, Macrae ML, Wells CM, Price JS (2018) Salinity change and organic matter accumulation rates in saline boreal ponds near Fort Murray, Alberta, Canada. *Catena* 165C: 425–433.

Data collection and analysis as well as manuscript writing was completed by O. Volik. Co-authors provided important suggestions for data interpretation and editorial revisions. O. Volik produced all figures and tables.

Chapter four is published as:

Volik O, Petrone RM, Wells CM, Price JS (2017) Impact of salinity, hydrology and vegetation on long-term carbon accumulation in a saline boreal peatland and its implication for peatland reclamation in the Athabasca Oil Sands Region. *Wetlands*. DOI: 10.1007/s13157-017-0974-5

Data collection and analysis, and manuscript writing was completed by O. Volik with final edits from the co-authors. All figures and tables were produced by O. Volik.

Chapter five is prepared for submission as:

Volik O, Petrone RM, Quanz M, Rooney R, Macrae ML, Price JS. Environmental controls on CO₂ exchange along salinity gradient in a saline boreal fen in the Athabasca Oil Sands Region.

Data collection and analysis, and manuscript writing was completed by O. Volik with final edits from the co-authors. All figures and tables were produced by O. Volik.

Abstract

Saline boreal fens represent potential models for post-mining landscape reclamation in the Athabasca Oil Sands Region (AOSR) (Canada) where wetland construction is challenged by salinization. One of the key indicators of reclamation success is the accumulation of organic carbon within constructed fens, and a better understanding of the drivers of carbon sequestration in natural saline fens can be useful for advancing fen construction in this region. As such, this thesis aims to determine the main environmental controls on carbon uptake and its long-term storage in a saline boreal fen near Fort McMurray (Alberta, Canada) by: 1) reconstructing past salinity change; 2) determining relations between reconstructed salinity, hydrological conditions, vegetation and organic matter accumulation rates (OMAR) over the last ~100 years in open-water areas (ponds) within the fen; 3) investigating the effects of salinity, vegetation and hydrology on the long-term apparent rate of carbon accumulation (LARCA) within the peatland; and 4) assessing CO₂ fluxes within the peatland and open-water areas.

Past salinity change was investigated using paleolimnological analysis of sediment cores from three ponds situated within the fen. Salinity fluctuations were reconstructed using weighted-averaging transfer functions based on diatoms and an environmental dataset from 32 saline boreal ponds. Results reveal complex “precipitation – surface water – groundwater” interactions associated with differences in the hydrologic functioning of the studied ponds, and their connectivity with shallow groundwater aquifers and adjacent wetlands. Relationships between cumulative departure from mean precipitation (CDLM) and diatom-inferred (DI) salinity suggest that precipitation may control salinity both directly and indirectly. In ponds recharged predominantly by meteoric water, precipitation may govern salinity directly by dilution of salt content in water, so that increases in precipitation result in a salinity decline. In ponds situated within a saline groundwater discharge zone, salinity may be influenced by precipitation indirectly through recharge of the saline aquifer, so increases in precipitation lead to rises in salinity. Our study suggests that complex DI-salinity response to precipitation change, coupled with notable range of DI-salinity fluctuation within natural saline fens should be considered while designing saline constructed wetlands and predicting their potential resilience under climate change.

Median OMAR ($181 \text{ g m}^{-2} \text{ yr}^{-1}$) of the site suggests that ponds situated within saline boreal fens OMAR comparable to freshwater boreal and subarctic ponds, and reconstructed salinity levels (3–21 ppt) did not severely affect organic matter accumulation. Strong significant positive (Lager Pond), strong significant negative (South Pond), and weak insignificant (Pilsner Pond) correlations between OMAR and DI-salinity were observed, suggesting that relations between organic matter accumulation and salt content are not straightforward, and salinity was not the main control on OMAR. Macrofossil data showed that OM accumulation was mainly driven by water level, type of primary producers and pond regime. OMAR was the highest during the transition from peatland to ponds due to low decomposition rates resulting from high inputs of relatively resistant plant litter, and anoxic conditions. A macrophyte-dominated pond regime was associated with higher OMAR relative to phytoplankton-dominated regime.

LARCA within the fen was studied using two peat sediment cores. Changes in LARCA in the less saline part of the fen correlate well with water table fluctuations and seem not to be affected by low salinity ($\text{EC} < 5 \text{ mScm}^{-1}$). The highest LARCA values are related to wet conditions; however, prolonged inundations coupled with high salinity ($\text{EC} > 10 \text{ mScm}^{-1}$) appear to have negative effect on LARCA. In the southern more saline part of the fen relationships between LARCA and hydrology are complicated by salinity probably through the impact on the net primary productivity. The influence of salinity on LARCA is determined by salinity level, and there is a threshold value (probably 10 mScm^{-1}) after which salinity can significantly affect “LARCA – hydrology” links. Mean LARCA of the site ($19.7 \text{ gm}^{-2} \text{ yr}^{-1}$) is lower than in western continental fens, but it is comparable to the average rate reported for western Canadian peatlands. The northern less saline part of the fen has LARCA of $29.67 \text{ gm}^{-2} \text{ yr}^{-1}$ that is close to LARCA in rich fens, but LARCA in the southern part is considerably lower ($9.79 \text{ gm}^{-2} \text{ yr}^{-1}$).

Environmental controls on net ecosystem exchange (NEE), ecosystem respiration (R), and gross primary productivity (GEP) within the fen were studied using community-scale CO_2 measurements along a salinity gradient. Strong positive correlations between NEE, GEP, leaf area index (LAI), and vegetation biomass within terrestrial areas and strong positive correlation between GEP and vegetation density within aquatic areas illustrated importance of vegetation properties for carbon uptake. CO_2 fluxes within peatland were driven primary by water table depth, and electrical conductivity as revealed by strong negative correlations between these

variables and NEE, GEP, and R. Links between CO₂ exchange and environmental factors were influenced by microtopographical differences, and additional controls (e.g., soil moisture, availability of magnesium, manganese and calcium) on NEE, GEP, and R were found within depressions. Strong negative correlation between R and water table depth (WTD), coupled with strong positive correlation between R and belowground biomass within ridges and no significant correlation between WTD and R within depressions possibly suggested predominance of root and/ or root-associated microbial respiration within depressions and prevalence of microbial respiration within ridges. Within open water areas, GEP and R were related to phosphate concentration as suggested by strong positive correlation. In contrast to terrestrial areas, EC had no relations to CO₂ fluxes, and higher GEP was found in mesosaline ponds comparatively to hyposaline ones. This study revealed importance of development of appropriate planting schemes for terrestrial and open-water areas to achieve sustainable CO₂ uptake within constructed fens.

Acknowledgements

I extend my sincere appreciation to following people; without their help this work would not have been possible:

My advisor, Prof. Richard Petrone, for his support, enthusiastic encouragement and useful critiques of this research work;

My thesis committee members, Prof. Roland Hall, Prof. Merrin Macrae, Prof. Jonathan Price for their patient guidance and support;

Prof. Nigel Roulet for being my external examiner and providing me with valuable suggestions.

Corey Wells for breaking ground on Saline Fen functioning and numerous discussions on salinity change;

Current and previous members of Hydrometeorology Lab, Wetlands Hydrology Lab, WATER Lab, Macrae's Lab, Strack's Lab, PEARL, The Cooper Lab (Meaghan Quantz, George Sutherland, James Sherwood, Vito Lam, Tristan Gingras-Hill, Melody Fraser, Greg Carron, Adam Green, Eric Kessel, Dr. Scott Ketcheson, Matthew Elmes, Sarah Scarlett, Jessica Williamson, Kate Jamieson, Dr. Felix Nwaishi, Dr. Johan Wiklund, Casey Remmer, Eva Mehler, Prof. Maria Strack, Dr. Martin Brummell, Kimberley Murray, Dr. Kathleen Laird, Andrea Borkenhagen, Andrew Pantel) for help with field work and lab analyses and discussions of the results.

My special thanks go to all the faculty and staff of the Department of Geography and Environmental Management at University of Waterloo for their assistance and support during this project.

Finally, I wish to thank my family for their support and encouragement throughout my study.

Table of contents

Examining Committee Membership	ii
Author’s Declaration	iii
Statement of Contributions	iv
Abstract	vi
Acknowledgements	ix
Table of Contents	x
List of Figures	xiv
List of Tables	xvii
List of Abbreviations	xix
1. Introduction	1
1.1. Background and rationale of research	1
1.2. Objectives and thesis structure	3
2. Long-term precipitation-driven salinity change in a saline, peat-forming wetland in the Athabasca Oil Sands Region, Canada: a diatom-based paleolimnological study	5
2.1. Introduction	5
2.1.1. <i>Study area</i>	7
2.2. Materials and methods	8
2.2.1. <i>Field work</i>	8
2.2.2. <i>Laboratory analyses of sediments</i>	11
2.2.3. <i>Diatom-based transfer function development</i>	11
2.2.4. <i>Estimation of cumulative departure from long-term mean precipitation</i>	12
2.3. Results	13
2.3.1. <i>Environmental gradients and distribution of modern diatom assemblages</i>	13
2.3.2. <i>Development of diatom-based transfer function</i>	15

2.3.3. <i>Sediment core lithology and chronology</i>	16
2.3.4. <i>Fossil diatom assemblages</i>	18
2.3.5. <i>Past salinity changes</i>	20
2.3.6. <i>Precipitation variability in 1922–2015 in Fort McMurray area</i>	21
2.4. Discussion	21
2.4.1. <i>Salinity fluctuation and precipitation change</i>	21
2.4.2. <i>Limitations of the study and future research</i>	24
2.4.3. <i>Implications for wetland reclamation in the Athabasca Oil Sands Region</i>	25
2.5. Acknowledgements	27
3. Organic matter accumulation and salinity change in open water areas within a saline boreal fen in the Athabasca Oil Sands Region, Canada	28
3.1. Introduction	28
3.2. Materials and methods	29
3.2.1. <i>Site description</i>	29
3.2.2. <i>Sediment analyses</i>	31
3.2.3. <i>Statistical analyses</i>	33
3.3. Results	33
3.3.1. <i>Chronology, sediment core lithology, OMAR change, and macrofossil assemblages</i>	33
3.3.2. <i>Diatom assemblages and salinity reconstruction</i>	38
3.3.3. <i>Diatom-inferred salinity and OMAR relations</i>	39
3.4. Discussion	41
3.4.1. <i>Salinity change and OM accumulation</i>	41
3.4.2. <i>Implications for fen construction in the Athabasca Oil Sands Region</i>	43
3.5. Conclusion	45
3.6. Acknowledgements	46
4. Impact of salinity, hydrology and vegetation on long-term carbon accumulation in a saline boreal peatland and its implication for peatland reclamation in Athabasca oil sands region	47
4.1. Introduction	47
4.2. Methods	49

4.2.1. <i>Study site</i>	49
4.2.2. <i>Collection of peat cores</i>	51
4.2.3. <i>Laboratory analyses</i>	52
4.2.4. <i>Environmental and plant community data</i>	53
4.3. Results	54
4.3.1. <i>Chronology, macrofossils and long-term apparent rate of carbon accumulation</i>	54
4.3.2. <i>Recent environmental gradients and vegetation</i>	57
4.4. Discussion	60
4.4.1. <i>Local-scale differences in LARCA within a saline fen</i>	60
4.4.2. <i>Carbon accumulation in a saline fen versus freshwater western continental fens</i>	61
4.4.3. <i>Implications for wetland reclamation in the Alberta Oil Sands Region</i>	62
4.6. Acknowledgements	63
5. Environmental controls on CO₂ exchange along a salinity gradient in a saline boreal fen in the Athabasca Oil Sands Region	65
5.1. Introduction	65
5.2. Materials and methods	67
5.2.1. Study site	67
5.2.2. <i>Community-scale CO₂ fluxes</i>	69
5.2.3. <i>Environmental variables</i>	73
5.2.3. <i>Vegetation sampling</i>	73
5.2.4. <i>Statistical analyses</i>	74
5.3. Results	74
5.3.1. <i>Spatial variability in CO₂ fluxes</i>	74
5.3.2. <i>Controls on CO₂ fluxes within peatland</i>	75
5.3.3. <i>Controls on CO₂ fluxes within open-water areas</i>	78
5.4. Discussion	81
5.4.1. <i>CO₂ fluxes in peatland areas</i>	83
5.4.2. <i>CO₂ flux within open-water areas (ponds)</i>	85
5.4.3. <i>Implications for fen construction in AOSR</i>	86

5.5. Conclusion	88
5.6. Acknowledgements	89
6. Summary	90
7. General conclusions and recommendations	93
References	97
Appendix A. Environmental dataset and results of statistical analyses used for diatom- based transfer function development	114
Appendix B. Description and chronology of cores North-1 and South-1 and environmental dataset from 40 vegetation plots along salinity gradient at Saline Fen	119
Appendix C. Spearman's rank-order correlation coefficients between net ecosystem exchange (NEE), respiration (R), gross ecosystem productivity (GEP) and environmental variables	124

List of Figures

Figure 2.1. (a) Regional map showing the location of the study area within Alberta, (b) map showing locations of Saline, Eastern Saline and Southern Saline sites near Fort McMurray, Alberta, (c) map of the study sites including locations of 32 ponds sampled in August, 2015 and locations of sediment cores (Lager-1, Pilsner-1, and South-1)	10
Figure 2.2. Canonical correspondence analysis (CCA) ordination biplot based on the mean environmental variables of depth, salinity, electrical conductivity, DO, pH, and concentrations of Cl^- , SO_4^{2-} , Ca^{2+} , Mg^{2+} , K^+ of (a) species, and (b) ponds	15
Figure 2.3. Physicochemical properties, ^{210}Pb , ^{137}Cs and ^{214}Bi activities, ^{210}Pb age - cumulative mass and ^{210}Pb age-depth models for cores Lager-1 (a), Pilsner-1 (b), South-1 (c)	17
Figure 2.4. Relative abundance of diatoms and diatom-inferred salinity for cores (a) Lager-1, (b) Pilsner-1, and (c) South-1	19
Figure 2.5. Variation in precipitation in 1922–2014 for Fort McMurray area (Alberta Landscape and Landuses 2015), (a) CDLM and (b) diatom-inferred salinity change in Lager, Pilsner and South Ponds.....	20
Figure 3.1 (a) regional map showing the location of the study site within Alberta, Canada; (b) map of the study site, including locations of sediment cores; (c) cross-section of the study site along A–B transect (shown on Figure 3.1(b)) including locations of sediment cores	31
Figure 3.2. Lithology, chemical properties, and age-depth models of cores Lager-1 (a), Pilsner-1 (b), South-1 (c)	34
Figure 3.3. Organic matter concentration, sediment and organic matter accumulation rates, diatom-inferred (DI) salinity (from Volik et al. 2017), and macrofossil assemblages in core Lager-1	35
Figure 3.4. Organic matter concentration, sediment and organic matter accumulation rates, diatom-inferred (DI) salinity (from Volik et al. 2017), and macrofossil assemblages in core Pilsner-1	37
Figure 3.5. Organic matter concentration, sediment and organic matter accumulation rates, diatom-inferred (DI) salinity (from Volik et al. 2017), and macrofossil assemblages in core South-1	38
Figure 3.6. The relationship between organic matter accumulation rate and diatom-inferred salinity in cores Lager-1 (a), Pilsner-1 (b), and South-1 (c)	40
Figure 4.1 a) regional map showing the location of the study area within Alberta; b) map showing locations of study site near Fort McMurray, Alberta; c) map of	

the study site including locations of peat cores (North-1, South-1) and vegetation plots	51
Figure 4.2. Age – depth models of the cores North-1 (a) and South-1 (b) and cumulative peat mass – depth models of the cores North-1 (c) and South-1 (d)	54
Figure 4.3. Macrofossil assemblages and LARCA in core North-1	56
Figure 4.4. Macrofossil assemblages and LARCA in core South-1	57
Figure 4.5. CCA ordination biplot based on soil electrical conductivity, water table depth, soil moisture and temperature	59
Figure 5.1 (a) Regional map showing the location of the study site within Alberta, Canada; (b) map showing location of Saline Fen near Fort McMurray, Alberta; (c) map of the study site, including locations of peatland and pond plots	68
Figure 5.2. Net ecosystem exchange (NEE), gross ecosystem productivity (GEP) and ecosystem respiration (R) within peatland (a) and open-water areas (b)	75
Figure 5-3 Variations in net ecosystem exchange (NEE), gross ecosystem productivity (GEP) and ecosystem respiration (R) with (a) electrical conductivity (EC), (b) water table depth (WTD), (c) soil moisture (SM), (d) soil temperature (ST), (e) leaf area index (LAI), and (f) photosynthetically active radiation (PAR) within ridges and depressions	77
Figure 5.4. Nutrient availability (measured by PRS Probes) within ridges (a) and depressions (b) along a salinity gradient	78
Figure 5.5. Variation in net ecosystem exchange (NEE), gross ecosystem productivity (GEP) and ecosystem respiration (R) with (a) water depth (D), (b) water temperature (WT), (c) electrical conductivity (EC), (d) pH, (e) dissolved oxygen concentration, (f) chlorophyll a concentration, and (g) vegetation density (VD) within open-water areas	80
Figure 5.6. Nutrient concentrations in mesosaline (a) and hyposaline (b) ponds in the studied saline fen	81
Figure 5.7. Correlations between net ecosystem exchange (NEE), gross primary productivity (GEP), ecosystem respiration (R) and environmental variables (electrical conductivity (EC), water table depth (WTD), soil moisture (SM), leaf area index (LAI), aboveground biomass (AB), belowground biomass (BB), seasonal increase in belowground biomass (BBI), soil organic matter (SOM), availability of calcium (Ca ²⁺), manganese (Mn) and magnesium (Mg ²⁺) (measured by PRS Probes), concentration of phosphates (PO ₄ ³⁻), vegetation density (VD)) within depressions, ridges and ponds in the studied saline fen	83

Figure 7.1. Conceptual diagram of controls on carbon uptake and long-term storage in a saline boreal fen. Broken lines indicate that $EC > 10 \text{ mS cm}^{-1}$ has an effect on carbon storage	94
Figure A-1. PCA ordination diagram of 32 ponds used for training set development (a), and CA ordination diagram of 32 ponds and 16 diatom species used for training set development (b)	118
Figure B-1. Lithology of cores North-1 (a) and South-1 (b). Moisture and organic matter contents are shown as presents while bulk density and ash-free density are shown as g cm^{-3}	121
Figure B-2. Soil electrical conductivity (a), moisture (b), water table depth (c), and temperature (d) of 40 vegetation plots along salinity gradient at Saline Fen	123

List of Tables

Table 2.1. Summary of core details and water chemistry data, and size and average depths of Spruce, Lager, Pilsner, and South Ponds	9
Table 3-1. Summary of core details	32
Table 5.1. Plant assemblages, percent cover, soil organic matter (SOM) in %, bulk density (BD) in gcm^{-3} , porosity (P), specific yield (Sy), aboveground biomass (AB) in gcm^{-3} , seasonal increase in belowground biomass (BBI) in gcm^{-3} , belowground biomass (BB) in gcm^{-3} at studied peatland plots	71
Table 5.2. Average depth and electrical conductivity (EC) in June-August, vegetation density (VD) and macrophyte assemblages at pond plots	72
Table A-1. List of sampled ponds including their coordinates (Coord), depth in m (D), major ion concentrations (mg L^{-1}), salinity (ppt) in May (Sal_May) and August (Sal_Aug), conductivity (mS cm^{-1}) in May (Cond_May), and August (Cond_Aug), pH, dissolved oxygen in mg L^{-1} (DO), chlorophyll <i>a</i> concentration in ug L^{-1} (Chl a)	114
Table A-2 – Eigenvalues, percent explained variance and loadings of the first two axes for principal component analysis (PCA), canonical analysis (CA), and canonical correspondence analysis (CCA)	116
Table B-1. Radiocarbon dates for cores North-1 and South-1	119
Table C-1. Spearman’s rank-order correlation coefficients between net ecosystem exchange (NEE), respiration (R), gross ecosystem productivity (GEP) and environmental variables (electrical conductivity (EC), water table depth (WTD), soil moisture (SM), leaf area index (LAI), soil temperature (ST), and photosynthetically active radiation (PAR)) within peatland plots during May – August	124
Table C-2. Spearman’s rank-order correlation coefficients between net ecosystem exchange (NEE), respiration (R), gross ecosystem productivity (GEP) and peat hydro-physical properties (bulk density (BD), porosity (P), specific yield (SY), soil organic matter (OM), aboveground biomass (AB), belowground biomass (BB) and increase in belowground biomass (BBI)) within peatland plots, with ridge and depression fluxes presented separately	125
Table C-3. Spearman’s rank-order correlation coefficients between net ecosystem exchange (NEE), respiration (R), gross ecosystem productivity (GEP), electrical conductivity in July-August (EC) and nutrient availability within peatland plots during peak season (July-August)	125
Table C-4. Spearman’s rank-order correlation coefficients between net ecosystem exchange (NEE), respiration (R), gross ecosystem productivity (GEP) and environmental variables (depth (D), water temperature (WT), electrical	

conductivity (EC), pH, dissolved oxygen (DO), chlorophyll a concentration (Chl a), vegetation density (VD), and photosynthetically active radiation (PAR)) within pond plots during June – August	126
Table C-5. Spearman’s rank-order correlation coefficients between net ecosystem exchange (NEE), respiration (R), gross ecosystem productivity (GEP) and major ion concentrations within pond plots in August	126

List of Abbreviations

A	Area
AB	Aboveground Biomass
AOSR	Athabasca Oil Sands Region
AR	Peat Accumulation Rate
ARCA	Actual Carbon Accumulation Rate
BB	Belowground Biomass
BBI	Increase in Belowground Biomass
BD	Bulk Density
BP	Before Present
BPR	Boreal Plains Region
C/N	Carbon to Nitrogen Ratio
CA	Correspondence Analysis
cal. yr	Calibrated Years
CCA	Canonical Correspondence Analysis
CDLM	Cumulative Departure from Long-term Mean Precipitation
CF	Conversion Factor
CRS	Constant-Rate-of-Supply
DI	Diatom-inferred
DO	Dissolved Oxygen
DOC	Dissolved Organic Carbon
EC	Electrical Conductivity
EC _{av}	Average Soil Electrical Conductivity
EC _{max}	Maximal Soil Electrical Conductivity
EC _{min}	Minimal Soil Electrical Conductivity
FDP	Fresh & Dry Plot
FWP	Fresh & Wet Plot
GEP	Gross Ecosystem Productivity
HDP	Strongly Saline & Dry Plot
HWP	Strongly Saline & Wet Plot
LAI	Leaf Area Index
LARCA	Long-term Apparent Rate of Carbon Accumulation
LOI	Loss-on-Ignition
LORCA	Long-term Apparent Rate of Carbon Accumulation
M	Molar Mass
MDP	Moderately Saline & Dry Plot
MWP	Moderately Saline & Wet Plot
N	Molar Volume
NEE	Net Ecosystem Exchange
NSERC	Natural Science and Engineering Research Council
OC	Organic Carbon Content
OM	Organic Matter
OMAR	Organic Matter Accumulation Rate
p	Probability Value
PAR	Photosynthetically Active Radiation
PC	Principle Component

PCA	Principle Component Analysis
pH	Potential of Hydrogen
P	Porosity
PRS	Plant Root Simulator
R	Ecosystem Respiration
r	Pearson Product-Moment Correlation Coefficient
r ²	Coefficient of Determination
RMSE	Root-Mean-Square Error
SAR	Sediment Accumulation Rate
SD	Standard Deviation
SDP	Slightly Saline & Dry Plot
SM	Soil Moisture
SMav	Average Soil Moisture
SMmax	Maximal Soil Moisture
SMmin	Minimal Soil Moisture
SOM	Soil Organic Matter
sp.	Unspecified Species
spp.	Unspecified species
ST	Soil Temperature
SWP	Slightly Saline & Wet Plot
Sy	Specific Yield
T	Temperature
Tav	Average Soil Temperature
TFT	Transfer Function Technique
Tmax	Maximal Soil Temperature
Tmin	Minimal Soil Temperature
TN	Total Nitrogen
TRACA	True Carbon Accumulation Rate
USA	United States of America
V	Volume
VD	Vegetation Density
WD	Water Depth
WT	Water Temperature
WTD	Water Table Depth
WTav	Average Water Table Depth
WTD	Water Table Depth
WTmax	Maximal Water Table Depth
WTmin	Minimal Water Table Depth

1. Introduction

1.1. Background and rationale of research

Covering about 3.5 – 8.5 % (5.3 – 12.8 million km²) of the earth's surface (Zedler and Kercher 2005), wetlands represent a unique combination of terrestrial, hydrological, and climatic conditions, so they can be considered as an overlap between aquatic and upland environments. Depending on the amount of dissolved salts in water, wetlands are divided into freshwater and saline systems (National Wetlands Working Group 1997). The greatest concentration of saline wetlands is found in coastal regions affected by sea water (Price 1990); however, saline wetlands are also known to be present in the continental interior where they occupy depressions and contain an increased quantity of dissolved salts due to saline groundwater percolating to the surface, or/and due to intensive evaporation in arid regions (National Wetlands Working Group 1997). These saline peat-forming wetlands are typically associated with the discharge of saline groundwater, and thus can be classified as fens – peat landforms fed mainly by minerogenous water (National Wetlands Working Group 1997).

Saline fens have been reported in Western Boreal Plains (WBP) (Slave River and Athabasca River watersheds and along the western shore of Lake Winnipegosis (Trites and Bayley 2009a; 2009b; Grasby and Betcher 2002; Purdy et al. 2005)). WBP is a hub of intensive bitumen sands mining and oil extraction, and since the beginning of commercial development of the Athabasca Oil Sands in the 1960–70's, more than 700 km² of natural land has been destroyed by surface mining. The principal condition under which oil sands mining gets its permit is that at the completion of the mining, the land should be reclaimed in such a way that its ecological capacity would become equivalent to one before the mining took place (Alberta Environment 2008). Because wetlands occupied significant portion of the original landscape (Vitt et al. 1996), about 30% of post-mined area should be reclaimed back to wetlands (Alberta Environment 2008). Until recently, reclamation projects were aimed mostly at the construction of marshes, but during the last decade the emphasis of reclamation efforts has shifted to fens, a dominant ecosystem in the pre-disturbed landscape (Price et al. 2010; Vitt and House 2015). However, fen construction is greatly challenged by salinization as mining disturbs the natural stratification of sediments, and previously isolated saline layers may become mixed with others, exposing salt-

reach layers at the surface (Ketcheson et al. 2016). In constructed wetlands, dissolved salts decrease water availability for plants by decreasing the osmotic potential of the soil solution and interfere with nutrient uptake and redistribution in the plant if the aforementioned salts are accumulated above a certain level; some ions (boron, chloride, sodium and others) become toxic at certain concentrations (Trites and Bayley 2009a; Kessler et al. 2010). Naturally saline communities offer appropriate models for reclamation in areas affected by salinity (Purdy et al. 2005; Wells and Price 2015a), and understanding controls on carbon sequestration in naturally saline fens can be helpful for furthering the landscape reclamation process as one of the key aspects of “equivalent capacity” is the carbon storage function of the system (Environment and Parks 2015). Saline fens were considered targets for reclamation (Environment and Parks 2015), so an understanding of temporal and spatial changes in carbon accumulation associated with differences in levels of dissolved salts should be useful for determining acceptable salinity levels that would not severely affect carbon accumulation at those constructed saline wetlands. Identification of the main controls on carbon accumulation under saline conditions will enhance development of constructed fen design because an understanding of those controls will help to choose and create settings (e.g., basin topography, microtopographical features, composition of plant assemblages, and planting scheme) that will allow constructed fens to function similarly to natural analogs in terms of carbon sequestration.

Carbon sequestration, the process of CO₂ uptake from the atmosphere and its long-term storage (Chapin et al. 2006), is one of the fundamental functions of the peat-forming wetlands (Gorham 1991) with peat accumulating potentials related to the balance between evapotranspiration and precipitation, and hydrologic connectivity with local water bodies and nearby uplands (Petroni, et al. 2011). Despite relatively low carbon accumulation rates (in average about 20-40 g C per m² per year (e.g. Botch et al. 1995; Clymo et al. 1998; Vitt et al. 2000; Turunen et al. 2002), during the Holocene northern peatlands have stored about 500±100 Gt of carbon (Yu 2012) that comprise about a quarter of the world soil carbon stock (2376-2456 Gt) (Batjes 1996) and about 80% of the global vegetation carbon stock (610 Gt) (Yu et al. 2012). Such a significant amount of carbon was deposited mainly because over millennia, the photosynthetic production of living plants exceeded decomposition of organic debris under anoxic conditions within the waterlogged peat column (Clymo et al. 1998).

Carbon sequestration in peatlands is driven by regional and site- specific factors such as precipitation and temperature regime (Malmer et al. 2005; Beilman et al. 2009), basin topography (Korhola et al. 1996; Van Bellen et al. 2011), vegetation and hydrology (Loisel and Garneau 2010; Van Bellen et al. 2011). However, in saline peatlands, salinity may modify the effect of these environmental variables on carbon accumulation as elevated salt content can affect plant productivity and litter decomposition (Neill 1993; Curco et al. 2002; Willis and Hester 2004; Neubauer 2013). Although a pioneering study of organic matter accumulation in saline wetlands by Trites and Bayley (2009a) has shown an ability of these wetlands to accumulate organic matter despite increased salt content, and saline fens are known to accumulate up to 1.5m of peat (Wells and Price 2015a), it is unclear how different levels of salinity impact carbon sequestration. The magnitude of variability in carbon accumulation in response to changes in environmental parameters may be different under hypo- , meso- and hypersaline conditions, so controls on carbon capture and long-term storage along a salinity gradient should be identified to improve our understanding of functioning of saline fens.

1.2. Objectives and thesis structure

The overall goal of this research is to determine the main environmental controls on carbon uptake and long-term storage along a salinity gradient within a saline, boreal, peat-forming wetland that represents an adequate model for reclamation in the Athabasca Oil Sands Region. The specific research objectives are:

- 1) to reconstruct temporal salinity change within the wetland using diatom-based transfer function and assess the main controls on salinity fluctuation over time;
- 2) to examine the main controls on organic matter accumulation rate (OMAR) in open-water areas within the wetland over time;
- 3) to evaluate degree of variability in long-term carbon accumulation rates within terrestrial areas of the wetland and to assess the main drivers of this variability;
- 4) to assess the main controls on recent carbon uptake along a salinity gradient.

The thesis consists of 6 chapters that are structured to fit the manuscript option at the University of Waterloo. The first chapter presents a general introduction to saline boreal wetlands, carbon accumulation in peatlands, and wetland reclamation in the Athabasca Oil Sands Region as well

as outlines the overall aim and specific questions of the research. Each of the subsequent chapters consists of a manuscript that addresses one of the questions of the thesis.

Chapter two addresses the first objective by assessing salinity change in a saline boreal fen over the last ~100 years using paleolimnological approach and examining the impact of precipitation change on salinity fluctuation. Chapter three addresses the second objective of the thesis by determining changes in organic matter accumulation in open-water areas within the wetland and by evaluation impact of salinity, water level, and vegetation on rates of organic matter accumulation. Chapter four addresses the third objective of the thesis by assessing changes in long-term apparent rate of carbon accumulation (LARCA) in more saline and less saline terrestrial parts of the wetland and by evaluating relations between LARCA and changes in salinity, water level, and vegetation inferred from macrofossils. Chapter five addresses the fourth objective of the thesis by determining effect of environmental factors on net ecosystem exchange, ecosystem productivity and ecosystem respiration along a salinity gradient.

Chapter six presents a summary of the conclusions from each chapter and provides a synthesis of the implications of the findings for fen construction in the Athabasca Oil Sands Region.

Three appendices are located at the end of the thesis: Appendix A contains an environmental dataset and results of statistical analyses used for development of diatom-based transfer function; Appendix B presents description and chronology of cores North-1 and South-1 and environmental dataset from 40 vegetation plots along salinity gradient at Saline Fen; Appendix C contains correlation coefficients between net ecosystem exchange (NEE), respiration (R), gross ecosystem productivity (GEP) and environmental variables.

2. Long-term precipitation-driven salinity change in a saline, peat-forming wetland in the Athabasca Oil Sands Region, Canada: a diatom-based paleolimnological study

2.1. Introduction

Alberta's boreal peat forming wetlands are of increasing concern as a the sub-humid Boreal Plains region (BPR) contains the Athabasca Oil Sands Region (AOSR), a hub of intensive bitumen sands mining and extraction where extensive areas of wetlands are being removed. According to provincial guidelines (Alberta Environment and Parks 2015), areas disturbed by surface mining (approximately 700 km² (Government of Alberta Energy 2017) must be reclaimed to an "equivalent land capacity" containing ~33% wetlands by area. However, this task is challenged by the potential for wetland salinization, due to the elevated ionic content in tailings and reclamation materials (tailings sands, petroleum coke) (Alberta Environment and Parks 2015). As target conditions, the expected outcomes of reclamation, should depend on pre-disturbance land use, coupled with post-mining site characteristics (such as pH and electrical conductivity). As such, naturally saline boreal fens (minerotrophic peat-forming wetlands) have been suggested as appropriate models for reclamation in areas where establishment of other wetland types is impossible due to elevated salt content (Purdy et al. 2005; Trites and Bayley 2009b; Alberta Environment and Parks 2015). Thus, understanding the properties and functions of saline boreal wetlands will be useful for guiding and improving wetland reclamation.

Recent research efforts have been devoted to understanding the contemporary hydrology, geochemistry, and ecology of saline boreal fens (Purdy et al. 2005; Trites and Bayley 2009a; 2009b; Phillips et al. 2015; Wells and Price 2015a, b). However, less is known about changes in salinity, a defining feature of saline fens, and about controls on long-term salinity fluctuation. Gaining knowledge of the drivers and past trends of salinity, the sum of all ion concentrations (Williams and Sherwood 1994), in natural saline wetlands will improve our understanding of salt dynamics in artificial wetlands and will help to create appropriate reclamation strategies. Long-term relations between salinity and precipitation are of particular interest because precipitation plays an important role in the wetland water balance within the BPR (Ferone and Devito 2004), and it is one of the main drivers of salinity distribution and fluctuation in saline wetlands (Heagle et al. 2013). In addition, small boreal lakes within the BPR, such as those found in saline

systems, are known to be sensitive to variations in the precipitation – evaporation balance (Smerdon et al. 2005). Thus, a better understanding of the precipitation – salinity linkage in saline boreal fens can be useful for predicting the potential resilience of constructed saline wetlands under climate change, and for the development of new approaches for salinity control.

Saline boreal fens include abundant open water areas (ponds) (Wells and Price 2015a), and sediment sequences accumulated in these ponds can provide useful information on wetland development and past environmental conditions including salinity (Smol et al. 2001). Diatoms have constituted one of the main indicators of past environmental changes of aquatic ecosystems because of their sensitivity to various environmental variables, global distribution, occurrence in wide variety of aquatic environments, and abundance in sediment records and modern environments (Battarbee et al. 2001). These algae have a relatively short generation time, so composition of their assemblages changes quickly in response to shifts in environmental conditions. Moreover, diatoms are often present in a high number, so quantitative numerical analysis can be performed (Gasse et al. 1995; Battarbee et al. 2001). Diatom distribution has been repeatedly shown to correlated with salinity (Cumming and Smol 1993; Laird et al. 1996; 2000; Fritz et al. 1993; Wilson et al. 1994; 1996). It has been suggested that salinity may influence diatoms through: 1) increased nutrient demand as algal cells have to produce N-rich osmolytes to survive under an osmotic stress (Saros and Fritz 2000), 2) through the effect on uptake of compounds involved in nutrient cycling, or 3) through nutrient availability in the water column (Fritz 2013). Because each diatom species has a different salinity tolerance (range of salinity values at which the species can survive) and salinity optima (salinity level that is associated with the highest abundance of the species), it is possible to use quantitative approaches for salinity reconstruction (Fritz 2013).

The transfer function technique (TFT) based on weighted-averaging calibration and regression has been proven to be the most useful tool for quantitative estimation of changes in water salinity and electrical conductivity, and has been widely applied across North America, Australia and other parts of the world (Cumming and Smol 1993; Gasse et al. 1995; Laird et al. 1996; Pienitz et al. 1992; 2000; Fritz et al. 1993; Wilson et al. 1994; 1996; Reed et al. 2012). High accuracy of salinity reconstruction using TFT can be expected when: 1) salinity has a strong effect on diatom assemblages (Fritz et al. 2010; 2013), 2) past fluctuation exceeds the

standard error of prediction, but does not exceed the central range of the modern training set (Birks 1998; Fritz et al. 2013), and 3) relationships between species and salinity are constant over time (Fritz et al. 2013). While the reconstruction of salinity can be biased to some extent by a number of issues associated with preservation, taphonomy, statistical analyses of diatom assemblages and environmental datasets, and calibration (Fritz et al. 2010), consistency between diatom-inferred (DI) salinity and historic salinity measurements (Fritz et al. 1990) suggests that TFT can be used for salinity reconstruction with a high level of confidence. Therefore, the purpose of this study is to develop a diatom-based transfer function and apply it to diatom assemblages in sediment cores from a saline boreal wetland near Fort McMurray, to provide insight into past salinity changes and their causes. A better understanding of temporal variations in salinity, as well as drivers of these changes will improve our knowledge on the hydrologic and geochemical functioning of these boreal peatlands, which is essential for the development of efficient reclamation practices (Ferone and Devito 2004). We address the following questions: 1) What is the scale of temporal variability in pond salinity over the last century? and 2) Has salinity change been associated with variations in precipitation in the Fort McMurray area? This paper is a part of a larger study on salinity fluctuations and carbon storage in saline boreal wetlands. Thus, the results reported here will be used to determine the relationships between salinity fluctuations and carbon accumulation in ponds, as well as the role of open water areas in carbon sequestration of a whole saline boreal peat-forming wetland.

2.1.1. Study area

The study was carried out in a complex of three natural saline fens (western fen (hereafter, Saline) (56°34'28.84" N, 111°16'38.39" W), south-eastern fen (hereafter, Southern Saline) (56°33'56.32"N, 111°16'20.18"W), and eastern fen (hereafter, Eastern Saline) (56°34'9.28"N, 111°15'9.98"W)) situated about 10 km south-east of Fort McMurray, Alberta (Figure 2.1(a), (b)). The region is characterized by a sub-humid climate with cold winters and warm, dry summers. Average January and July temperatures for the Fort McMurray area during 1981–2010 were -19°C and +16.6°C, respectively (Government of Canada 2017). Mean annual temperature was 0.2°C, and mean annual precipitation was 460 mm (Government of Canada 2017). The fens are characterized by notable gradients in electrical conductivity, and the electrical conductivity of near-surface groundwater in Saline varies from 0.5 mS cm⁻¹ in the

northern part to 120 mS cm⁻¹ in the southern part. Surface and ground waters are dominated by Na⁺ and Cl⁻ (Wells and Price 2015a; 2015b). Wetland vegetation is dominated by Baltic rush (*Juncus balticus* Willd.), seaside arrow grass (*Triglochin maritima* L.), sweetgrass (*Hierochloa hirta* (Schrank) Borbás), narrow reed grass (*Calamagrostis stricta* (Timm.) Koeler), and foxtail barley (*Hordeum jubatum* L.). However, halophyte plants are abundant in the in more saline parts, including sea plantain (*Plantago maritima* L.), red swampfire (*Salicornia rubra* A. Nelson), and horned seablite (*Suaeda calceoliformis* (Hook.) Moq.).

Numerous shallow ponds are situated within the wetland complex, predominantly in the southern and central parts. Average pond salinity ranges from 1 to 40 ppt. Typically, surface areas of the ponds vary from 1 m² to 1.2 ha although smaller depressions (surface area about 0.5 m²) filled with water are abundant. Most large ponds have irregular shapes, while small ponds are typically circular and located in deep depressions with steep margins. The ponds have average depths of 0.4–0.5 m, with many of the ponds drying out during the late summer. Thirty-two permanent ponds from Saline, Southern Saline, and Eastern Saline were used for this study (Figure 2.1(c)) including Lager, Pilsner and South Ponds, where three sediment cores were collected.

2.2. Materials and methods

2.2.1. Field work

Three sediment cores (Lager-1, Pilsner-1 and South-1) were taken from Lager, Pilsner, and South Ponds, respectively (core locations, core lengths, coring details are in Table 2-1 and Figure 2.1), all from Saline Fen. The cores were extruded and sectioned into 1-cm increments in the field and refrigerated at 4°C until further processing.

For the diatom training set development, ponds were selected based on the following criteria: 1) limited connectivity with adjacent ponds to reduce possible inputs of allochthonous material, 2) permanence of ponds to minimize the effects of regular drying out on the composition and preservation of diatom assemblages (Gasse et al. 1997), and 3) fine-grained structure of bottom sediments, as a preliminary investigation conducted in July, 2014 revealed a lack of diatoms in ponds with coarse-grained peaty bottom material. Only 32 ponds in total fulfilled these criteria

and were used for the study. This set encompasses ~75% of the ponds in Southern Saline and Eastern Saline, and ~30% of ponds in Saline, and captures the full range of pond salinity in the study area. Thus, the pond set seems to be sufficient for the development of a training set although the number of the ponds was smaller than has been recommended (Reavie and Juggins 2011; Reavie and Edlund 2013). Pond surface sediment samples (upper 0.3 cm) were taken on August 10, 2015 using a plastic tube (5 cm in diameter) pushed into sediments.

Temperature, conductivity and salinity were measured on 15 May, 2015 and 10 August, 2015, and pH and dissolved oxygen (DO) were measured on 10 August, 2015 using a hand-held probe YSI Professional Plus (YSI Incorporated, USA). Depths of the ponds were measured on 10 August, 2015. Surface water samples (from ~20 cm depth) from each pond were collected on 10 August, 2015. The water samples were filtered (0.45 µm cellulose acetate filters) within 24 hours and frozen upon delivery to the Biogeochemistry Lab at the University of Waterloo, where they were analyzed for major ions (DIONEX ICS3000).

Table 2.1. Summary of core details and water chemistry data, and size and average depths of Spruce, Lager, Pilsner, and South Ponds

	Lager Pond	Pilsner Pond	South Pond
Area, ha	~0.95	~0.13	~1.28
Average depth, m	0.49	0.46	0.43
Salinity, ppt	7.47	14.57	11.31
Conductivity, mS cm ⁻¹	10.6	18.7	18.9
Total dissolved salts, mg L ⁻¹	8404	15,580	12,337
Dissolved oxygen, mg ⁻¹	5.68	5.31	7.64
pH	7.44	6.82	7.61
Core name	Lager-1	Pilsner-1	South-1
Core length, cm	31 (only upper 22 cm is used for this study)	41 (only upper 28 cm is used for this study)	43 (only upper 28 cm is used for this study)
Coring site coordinates	56°34'7.85"N 111°16'11.83"W	56°34'6.53"N 111°16'7.56"W	56°34'3.46"N 111°16'0.41"W
Coring date	15 Jun 2014	13 May 2015	13 May 2015
Coring device	plastic tube (diameter 8.5 cm) pushed into sediments	Maxi-Glew gravity corer	Maxi-Glew gravity corer

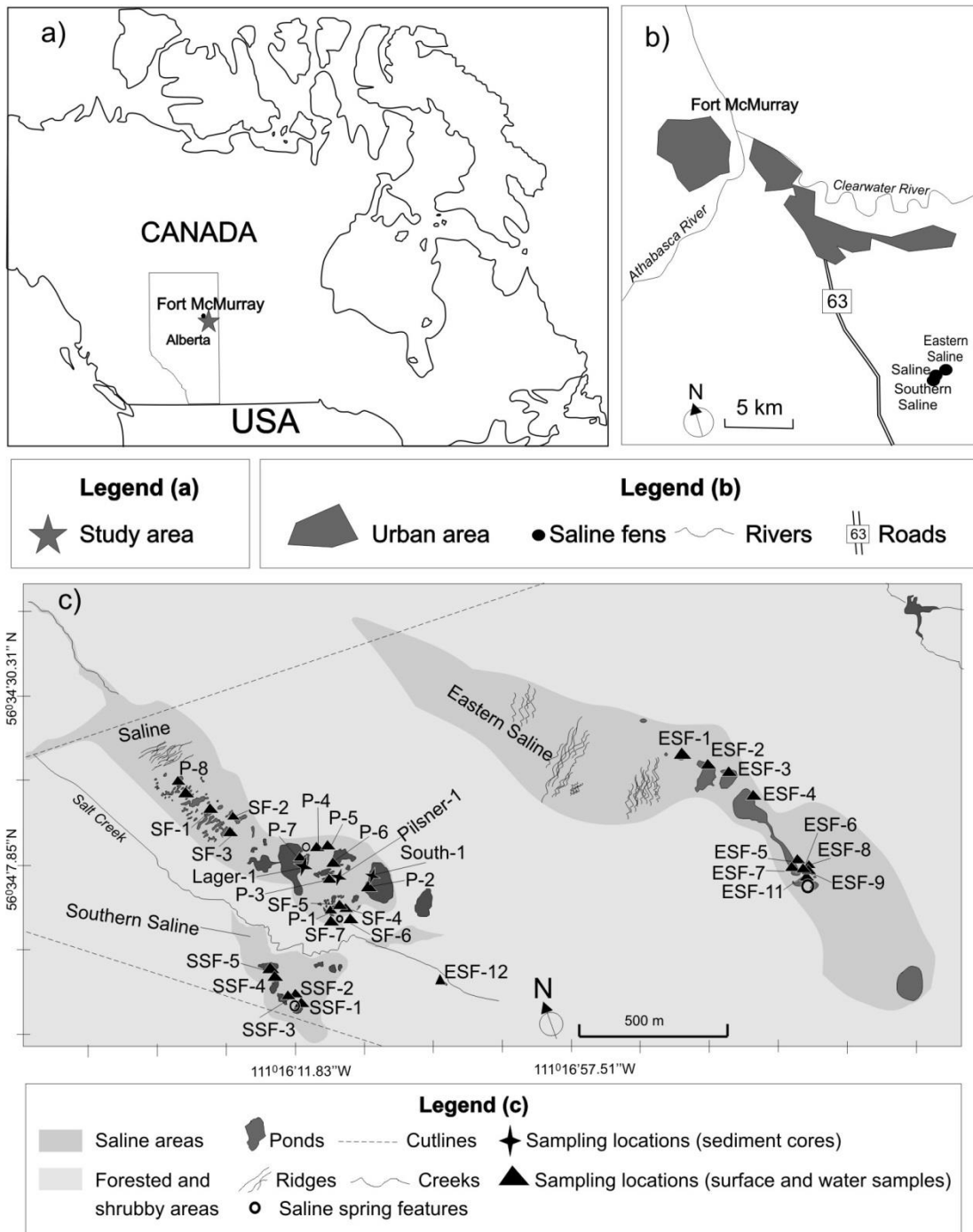


Figure 2.1. (a) Regional map showing the location of the study area within Alberta, (b) map showing locations of Saline, Eastern Saline and Southern Saline sites near Fort McMurray, Alberta, (c) map of the study sites including locations of 32 ponds sampled in August, 2015 and locations of sediment cores (Lager-1, Pilsner-1, and South-1).

2.2.2. Laboratory analyses of sediments

Sediment core subsamples of 1 cm³ were taken every 2 cm and measured for moisture, organic matter, carbonate and mineral matter by loss-on-ignition (LOI) following Heiri et al. (2001) by sequential heating at temperatures of 90°C, 550°C and 950°C for 24, 4 and 2 hours, respectively. To establish sediment core chronology for the past ~150 years, sediments samples were taken at every 1 cm (upper 5 cm) and every 2 cm (below 5 cm) and measured for activities of ²¹⁰Pb, ²¹⁴Bi, ¹³⁷Cs activities by gamma ray spectroscopy from a measured weight (0.7 to 3 g) of freeze-dried sediment that was packed into plastic tubes to a height of 35 mm and sealed with a silicone septum (Supelco®) followed by 1 cm³ of 2-ton epoxy resin (Devcon® product no. 14310) for at least 2 weeks before analysis. Supported ²¹⁰Pb activity was estimated from the average total ²¹⁰Pb activity of the bottom samples characterized by relatively constant activity. In addition, mean values of ²¹⁴Bi activity were used to determine depth where background ²¹⁰Pb activities had been reached. Samples were measured for 23–47 hours using an ORTEC digital gamma ray spectrometer at the WATER Lab (Department of Biology, University of Waterloo). Dates were calculated using the constant-rate-of-supply (CRS) model (Appleby and Oldfield 1978), and error terms for dates were estimated following Binford (1990).

For diatom analyses, subsamples of 0.2–0.3 g were processed for slide preparation following the methods of Battarbee et al. (2001). The samples were taken from the surface sediments for training set development. From cores Lager-1 and South-4 subsamples were taken every 2 cm. Below 10 cm depth in core Pilsner-1, sediments were composed of coarse peaty material that could be potentially barren of diatoms, and consequently the upper part of the core was subsampled at 1-cm increments to ensure enough samples were obtained for salinity reconstruction. Cleaned diatom slurries in water were dried onto cover slips and mounted onto glass slides using Naphrax (refraction index 1.7). Diatom identification was performed at 1000X magnification following Spaulding et al. (2010). At least 300 valves in each sample were identified and enumerated, and relative abundance and total diatom concentration values were calculated following the methods of Battarbee et al. (2001). Data were plotted using C2 by Juggins (2011).

2.2.3. Diatom-based transfer function development

Development of a diatom-based salinity model followed Cumming and Smol (1993) and Wilson et al. (1994) to make our results comparable to what was reported from the Northern Great Plains (Cumming and Smol 1993; Fritz et al. 1993) and Interior Plateau regions (Wilson et al. (1994)). A total of 17 environmental variables (salinity, conductivity, depth, pH, dissolved oxygen (DO), concentrations and proportions of Cl^- , SO_4^{2-} , Ca^{2+} , Mg^{2+} , K^+) were used for analyses. Due to a skewed distribution, salinity and conductivity, pH and DO were log-transformed, and depth was square-root transformed prior to analyses. Concentrations of major ions (Cl^- , SO_4^{2-} , Ca^{2+} , Mg^{2+} , K^+) were analysed as both log-transformed concentrations and as proportions. The study sites have very low carbonate content (except ESF-12 and Lager Pond), and because carbonate concentration was below detection limits in > 90% of the lakes, it was discarded from the set of environmental variables.

Principal components analysis (PCA) and correspondence analysis (CA) were used to identify the main environmental gradients and spatial differences in diatom community composition among sites, respectively. Relations between modern diatom assemblages and environmental variables were assessed based on canonical correspondence analysis (CCA). We determined the strength of the relationship between diatom assemblage composition and DI-salinity, by assessing the correlation between sample scores of the fossil assemblages in a CCA of modern assemblages constrained to salinity as the sole environmental variable. All ordinations were performed using PAST 3.06 (Hammer et al. 2001), and the significance of ordination axes was explored using Monte Carlo permutation tests. Software C2 by Juggins (2003) was used for calculation of Hill's diversity index, species optima and tolerances (by weighted-averaging regression), error estimation (999 bootstrap cycles), calibration of salinity model (with classical deshrinking and inverse deshrinking) and salinity reconstructions. Taxon optima and tolerances were calculated based on an arithmetic average of May and August salinity measurements and were used for development of diatom-based salinity inference models. Squared chord distance between diatom assemblages from fossil and modern samples was used to determine dissimilarity between fossil and modern samples and to determine whether fossil samples have analogs in the modern training set. Squared chord distance was measured in PAST 3.06.

2.2.4. Estimation of cumulative departure from long-term mean precipitation

Cumulative departure from long-term mean precipitation (CDLM) is a variable that is useful for evaluation of the temporal relationship between precipitation and ground water level (Weber and Stewart 2004). CDLM calculation was performed following Weber and Stewart (2004) and included: 1) estimating the mean for a set of rainfall data, 2) subtracting the mean value from each annual value to determine departures, and 3) accumulating the departure values over the studied time span. We used historical data on precipitation in the Fort McMurray region for 1922–2014 from Alberta Landscape and Landuses (2015).

2.3. Results

2.3.1. Environmental gradients and distribution of modern diatom assemblages

The combined 32-pond dataset was characterized by notable gradients in salinity and electrical conductivity, and exhibited a strong correlation ($r=0.97$, $p<0.05$) between salinity and conductivity. Water salinity varied from 1 to 36 ppt in May and from 1 to 42 ppt in August (Appendix 1). Water electrical conductivity ranged from 2 to 57 mS cm^{-1} in May and 3 to 68 mS cm^{-1} in August. All ponds were strongly dominated by Na^+ and Cl^- , with an average $\text{Cl}^- : \text{SO}_4^{2-}$ ratio of 42:1 (Appendix 1). PCA of the water chemistry data shows that the first PC axis represents positive relations between variables associated with ionic content (salinity, conductivity, Cl^- , SO_4^{2-} , Na^+ concentrations) and accounts for 56.4% of the variation (Appendix 1). In contrast, the gradient found along the second PC axis is associated with the $\text{Cl}^- : \text{SO}_4^{2-}$ ratio and accounts for 12.1% of the variation (Appendix 1). Pond depth, pH and DO were not characterized by notable spatial gradients, and PCA shows that these variables are associated with secondary axes and account for less than 5% of the variation.

Twenty-five species from 32 ponds were identified, but only 16 species were present at >1% in at least two ponds and used for diatom-salinity transfer function development. CA shows that differences in overall species composition of Saline, Eastern Saline and Southern Saline were not remarkable. However, two distinct pond groups (ponds associated with hyposaline species and ponds associated with mesosaline species) were observed. According to the species distribution, Axis 1 ($\lambda=0.80$) accounts for 30.5% of the variation in the diatom dataset and reflects a salinity/conductivity gradient (Appendix 1). Taxa associated with hyposaline conditions, such as *Staurosira construens* var. *venter* (Ehrenberg) P.B. Hamilton, *Staurosirella*

pinnata (Ehrenberg) D.M.Williams & Round and *Cocconeis placentula* var. *lineata* (Ehrenberg) Van Heurck, are located to the left along Axis 1, whereas species associated with mesosaline conditions, such as *Diploneis stroemii* Hustedt, *Parlibellus cruciculus* (W. Smith) Witkowski, Lange-Bertalot & Metzeltin, are positioned to the right along Axis 1. Axis 2 ($\lambda=0.39$) accounts for 14.8% of the variation in the diatom data and appears to be associated with brine composition. Sulphate tolerant taxa, such as *Navicula salinarum* Grunow (Staats et al. 1999), are positioned high along Axis 2, while species intolerant to elevated sulphate concentration, such as *Navicymbula pusilla* (Grunow in A. Schmidt) Krammer (Saros and Fritz 2000), are positioned low along Axis 2.

In a CCA exploring relations between distributions of diatom assemblages and environmental gradients Axis 1 ($\lambda=0.69$, $p<0.05$) and Axis 2 ($\lambda=0.27$, $p<0.05$) capture 43.45% and 16.0% of the variation, respectively (Appendix 2). Salinity ($r = -0.86$, $p <0.05$), conductivity ($r = -0.86$, $p <0.05$), and concentrations of Cl^- ($r = -0.88$, $p <0.05$), SO_4^{2-} ($r = -0.82$, $p <0.05$) are most strongly correlated with CCA Axis 1, suggesting strong association of these variables with diatom assemblage composition among ponds (Figure 2.2). DO and lake-water pH have a weak association with variation in diatom assemblage composition based on the short length for these vectors (Figure 2.2). CCA shows that the distributions of *D. stroemii*, *P. cruciculus*, *Anomoeoneis sphaerophora* fo. *costata* (Kützing) A.-M.Schmid, *Nitzschia tubicola* Grunow in Cleve & Grunow, *Halamphora coffeaeformis* (Agardh) Levkov, *N. salinarum*, *Craticula halophila* (Grunow) D.G.Mann, *N. pusilla* are positively related to variables associated with salt content (salinity, conductivity, concentration of Cl^- , SO_4^{2-}), while *S. construens* var. *venter*, *S. pinnata*, *Pseudostaurosira brevistriata* (Grunow) D.M.Williams & Round, *C. placentula* var. *lineata*, *Navicula cryptocephala* Kützing, *Cyclotella meneghiniana* Kützing and *Navicula peregrina* (Ehrenberg) Kützing demonstrate negative relations with these variables. A separation of ponds and species into two distinct groups associated with the salinity gradient is evident (Figure 2.2 (a), (b)).

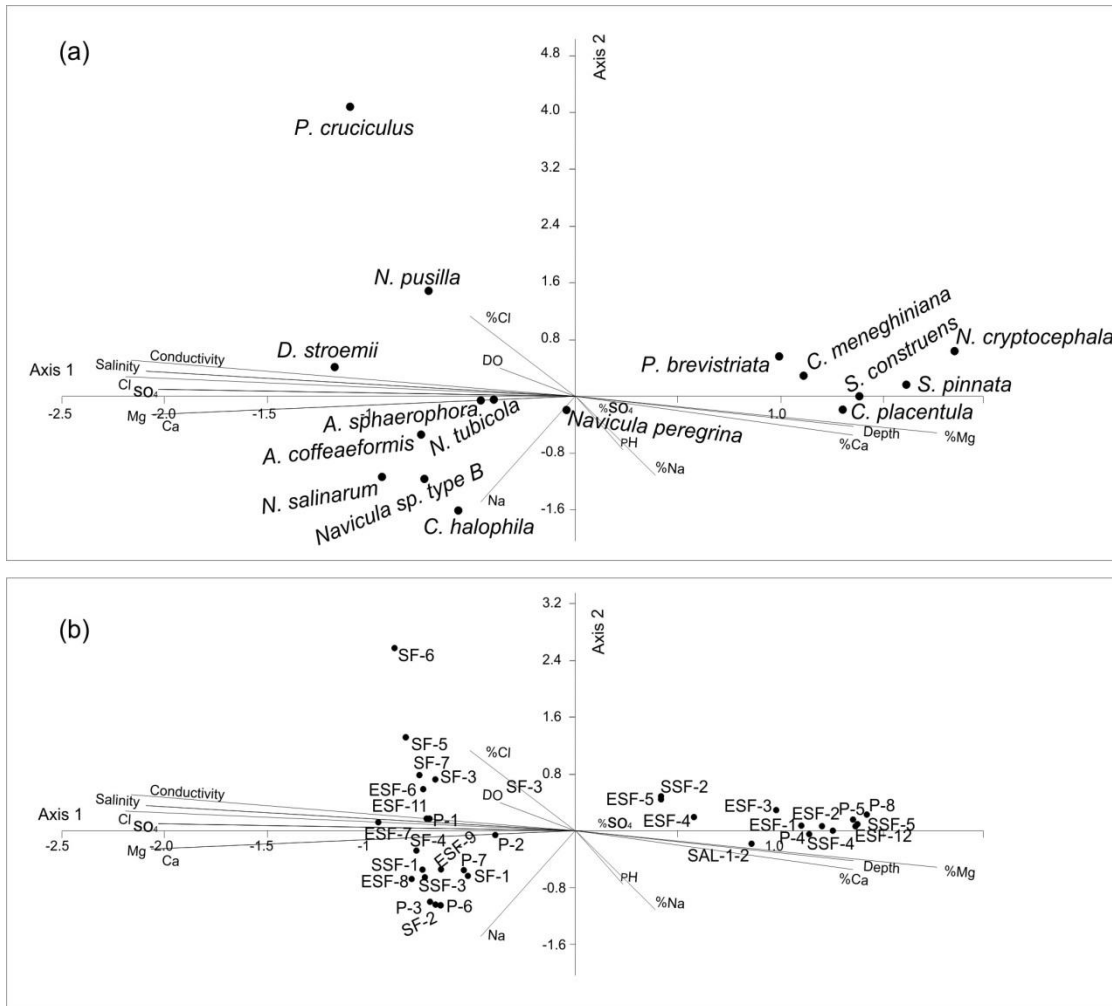


Figure 2.2. Canonical correspondence analysis (CCA) ordination biplot based on the mean environmental variables of depth, salinity, electrical conductivity, DO, pH, and concentrations of Cl^- , SO_4^{2-} , Ca^{2+} , Mg^{2+} , K^+ of (a) species, and (b) ponds.

2.3.2. Development of diatom-based transfer function

Diatom-inferred salinity transfer functions based on inverse de-shrinking provided more robust performance statistics (RMSE=0.17, $r^2=0.79$) than those based on classical deshrinking (RMSE=0.19, $r^2=0.79$). Thus, we used the weighted-averaging transfer function with classical de-shrinking for salinity reconstruction in the wetland cores. Diatom weighted-average salinity optima cover the salinity gradient observed in Saline and vary from 3 to 34 ppt. Most taxa have weighted-average optima in the hyposaline (3–20 ppt) range of salinity and only *D. stroemii*, *P. cruciculus* and *N. tubicola*, *N. pusilla* have optima in the mesosaline (20–50 ppt) range

(Appendix A). Differences between salinity optima and tolerances based on weighted-averaging and bootstrapping are not significant ($p > 0.05$) suggesting reliability of salinity inference models. The correlation between diatom-inferred salinity and average measured salinity in the 32 ponds studied is significant and strong ($r = 0.98$, $p < 0.05$). Based on measurements of squared chord distance, approximately 90% of diatom assemblages from fossil samples have analogs in the modern training set. One species (*Caloneis westii* (W. Smith) Hendey) present in the fossil assemblages was absent in the modern samples, and thus was not used for salinity reconstruction.

2.3.3. Sediment core lithology and chronology

Core Lager-1 consisted of firm gyttja (below 16 cm), peaty gyttja (16–9 cm) and gyttja (9–0 cm) (Figure 2.3(a)). Core Pilsner-1 demonstrated a transition from peat to peaty gyttja at 16 cm followed by a shift (at 10 cm) to gyttja (Figure 2- 3(b)). Core South-1 was characterized by a transition from peat to gyttja at 22 cm (Figure 2.3(c)). All three cores were characterized by high water content ($> 80\%$ in average) and mean organic content of 63% (Figure 2.3).

Correlation between log-unsupported ^{210}Pb activity and cumulative dry mass for all three cores is strong ($r > 0.85$) and significant ($p < 0.05$) suggesting relatively constant sedimentation rates and negligible sediment mixing. In core Lager-1 the total activity of ^{210}Pb peaked at 3 cm, then decreased with increasing cumulative dry mass, reaching supported levels of 28 mBq g^{-1} at 18 cm (confirmed by ^{214}Bi activity), which correspond to a CRS-modeled date of 1922 (Figure 2.3(a)). Decreased total ^{210}Pb activity within the upper 3 cm of the core may have resulted from increased sedimentation rates or post-depositional remobilization of ^{210}Pb under steep redox gradients (Baskaran et al. 2014). In the core from Pilsner pond, the total activity of ^{210}Pb decreased with increasing cumulative dry mass, reaching supported levels of 24 mBq g^{-1} at 24 cm (confirmed by ^{214}Bi activity), corresponding to a CRS-modeled ^{210}Pb date of 1906 (Figure 2.3(b)).

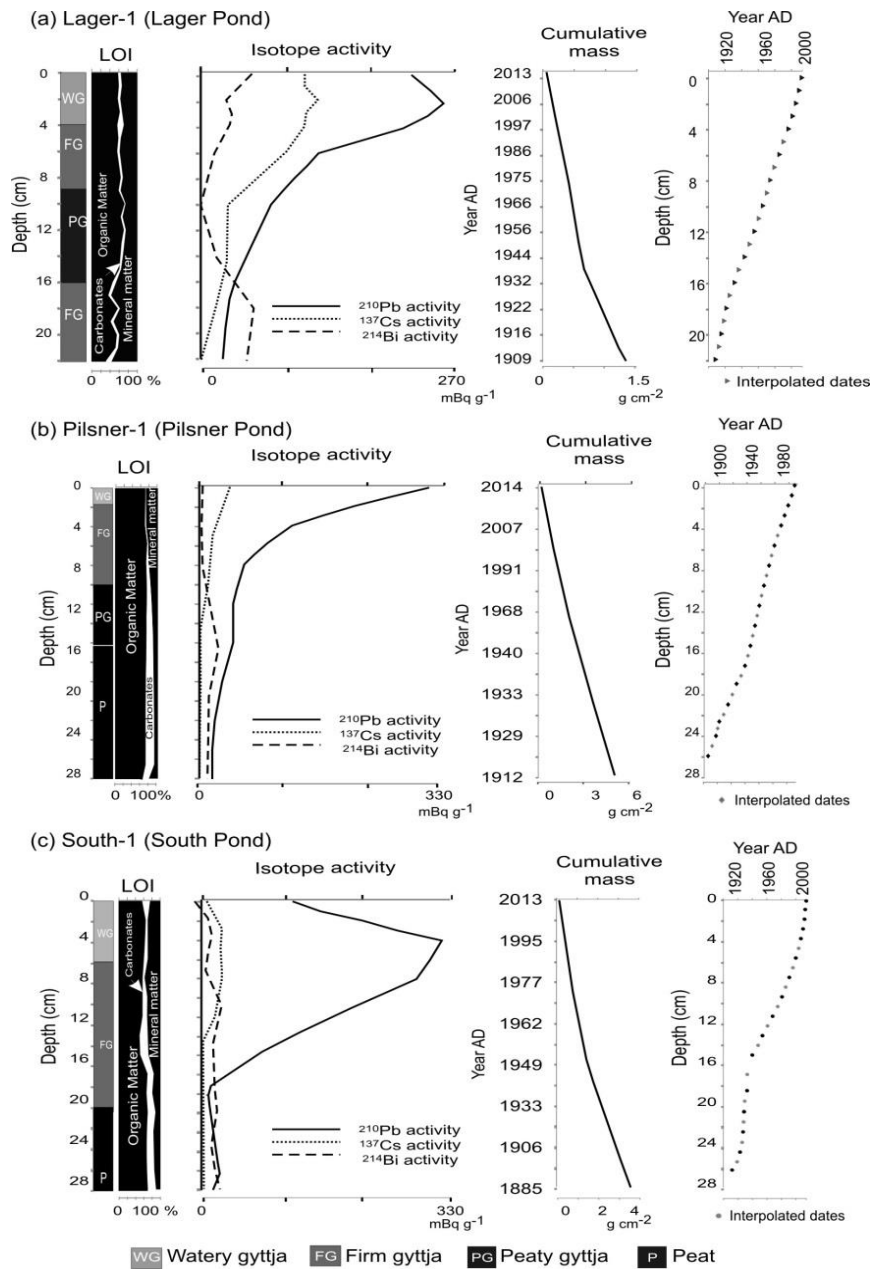


Figure 2.3. Physicochemical properties, ^{210}Pb , ^{137}Cs and ^{214}Bi activities, ^{210}Pb age - cumulative mass and ^{210}Pb age-depth models for cores Lager-1 (a), Pilsner-1 (b), South-1 (c).

In the core from South Pond, the total activity of ^{210}Pb decreased within the upper 4 cm similar to that observed in core Lager-1. Below 4 cm, the total activity of ^{210}Pb decreased down core with increasing cumulative dry mass, reaching supported levels of 3.5 mBq g⁻¹ at 20 cm depth (confirmed by ^{214}Bi activity), corresponding to a basal CRS-modeled ^{210}Pb date of 1933 (Figure 2.3(c)). However, the unsupported ^{210}Pb rises above background levels deeper in the core

at 24 cm depth before again returning to background levels. This creates two possible interpretations: 1) that background ^{210}Pb activity is reached at 20 cm and the rise in unsupported ^{210}Pb activity at greater depths is “noise”, confining the ^{210}Pb -datable record to the upper 16 cm of the core, or 2) the fall and then rise in unsupported ^{210}Pb activity with depth is indicative of a massive increase in sedimentation rate at 20 cm depth overlying more normal conditions below that depth, so the ^{210}Pb datable portion of the core extends to 28 cm. The second scenario seems most probable since a transition from gyttja to peat was observed below 20 cm, revealing a notable shift in lithology. This shift suggests that a change in conditions of sedimentation resulted in acceleration of the sedimentation rate.

^{137}Cs activity profiles in all three cores (Figure 2.3) do not demonstrate the expected peak in 1963 (Foster et al. 2006) and do not support ^{210}Pb chronology. This discrepancy is not surprising in saline nutrient-rich environments and can be attributed to the higher mobility of ^{137}Cs in organic-rich sediments, and high concentrations of competing ions such as Na^+ and K^+ , and ^{137}Cs mobilization under saline conditions (Foster et al. 2006).

2.3.4. Fossil diatom assemblages

The bottom portion (below 16 cm) of core Lager-1 was dominated by diatom taxa typical of hyposaline waters (*A. sphaerophora* f. *costata*, *N. peregrina*, *C. westii*), and the mesosaline indicator taxon *D. stroemii* appears between 22–18 cm (Figure 2.4(a)). At 16 cm, a shift to assemblages dominated by hyposaline taxa typical of hyposaline waters (*S. construens* var. *venter*, *H. coffeaeformis*, *N. salinarum*, *C. halophilla* and *N. peregrina*) was observed (Figure 2.4(a)).

The bottom part (below 10 cm) of core Pilsner-1 was virtually free of diatoms, whereas diatom assemblages above 10 cm were dominated by *N. salinarum*, *H. coffeaeformis*, *C. halophilla*, *N. tubicola*, *N. peregrina*. Mesosaline species (*P. cruciculus*) were most abundant at 3–5 cm (Figure 2.4(b)). As observed in Pilsner, diatoms were absent in the bottom of South Saline pond (below 22 cm in core). Between 22 and 18 cm assemblages were dominated by *S. pinnata* and *S. construens* var. *venter*, whereas above 16 cm, a rise in abundance of *N. pusilla*, *H. coffeaeformis*, *N. salinarum*, *N. peregrina* was observed although *S. pinnata*, *S. construens* var. *venter*, and *P. brevistriata* were present (Figure 2.4(c)).

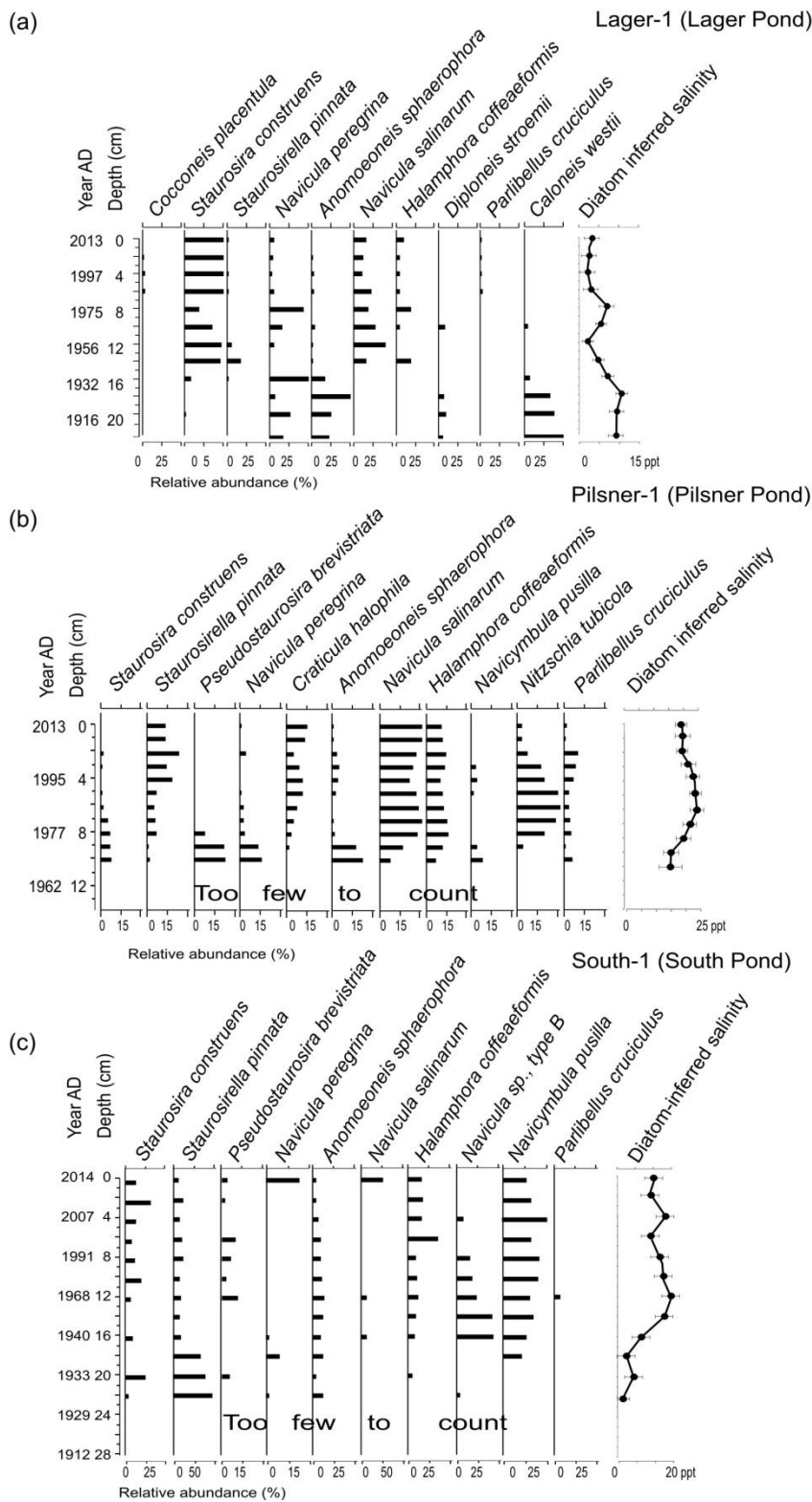


Figure 2.4. Relative abundance of diatoms and diatom-inferred salinity for cores (a) Lager-1, (b) Pilsner-1, and (c) South-1. Diatom taxa are organized by salinity optima.

2.3.5. Diatom-inferred salinity change

In Lager Pond, DI-salinity was the highest from 1909–1922, varying from 9 to 13 ppt, then declining to 3 ppt in ~1956 (Figure 2.5(a)). DI-salinity rose again (up to 9 ppt) between ~1956 and ~1975, followed by another decline. Since ~1986, DI-salinity has been relatively stable varying from 4 to 5 ppt in Pilsner Pond, a rise in DI-salinity (from 14 to 21 ppt) in ~1973–1995 followed by a decline to 16 ppt was observed (Figure 2.5(b)). In South Pond, in ~1931–1933 DI-salinity was the lowest (1–2 ppt) and then increased reaching 19 ppt in ~1954, before decreasing slightly from 19 to 15 ppt from ~1954–2000, and DI-salinity fluctuated between 10 and 17 ppt in ~2007–2014 (Figure 2.5(c)).

DI-salinity values are strongly associated with the main gradient in the distribution of diatom assemblages over time within each pond. Strong significant correlation ($r=0.88$, $p<0.05$) between CCA Axis 1 scores of the fossil assemblages and diatom-inferred salinity values was observed. Differences between measured salinity (Wells 2014) and DI-salinity in 2012 in studied ponds were not significant ($p>0.1$).

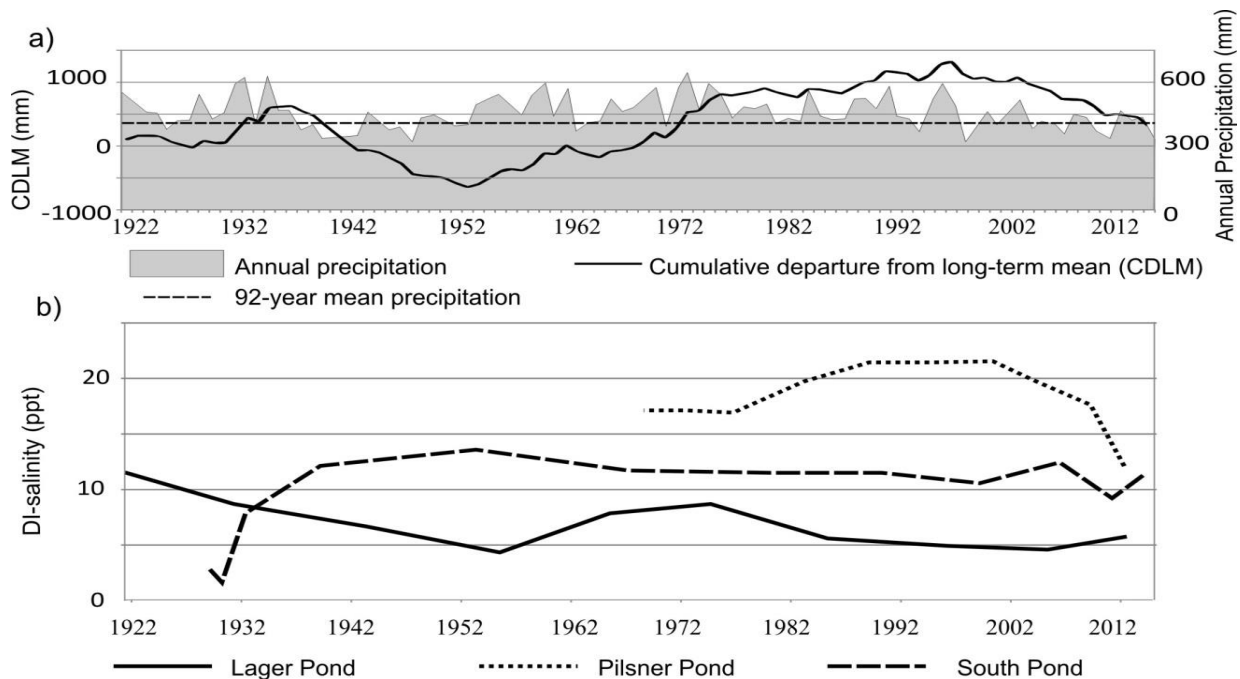


Figure 2.5. Variation in precipitation in 1922–2014 for Fort McMurray area (Alberta Landscape and Landuses 2015) (a), CDLM and (b) diatom-inferred salinity change in Lager, Pilsner and South Ponds.

2.3.6. Precipitation variability in 1922–2015 in Fort McMurray area

During 1922–2014, annual precipitation in Fort McMurray area varied from 242 mm (in 1998) to 675 mm (in 1973) with average of 431 mm (Figure 2.5(a)). CDLM ranged from -793 mm (in 1953) to 945 mm (in 1977). Rising CDLM occurred during 1922–1937 (up to 552 mm) and 1952–1997 (up to 945 mm), whereas declines occurred 1934–1952 (up to -793 mm) and 1997–2015 (up to -165 mm) (Figure 2.5(a)).

Complex relations between DI-salinity, precipitation and CDLM are apparent (Figure 2.5). In Lager Pond, the decline in CDLM during 1934–1952 coincided with a decrease in DI-salinity, followed by increase in CDLM and DI-salinity during 1960–1976 while a rise in CDLM in 1976–2012 corresponds to a decline in DI-salinity. In Pilsner Pond, a rise in DI-salinity in 1976–2012 corresponds to a decline in DI-salinity. In South Pond, a rise in DI-salinity in 1976–2012 coincided with the rise of CDLM, and the following decline in CDLM was accompanied by a decline in DI-salinity. In South Pond, rising CDLM during 1932–1936 corresponded with rising DI-salinity. Following this, an increase in DI-salinity during 1936–1952 coincided with decline in CDLM. A gradual decline in DI-salinity in 1952–2000 was accompanied by rise in CDLM. Although the CDLM demonstrated a decline in 1997–2014, rises in DI-salinity in 2006 and decline in 2012 were visible.

2.4. Discussion

2.4.1. Salinity fluctuation and precipitation change

Lake and pond dynamics and climate are connected in a complex way (Butcher et al. 2015), and effective moisture (precipitation minus evaporation) is known to have a strong effect on the ionic concentration and composition of inland waterbodies (Fritz 2013). However, groundwater input can complicate climate – water chemistry links (Vance et al. 1997; Telford et al. 1999; Smith et al. 2002; Hobbs et al. 2011). This study reveals a complex relationship between precipitation and pond DI-salinity resulting from differences in the hydrologic functioning of the studied ponds, and their connectivity with shallow groundwater aquifers and adjacent wetlands (Wells and Price 2015b).

Although studied ponds are located in close proximity, DI-salinity patterns (Figure 2.5(b)) do not coincide, and in some cases, are opposite suggesting the existence of different

mechanisms of pond salinity regulation. The observed difference in DI-salinity trends between Pilsner and Lager Pond (Figure 2.5) can be most likely explained by their relative positions within the landscape, as well as the potential for significant variability in saline spring discharge driven by long-term precipitation patterns. In Lager Pond, a direct relation between DI-salinity and CDLM was found between 1937 and 1976. A decrease in DI-salinity between 1937 and 1952 occurred during a period of long-term moisture deficit (a decline in the CDLM), where excess water was low and the opportunity for runoff or groundwater movement is limited in the BPR (Petroni et al. 2007; Devito et al. 2005). While the transport of saline groundwater to the fen is tied to the presence of a regional saline aquifer (the Grand Rapids) (Wells and Price 2015a), a period of low deep groundwater input during this period (expressed through low salinity levels in Lager Pond) may be indicative of the sensitivity of regional aquifers to long-term drought and precipitation cycles (Winter and Rosenberry 1998; Hayashi and Farrow 2014).

Between 1954 and 1976, a steady increase in annual precipitation is observed resulting in a steady decrease in the long-term moisture deficit (a rise of the CDLM) (Figure 2.5). During this period, DI-salinity at Lager Pond increased. The observed DI-salinity changes can be explained by the function of the saline fen as a saline discharge zone driven by a saline plume within a near-surface Cretaceous Formation, which is likely sensitive to regional wetting and drying cycles (Wells and Price 2015b). Consequently, a rise in CDLM (a decrease in the moisture deficit) may have intensified the regional groundwater flow and thus discharge of saline water to the fen and ponds. Similar salinity increases accompanied by rises in precipitation and lake level were reported from Kenosee Lake (Saskatchewan) (Vance et al. 1997) and Lake Awassa (Africa) (Telford et al. 1999), and was attributed to the intensification of saline groundwater input under the onset of wet conditions. Moreover, the impact of groundwater influx on lake salinity was observed at Elk Lake (Minnesota) (Smith et al. 2002) and Konya Basin (Turkey) (Reed et al. 1999). Although there is uncertainty in the magnitude of deeper groundwater flux to the present study site, as mineral sediments underlying the fen have low average hydraulic conductivity and thus low vertical groundwater flux (Wells and Price 2015a), the presence of a layer of sand and fine gravel (higher hydraulic conductivity) near the south-eastern end of Lager Pond (Wells 2014) supports the possibility of deeper groundwater discharge therein. Moreover, discharge of saline ground water can be assumed from the presence of relict saline spring features observed near the north-eastern end of Lager Pond (Wells and Price 2015a). This also coincides with the

findings of Wells and Price (2015b), suggesting that the studied fen was functioning as a saline spring with fluctuating discharge rates.

The influence of site-scale hydrology on salinity also plays an important role in salinity dynamics at the fen. Wells and Price (2015a) observed that steeper hydraulic gradients within the south fen supplied surface and subsurface flow northward, towards Lager Pond, and this flow (and thus salt transport) was enhanced when water tables were elevated due to higher hydraulic conductivities within the upper peat layers. An increase in DI-salinity at Lager Pond during the years following the long-term moisture deficit was likely driven by intra-wetland groundwater flow. Interestingly, an inverse relation between CDLM and DI-salinity in Lager Pond during 1976–2012 (wet cycle) is evident. Although it is possible that a decrease in DI-salinity during this period resulted from the dilution of pond water by precipitation, the simultaneous rise in salinity in Pilsner Pond suggests other mechanisms are at play. The observed difference in DI-salinity trends between Pilsner and Lager Pond can be most likely explained by their relative positions within the landscape and the degree of hydrologic connectivity between adjacent land units. The semi-permanent Pilsner Pond is situated within the south-central portion of the fen and is isolated from the adjacent non-saline wetlands (Figure 2.1). Fed horizontally by saline groundwater from the peatland and vertically via the connected saline Grand Rapids aquifer, the ponds only source of freshwater is through rainfall (Wells and Price 2015b). In contrast, Lager Pond is located within the saline fen's most narrow section and is the largest pond within the system. Its eastern and western shorelines are hydrologically connected during wet periods to the adjacent freshwater systems, where the exchange of both fresh surface and subsurface flow can take place (Wells and Price 2015b). Thus, in combination with precipitation, Lager Pond is more susceptible to dilution via adjacent freshwater systems during periods of elevated water table and may explain the decrease in salinity from 1976 and onward. High concentration of carbonates in Lager Pond also supports the influx of groundwater from adjacent wetlands dominated by carbonates (Wells and Price 2015b), in contrast to the rest of studied ponds in Saline that has overall low carbonate content.

In South Pond, DI-salinity demonstrates an opposite relationship with CDLM (except 1932–1936 and 2012–2014) and seems to be directly governed by precipitation rather than by deeper saline groundwater input. It was reported that rises in precipitation result in decreased

solute concentration in shallow lakes in the Boreal Plains (Cobbaert et al. 2014). Thus, dilution of salt by precipitation can explain the inverse relation between salinity in South Pond and precipitation. The semi-permanent features of South Pond also suggest that the pond is fed predominantly by precipitation as the pond dries up during the summer due to high evapotranspiration (Wells 2014).

2.4.2. Limitations of the study

This study developed a diatom-based salinity transfer function from the analysis of diatom assemblage composition in 32 relatively isolated ponds situated close together in adjacent saline wetlands and applied it to reconstruct past salinity variations in three saline boreal ponds over the last 90 years. The ponds have relatively similar ion compositions and pH, but different salinity levels, and thus, it can be assumed that the influence of the environmental factors other than salinity on diatom distribution should be limited. This was confirmed by a CCA which demonstrated the distribution of diatom assemblages among sites is strongly and significantly associated with salinity and ionic content of the pond water (Figure 2.2). In addition, salinity was considered the main driver of temporal changes in diatom assemblages from the sediment cores based on strong and significant correlation between the CCA Axis 1 scores of the fossil assemblages in the 32-pond training set constrained to salinity and the diatom-inferred salinity values obtained from samples in the sediment cores from the three ponds. The ponds used for development of the training set are small and shallow and do not have river inflows, and thus negative effects on the accuracy of the diatom-based salinity model due to transport before diatom burial coupled with mixing of planktonic, littoral, saline and freshwater taxa should be reduced (Fritz et al. 2010). The absence of allochthonous input is also confirmed by similar ecological requirements (except salinity) of diatom taxa as most species are eutrophic and alkalophilic with remarkable differences in salinity optima. Number of species in the studied ponds is lower compared to Great Plains or Interior Plateau (Cumming and Smol 1993; Fritz et al. 1993; Wilson et al. 1994; 1996) and this may reduce the accuracy of salinity inference (Fritz et al. 2010). However, the studied ponds are hypo- to mesosaline, so preservation of diatoms is better compared to those of the Great Plains or Interior Plateau, and thus salinity inference here should be more accurate (Ryves et al. 2006). Moreover, the accuracy of the salinity inference is also supported by the very high number (about 90%) of fossil samples that have adequate

modern analogs, coupled with a strong significant correlation between CCA Axis 1 scores of the fossil assemblages and diatom-inferred salinity values.

Diatom assemblages from the studied ponds are dominated by taxa that were reported from Great Plains, Interior Plateau and Yukon River basin (Cumming and Smol 1993; Fritz et al. 1993; Pienitz et al. 1992; Wilson et al. 1994). The main differences between diatom assemblages in this study and in studies mentioned above are: 1) the presence of *D. stroemii* and *P. cruciculus* that can comprise up to 20–30% of diatoms assemblages in some ponds, 2) low number of species (25 species were identified, and only 16 species were present at >1% in at least two ponds), and 3) high abundance of *S. construens* var. *venter* (maximum relative abundance of up to 95% was observed in some ponds). Estimated diatom salinity optima are notably different from those reported from the Great Plains and Interior Plateau (Cumming and Smol 1993; Fritz et al. 1993; Wilson et al. 1994) (Appendix A). Thus, it can be assumed that our inferences may be biased as the transfer function was based on a small training set and limited salinity gradient. However, a strong significant correlation ($p < 0.05$) and no significant difference ($p > 0.05$) between diatom-inferred salinity and average measured salinity in the 32 studied ponds, gives us *confidence* in transfer function development. Moreover, diatom-inferred salinities for studied ponds in 2012 were very close to what was observed in the field in summer 2012 (Wells 2014). The differences in salinity optima may result from differences in ion composition (Gasse et al. 1995; Herbst 2001) as previous estimates were done for lakes dominated mainly by sulphate (Cumming and Smol 1993; Fritz et al. 1993; Wilson et al. 1994). Moreover, PCA and CA suggested that $\text{Cl}^- : \text{SO}_4^{2-}$ ratios have an influence on the composition of diatom assemblages within the studied ponds. Other factors such as depth and substrate may also have an effect on salinity optima (Williams et al. 1990). Despite the fact that our inferences work well for the studied saline fen, they should be used with caution in other locations, and further studies with more extensive sampling of ponds with different brine composition are required to develop diatom-based salinity model that can be used in whole boreal region.

2.4.3. Implications for wetland reclamation in the Athabasca Oil Sands Region

Although constructed wetlands (fens) can be hydrologically isolated from an overburden dump (Price et al. 2010), it is expected that many constructed wetlands will have deeper

groundwater input from seepage zones on tailings sand beaches that are known to have elevated salt content (Ketcheson et al. 2016). Isolated wetlands are known to be subjected predominantly to local processes in which water is added or removed from the wetland itself through surficial processes (such as precipitation, evapotranspiration, run-off) and shallow groundwater input/output (Devito et al. 2012), and it has been reported that salinity within an hydrologically isolated constructed fen is controlled by precipitation diluting shallow saline groundwater (Kessel 2016). This study suggests that wetlands (or part of the wetlands such as open water areas) that are situated within seepage zones are not only controlled by these local processes, but can also be subject to variation in regional aquifers, and thus, their salinity can be driven, in part, by saline groundwater discharge.

Given the fact that observed relations between precipitation, groundwater discharge and salinity within the boreal fen are not straightforward, different salinity responses to the climate change within isolated and non-isolated constructed wetland can be expected. Future climatic changes in the AOSR will likely be associated with increases in temperature, precipitation and evapotranspiration (Ketcheson et al. 2016). Although salinity within the isolated wetlands may decline under increased precipitation, salt concentration within the wetlands located within seepage zones may rise due to intensification of saline groundwater input. This should be considered when designing the constructed wetlands because geomorphic and hydrogeological settings have to help to not only moderate regional climatic conditions (Ketcheson et al. 2016), but also to mitigate changes in saline groundwater influx. This study suggests the possible existence of precipitation threshold values that specify the amount of precipitation required for shifts in salinity levels. Determining actual levels of these thresholds under various local conditions (e.g., location, topography, substrate) can be useful for predicting the potential resilience of saline wetland ecosystems under climate change.

This study shows that connectivity to adjacent wetlands is important for explaining the spatial and temporal variations in salinity within the saline boreal fen, and influx of fresh water from surrounding wetlands may modify how fen salinity changes result from saline groundwater discharge and direct input of meteoric water. Consequently, incorporation of landscape connectivity into post-mined landscape design plans can be useful not only for maintaining water

balance of reclaimed area (Ketcheson et al. 2016), but also for salinity control that is one of the most important conditions for reclamation success.

2.5. Acknowledgements

We wish to thank Meaghan Quanz, Tristan Gingras-Hill, Adam Green, Volodymyr Sivkov and Kate Jamieson for help with core collection and field extraction, Casey Remmer and Eva Mehler for help with lab work, Johan Wiklund for ^{210}Pb dating and valuable comments, Vito Lam for water chemistry analyses, Dr. Kate Laird (Queen's University) and Dr. Sherilyn Fritz for help with diatom identification. We thank Dr. Thomas J Whitmore and Dr. Euan Reavie and anonymous reviewers for comments on an early draft of this work. Funding was provided by the Natural Science and Engineering Research Council (NSERC) of Canada, Collaborative Research and Development Program, co-funded by Suncor Energy Inc., Imperial Oil Resources Limited and Shell Canada Energy, NSERC Northern Supplement and Discovery Grants (Petronne), Northern Science Training Program (Volik, Petronne).

3. Organic matter accumulation and salinity change in open water areas within a saline boreal fen in the Athabasca Oil Sands Region, Canada

3.1. Introduction

Continental fens comprise up to 90% of western boreal peatlands (Vitt et al. 2009) and act as sinks and transformers of organic matter, water, and nutrients (Yu 2012) at the interface of terrestrial and aquatic boreal ecosystems. Since the 1960's anthropogenic impact on these peatlands has increased dramatically, especially in oil-producing Alberta where open-pit mining has destroyed thousands of hectares of the boreal landscape (Government of Alberta Energy 2017), more than 55% of which are fens (Vitt et al. 2009). Oil companies must reclaim disturbed areas to land of equivalent ecological capacity, and about 30% of the post-mined area must be reclaimed back to boreal wetlands (Alberta Environment and Parks 2015). Thus, the construction of boreal fens, the dominant type of wetlands in Alberta (Vitt et al. 2009), is crucial for reclamation success. Current attempts to construct self-sustaining boreal fens (e.g., Price et al. 2010) have faced several challenges with salinization being the most significant (Vitt and House 2015). Increased salt inputs from saline tailings and reclamation materials hinder establishment of moss-dominated fens, making naturally graminoid-dominated saline fens potential models for reclamation (Wells and Price 2015a; Environment and Parks 2015). The ability of ecosystems to accumulate organic matter (OM) is one of the key aspects of ecological capacity and a commonly used metric for assessing the success of peatland restoration or reclamation projects (Wortley et al. 2013). Therefore, it is relevant and timely to determine organic matter accumulation rates in naturally saline fens that can be useful for establishing targets for reclamation. Accumulation of OM within open water areas (ponds) is of particular interest because ponds compose a notable part of saline fens, (Wells and Price 2015a), and understanding the role of ponds in the OM storage in natural saline fens is necessary for an appropriate estimation of OM accumulation potential of constructed saline fens.

Saline fens are dynamic systems, and the reconstruction of past salinity within open water areas in a saline boreal fen (known as Saline Fen) situated in the Athabasca Oil Sands Region using diatom-based transfer function has revealed notable variation in salinity during the last ~100 years (Volik et al. 2017). Given that increases in salinity can affect plant productivity and microbial productivity (Herbert et al. 2015), OM accumulation in open water areas within the fen

may be expected to change in response to salinity fluctuations. A better understanding of the relationships between temporal changes in water salinity and OM accumulation in saline fens can be useful for prediction of constructed fen resilience under future environmental changes (e.g., climate warming) and salinity variation. In addition, estimation of OM accumulation rates under different salinity levels can be helpful for defining acceptable salinity ranges that will not hinder OM accumulation within constructed saline fens.

OM deposition in waterbodies is tightly connected to water depth and productivity of aquatic and adjacent terrestrial plant assemblages (Meyers and Ishiwatari 1995) that can complicate relations between OM accumulation rate and salinity. Consequently, water level fluctuation and type of vegetation in and near the waterbody should be taken into account while looking at changes in OM deposition with respect to salinity. Information on past local vegetation assemblages may be provided by the study of plant macrofossils such as seeds, leaves, fruits, etc.; moreover, macrofossil analysis has been widely used for reconstructing small-scale environmental changes (Mauquoy et al. 2010). This study aims to estimate the apparent organic matter accumulation rate (OMAR) in open water areas (Lager, Pilsner, and South Ponds of Saline Fen) where past salinity was reconstructed by Volik et al. (2017) and address the following questions: 1) How has OMAR changed over time? 2) Has variability in OMAR been associated with changes in diatom-inferred salinity reported by Volik et al. (2017)? 3) How have changes in OMAR been related to changes in water depth and vegetation revealed by macrofossil analysis? This paper is a part of a study on organic matter accumulation change along a salinity gradient in a saline boreal fen in the Athabasca Oil Sands Region, and results from this paper will provide insight into the role of open water areas in OM storage of the wetlands that is useful for assessment of carbon sequestration potential of constructed saline wetlands and improvement of constructed wetland design.

3.2. Materials and methods

3.2.1. Site description

The study was conducted at a saline boreal fen (further, Saline Fen) situated about 10 km south-east from Fort McMurray, Alberta (Figure 3.1). The climate of the study area was sub-humid with average January temperatures of -19 °C and July temperatures of +16.6 °C, and a

mean annual precipitation of 460 mm (Government of Canada 2017). The surface area of Saline Fen was about 27 ha, with an irregular shape and elongated northwest- southeast orientation. Electrical conductivity of shallow groundwater (<50 cm depth from the peat surface) varied from 5 mS cm⁻¹ to 120 mS cm⁻¹ (Wells and Price 2015b) while average pond water salinity ranged from 5 mS cm⁻¹ to 67 mS cm⁻¹. Surface water and groundwater were dominated by Na⁺ and Cl⁻ although Ca²⁺, Mg²⁺ and SO₄²⁻ were also present. The fen comprised a series of depressions, ridges and ponds, and the vegetation displayed a distinct pattern with ridges dominated by Baltic rush (*Juncus balticus* Willd.), sweetgrass (*Hierochloa hirta* (Schrank) Borbás), narrow reed grass (*Calamagrostis stricta* (Timm.) Koeler), and foxtail barley (*Hordeum jubatum* L.), and depressions dominated by seaside arrow grass (*Triglochin maritima* L.). In areas with the highest salinity, halophyte vegetation (e.g., sea plantain (*Plantago maritima* L.), horned seablite (*Suaeda calceoliformis* (Hook.) Moq.), and red swampfire (*Salicornia rubra* A.Nelson)) was observed. Small (0.5 m² to 1.2 ha) shallow (average depths of 0.4–0.5 m) ponds occupied about 19% of the fen and were situated predominantly in the southern and central parts (Wells and Price 2015a; 2015b). Most of the large ponds had irregular shape while small ponds were circular-shaped and located in deep depressions with steep margins. The majority of the ponds had semi-permanent features and was dry during late summer.

OMAR was assessed in Lager, Pilsner and South Ponds. Lager Pond covered ~0.95 ha and had average depth of ~0.5 m. It had irregular shape with an elongated embayment in the southern part. This permanent pond had an average salinity of 9 ppt and average pH of 8. While macrophytes (*Typha angustifolia* L., *Schoenoplectus* spp., and *Carex* spp.) grew intensively along the perimeter of the pond, the main axis of the pond was lacking aquatic vegetation. Pilsner Pond had an area of 0.13 ha and average depth of ~0.45 m, and had a segmented appearance with several round-shaped embayments. Nearshore areas of the pond dried out during late summer. The average salinity of the pond was about 16 ppt and average pH was 6. The major part of the pond was lacking aquatic vegetation although *Potamogeton* spp. sporadically occupied embayments. South Pond had area of 1.2 ha and average depth of ~0.43 m. It had an elongated shape with a round embayment in the northern part. The pond had semi-permanent features, and water depth near the shore dropped to zero during late summer. The average salinity of the pond was about 19 ppt and average pH is 7.5. The south-eastern shore of the pond was occupied by *Schoenoplectus* spp. and *Carex* spp. Emergent macrophytes were rare

along the north-western part of the pond. *Potamogeton* spp. were common in the northern part of the pond. An extensive brown-green microbial mat covered the majority of the bottom of South Pond.

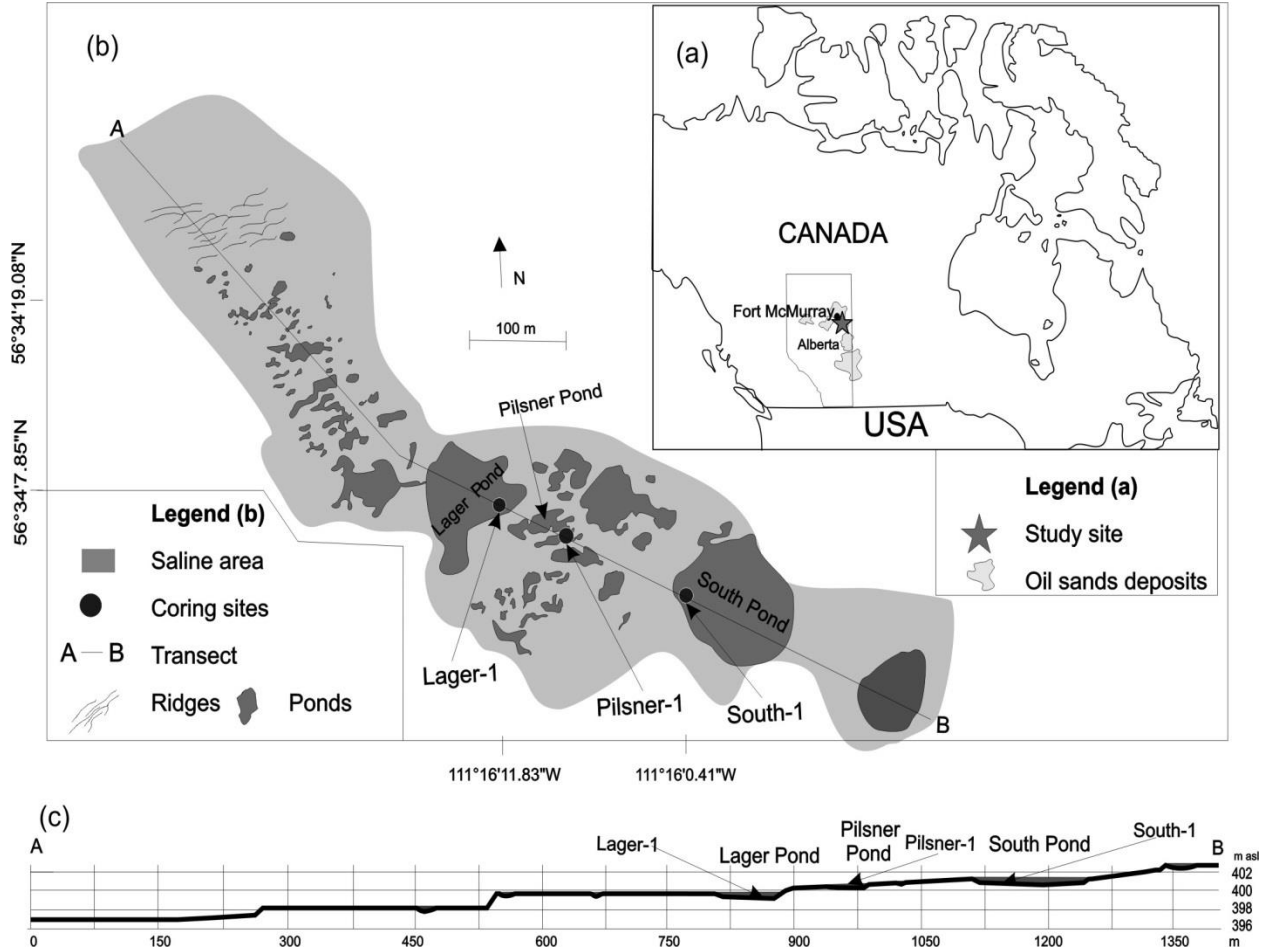


Figure 3.1. (a) regional map showing the location of the study site within Alberta, Canada; (b) map of the study site, including locations of sediment cores; (c) cross-section of the study site along A–B transect (shown on Figure 3.1(b)) including locations of sediment cores

3.2.2. Sediment analyses

Estimation of OMAR was performed on sediment cores Lager-1, Pilsner-1 and South-1 that were taken from Lager, Pilsner, and South Ponds, respectively (core locations, core lengths, coring details are in Figure 3.1 (c), Table 3.1, and Volik et al. (2017)). The cores were extruded and sectioned into 1-cm increments in the field and refrigerated at 4°C until further processing.

Table 3.1. Summary of core details (from Volik et al. 2017)

	Lager Pond	Pilsner Pond	South Pond
Core name	Lager-1	Pilsner-1	South-1
Core length, cm	31 (only upper 22 cm is used for this study)	41 (only upper 28 cm is used for this study)	43(only upper 28 cm is used for this study)
Coring site coordinates	56°34'7.85"N 111°16'11.83"W	56°34'6.53"N 111°16'7.56"W	56°34'3.46"N 111°16'0.41"W
Coring date	15 Jun 2014	13 May 2015	13 May 2015
Coring device	plastic tube (diameter 8.5 cm) pushed into sediments	Maxi-Glew gravity corer	Maxi-Glew gravity corer
Total number of subsamples:			
for LOI	23	25	29
for dating	14	15	17
for diatom analysis	12	25	15
for macrofossil analysis	12	13	15

Continuous subsamples of 1 cm³ at 1-centimeter resolution were taken and processed for loss-on-ignition (LOI) following Heiri et al. (2001) to estimate moisture, organic matter, carbonate and mineral matter in Lager-1, Pilsner-1 and South-1. Continuous sediment subsamples at 1-centimeter resolution (for upper 5 cm of all core) and at 2-centimeter resolution (below 5 cm) were taken from all three core to establish core chronology using measurements of ²¹⁰Pb, ²¹⁴Bi, ¹³⁷Cs activities by gamma ray spectroscopy in the WATER Lab (Department of Biology, University of Waterloo) (see Volik et al. 2017 for details). A constant rate of supply model was used to determine the age of the sediments and sediment accumulation rate (\pm standard deviation) (SAR) (Appleby and Oldfield 1978). Organic matter accumulation rate (\pm standard deviation) (OMAR) was calculated as a product of sediment accumulation rate and the organic matter content (OM) in each sample:

$$\text{OMAR}=\text{SAR}\times\text{OM} \quad (3.1)$$

For diatom analysis, subsamples of 0.2–0.3 g were taken and processed for slide preparation following the methods of Battarbee et al. (2001). Continuous subsamples at 2-centimeter resolution were taken from cores Lager-1 and South-4. Because the bottom part of core Pilsner-1 was composed of coarse peaty gyttja that could be potentially barren of diatoms, this core was subsampled at 1-cm increments to ensure enough samples were obtained for salinity reconstruction (see Volik et al. 2017 for details). Salinity reconstruction was performed using weighted-averaging transfer functions based on diatoms and an environmental dataset from 32 saline boreal ponds (see Volik et al. 2017 for details). The diatom-based salinity model was developed following method of Cumming and Smol (1993) and Wilson et al. (1994).

In addition, continuous subsamples of 5 cm³ (measured by water displacement) at 2-centimeter resolution were taken from all three cores for macrofossil analyses. Individual samples were gently washed through a 125 µm sieve, and identification and counting of plant macrofossils in each sample were conducted at x10 magnification. Following the method of Hughes and Barber (2003), all macrofossil remains in each sample were counted using a 100-cell grid graticule as a quadrat, using a five-point scale of abundance (1= rare, 2 = occasional, 3 = frequent, 4 = very frequent and 5 = abundant). Macrofossil diagrams were made using C2 by Juggins (2011).

3.2.3. *Statistical analyses*

Relations between diatom-inferred (DI) salinity and OMAR were explored using Pearson linear correlation between all obtained values of DI-salinity and OMAR for each core. Due to a skewed distribution, all values were log transformed before statistical analyses. All statistical analyses were performed in PAST 3.06 (Hammer et al. 2001).

3.3. Results

Detailed description, chronology and salinity reconstruction for cores Lager-1, Pilsner-1, and South-1 have been presented in Volik et al. (2017).

3.3.1. *Chronology, sediment core lithology, OMAR change, and macrofossil assemblages*

Age models (Figure 3.2) for all three cores were derived by interpretation of ²¹⁰Pb and ²¹⁴Bi activity profiles. Strong ($r>0.85$) and significant ($p<0.05$) correlation between log-

unsupported ^{210}Pb activity and cumulative dry mass was observed in all three cores, suggesting relatively constant sedimentation rates and negligible sediment mixing. A discrepancy between ^{137}Cs and ^{10}Pb activity profiles was found, and it was attributed to the higher mobility of ^{137}Cs in organic-rich saline environment (see Volik et al. (2017) for details).

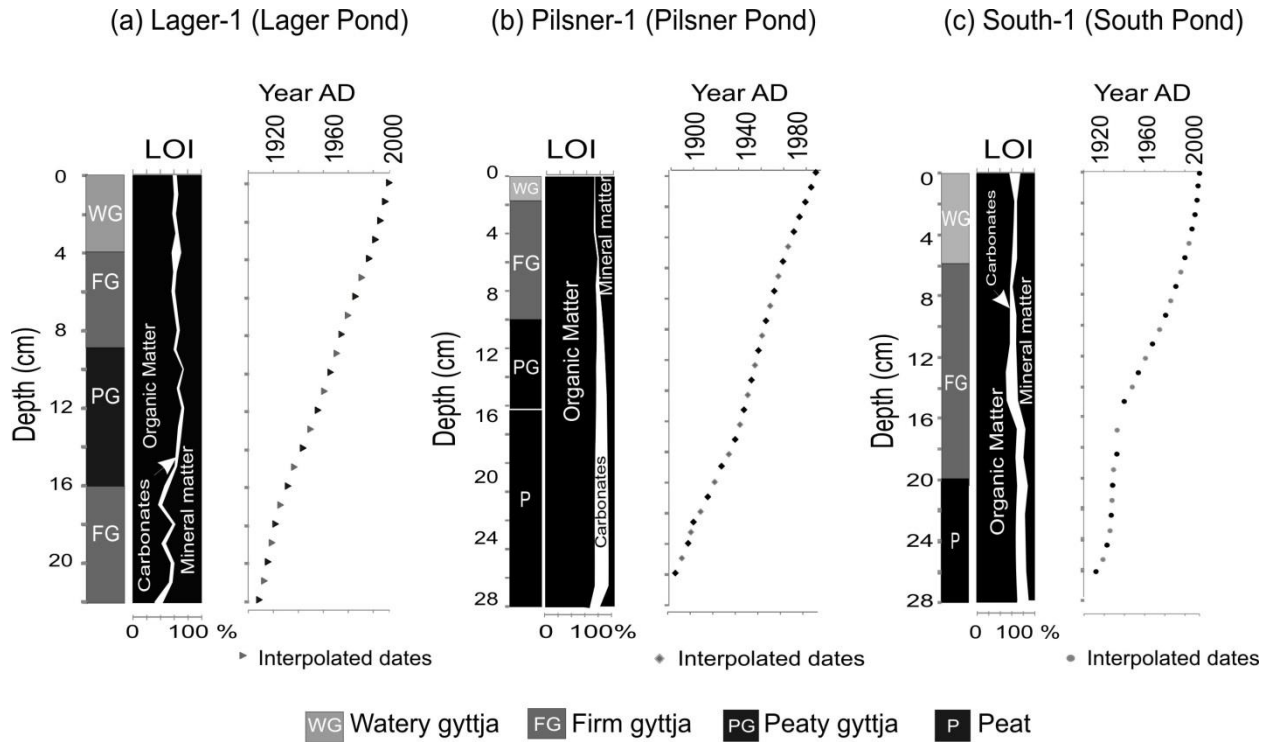


Figure 3.2. Lithology, chemical properties, and age-depth models of cores Lager-1 (a), Pilsner-1 (b), South-1 (c)

The bottom part (22–16 cm; deposited ~AD 1909–1932) of core Lager-1 was composed of firm gyttja with water content of $72.0 \pm 6.1\%$, organic matter content of $46.6 \pm 9.8\%$, mineral content of $47.2 \pm 8.1\%$, and carbonate content of $6.1 \pm 2.2\%$ (Figure 3.2(a)). This part of the core was characterized by the highest OM concentration (mean $0.23 \pm 0.3 \text{ g cm}^{-3}$), SAR (mean $294 \pm 84 \text{ g m}^2 \text{ yr}^{-1}$), and OMAR (mean $38 \pm 13 \text{ g m}^2 \text{ yr}^{-1}$) (Figure 3.3). Gyttja contained abundant unidentifiable debris, but rare remains of *Schoenoplectus* spp. and *Potamogeton* spp. were present (Figure 3.3). Above 16 cm, the core consisted of peaty gyttja (16–9 cm), firm gyttja (9–4 cm) and watery gyttja (4–0 cm) that had relatively similar water content (mean $87.0 \pm 1.0\%$), organic matter content (mean $61.7 \pm 4.8\%$), mineral content ($32.8 \pm 4.0\%$), and carbonate content (mean $5.4 \pm 2.3\%$) (Figure 3.2(a)). Mean OM concentration, SAR and OMAR were $0.13 \pm 0.02 \text{ g}$

cm⁻³, 36 ±11 g m² yr⁻¹, and 8±1 g m² yr⁻¹, respectively (Figure 3.3). Although plant remains were mostly unidentifiable in this portion of the core, abundant remains of filamentous cyanobacteria were found at 14–8 cm (dated to 1944–1975 AD) (Figure 3.3).

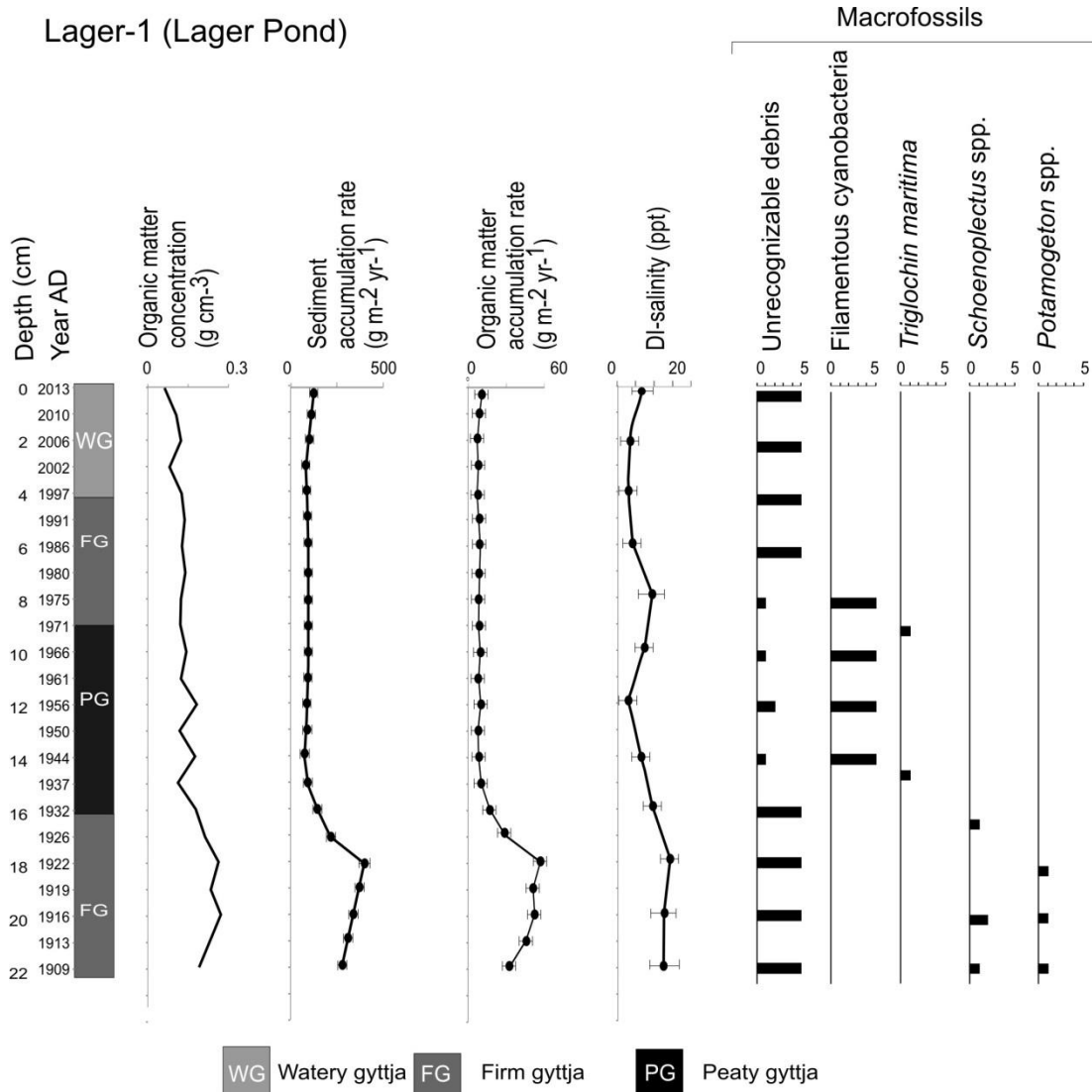


Figure 3.3. Organic matter concentration, sediment and organic matter accumulation rates, diatom-inferred (DI) salinity (from Volik et al. 2017), and macrofossil assemblages in core Lager-1

In core Pilsner-1, sediments below 18 cm consisted of peat (dated to 1885–1942 AD), with water content of 82.2±0.5%, organic matter content of 71.6±0.4%, mineral content of 9.8±0.9%, and carbonate content of 18.6±0.9% (Figure 3.2(b)). Peat was composed of well-

preserved stem bases of *T. maritima* and stems of *Atriplex* spp. (Figure 3.4). Mean values of OM concentration, OMAR, and SAR were $0.25 \pm 0.01 \text{ g cm}^{-3}$, $354 \pm 10 \text{ g m}^{-2} \text{ yr}^{-1}$, and $253 \pm 7 \text{ g m}^{-2} \text{ yr}^{-1}$, respectively (Figure 3.4). At 18–16 cm (dated to ~ 1942–1949 AD), a gradual transition to peaty gyttja was observed, with water content of $83.3 \pm 0.6\%$, organic matter content of $74.0 \pm 0.6\%$, mineral content of $13.8 \pm 2.5\%$, and carbonate content of $12.1 \pm 3.0\%$ (Figure 3.2b). This shift coincided with increases in OM concentration (mean $0.26 \pm 0.01 \text{ g cm}^{-3}$), SAR (mean $592 \pm 104 \text{ g m}^{-2} \text{ yr}^{-1}$), and OMAR (mean $430 \pm 80 \text{ g m}^{-2} \text{ yr}^{-1}$). Peaty gyttja contained well-preserved remains of *T. maritima* and *Schoenoplectus* spp. (Figure 3.4) Above 10 cm (dated to ~1969–2013 AD), the core was composed of gyttja with water content of $84.4 \pm 0.9\%$, organic matter content of $71.0 \pm 2.0\%$, mineral content of $25.6.8 \pm 2.6\%$, and carbonate content of $2.5 \pm 1.3\%$ (Figure 3. 2(b)). Mean OM concentration, SAR, and OMAR were $0.22 \pm 0.05 \text{ g cm}^{-3}$, $446 \pm 145 \text{ g m}^{-2} \text{ yr}^{-1}$, and $326 \pm 110 \text{ g m}^{-2} \text{ yr}^{-1}$, respectively (Figure 3.4). Gyttja contained rare remains of *Schoenoplectus* spp. and *Potamogeton* spp. (Figure 3.4)

At core South-1, sediments below 20 cm (dated to 1912–1932 AD) were composed of peat with water content of $85.2 \pm 0.4\%$, organic matter content of $67.6 \pm 1.2\%$, mineral content of $15.7 \pm 1.3\%$, and carbonate content of $16.7 \pm 1.8\%$ (Figure 3.2(c)). At 28–24 cm, OM concentration (mean $0.31 \pm 0.02 \text{ g cm}^{-3}$), SAR (mean $598 \pm 172 \text{ g m}^{-2} \text{ yr}^{-1}$), and OMAR ($401 \pm 115 \text{ g m}^{-2} \text{ yr}^{-1}$) were relatively stable, but sharp peaks in SAR ($14377 \pm 581 \text{ g m}^{-2} \text{ yr}^{-1}$) and OMAR (mean $9665 \pm 397 \text{ g m}^{-2} \text{ yr}^{-1}$) were observed at 24–20 cm (~1929–1933 AD) (Figure 3.5). This part of the core contained abundant remains of *T. maritima* and occasional stems of *Atriplex* spp., and abundant stem bases of *T. maritima* in growth position (Figure 3.5). At 20 cm, a transition from peat to gyttja was observed, with water content of $89.9 \pm 2.8\%$, organic matter content of $58.8 \pm 5.8\%$, mineral content of $29.4 \pm 5.8\%$, and carbonate content of $11.8 \pm 5.7\%$ (Figure 3.2(c)). Above 20 cm, OM concentration (mean $0.20 \pm 0.05 \text{ g cm}^{-3}$), SAR (mean $191 \pm 40 \text{ g m}^{-2} \text{ yr}^{-1}$), and OMAR ($110 \pm 30 \text{ g m}^{-2} \text{ yr}^{-1}$) were relatively stable, except the upper 4 cm of the core which was characterized by increased SAR (mean $525 \pm 169 \text{ g m}^{-2} \text{ yr}^{-1}$) and OMAR ($317 \pm 84 \text{ g m}^{-2} \text{ yr}^{-1}$) (Figure 3.5). This part of the core consisted of highly decomposed gyttja with occasional remains of *T. maritima*, *Schoenoplectus* spp. and *Potamogeton* spp. Green-coloured thin (0.5–1 cm) horizontal parallel laminae of the *microbial mats* were observed in the upper part of the core (4–0 cm; Figure 3.5).

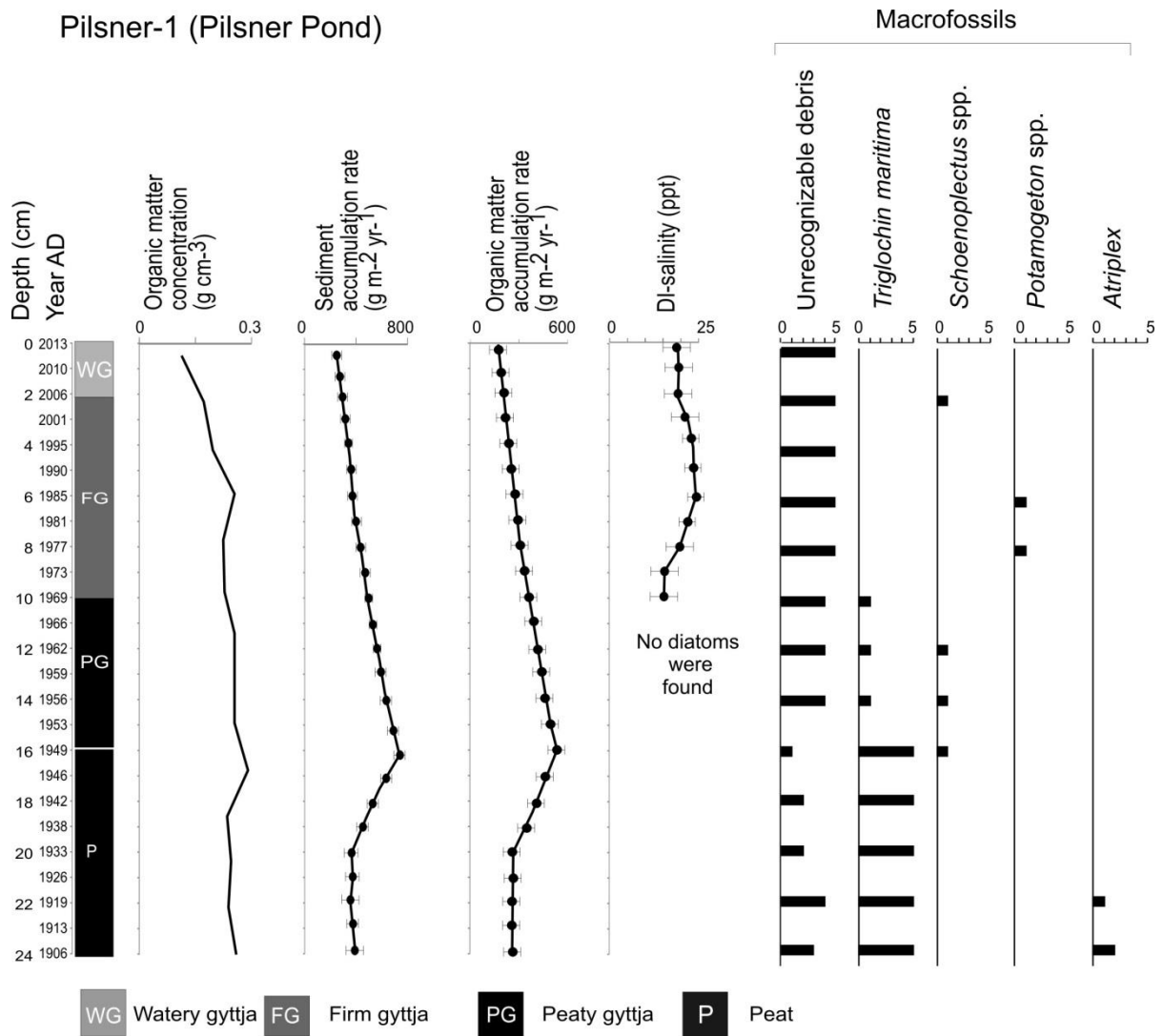


Figure 3.4. Organic matter concentration, sediment and organic matter accumulation rates, diatom-inferred (DI) salinity (from Volik et al. 2017), and macrofossil assemblages in core Pilsner-1

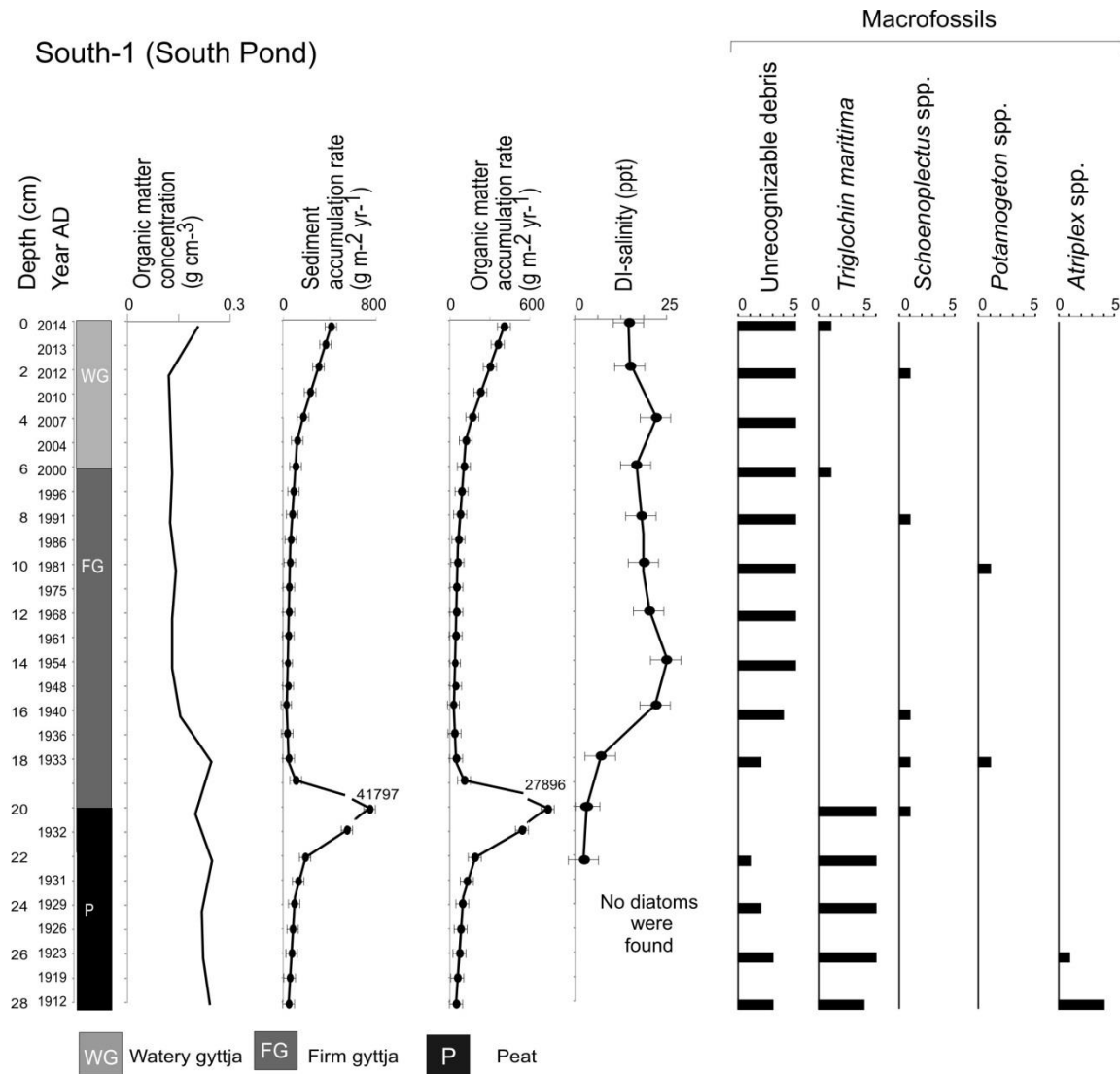


Figure 3.5. Organic matter concentration, sediment and organic matter accumulation rates, diatom-inferred (DI) salinity (from Volik et al. 2017), and macrofossil assemblages in core South-1

3.3.2. Diatom assemblages and salinity reconstruction

A total of 15 species with relative abundance more than 1% were found in the three studied cores. Diatom assemblages in all three cores were composed of taxa typical of hyposaline and mesosaline waters (*Staurosirella pinnata* (Ehrenberg) D.M.Williams & Round, *Staurosira venter* (Ehrenberg) Cleve & J.D.Möller, *Navicymbula pusilla* (Grunow) Krammer, *Halamphora coffeaeformis* (Agardh) Levkov, *Platessa salinarum* (Grunow) Lange-Bertalot,

Anomoeoneis costata (Kützing) Hustedt, *Navicula peregrina* (Ehrenberg) Kützing, *Caloneis westii* (W. Smith) Hendey, *Craticula halophila* (Grunow) D.G.Mann, *Diploneis stroemii* Hustedt, *Parlibellus cruciculus* (W. Smith) Witkowski, Lange-Bertalot & Metzeltin). Bottom parts of cores Pilsner-1 and South-1 were virtually free of diatoms (Volik et al. 2017).

To reduce biases for transfer function development and salinity reconstruction, only small shallow ponds with relatively similar ion compositions and pH, and without river inflows were included into training sets of species and environmental data (Volik et al. 2017). Small size of the training sets (32 ponds) used for transfer function development may potentially represent a bias for salinity reconstructions (Volik et al. 2017). Despite the small sample size of the training sets (32 ponds), the diatom-based salinity model produced a strong significant correlation ($r > 0.9$, $p < 0.05$) between DI- salinity and average measured salinity in the studied ponds. Moreover, DI-salinities for studied ponds in 2012 were very close to what was observed in the field in summer 2012 by Wells (2014). As revealed by measurements of squared chord distance, approximately 90% of diatom assemblages from fossil samples had analogs in the modern training set.

3.3.3. DI-salinity and OMAR relations

In core Lager-1, the correlation between DI-salinity and OMAR was strongly positive and significant ($r = 0.77$, $r^2 = 0.60$, $p < 0.05$) (Figure 3.6(a)). The correlation between DI-salinity and OMAR in core Pilsner-1 was weak and insignificant ($r = -0.34$, $r^2 = 0.12$, $p > 0.05$) (Figure 3.6(b)). Core South-1 was characterized by strong and significant negative ($r = -0.97$, $r^2 = 0.93$, $p < 0.05$) (Figure 3.6(c)) correlation between DI-salinity and OMAR.

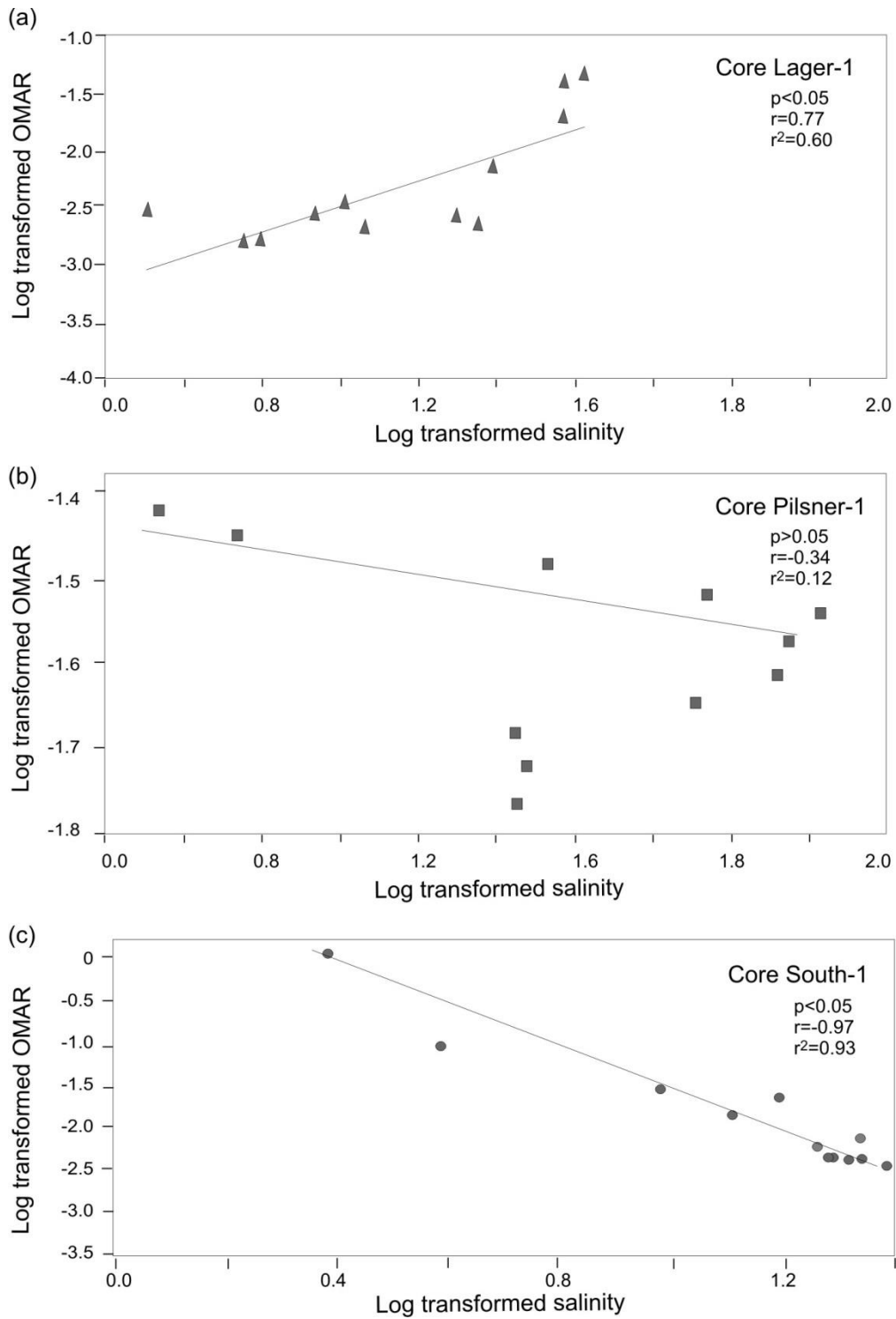


Figure 3.6. The relationship between organic matter accumulation rate and diatom-inferred salinity in cores Lager-1 (a), Pilsner-1 (b), and South-1 (c)

3.4. Discussion

3.4.1. Salinity change and OM accumulation

Open water areas (ponds) are integral parts of saline boreal fens because they are hydrologically connected with the surrounding peatlands (Wells and Price 2015a, 2015b), and play an important hydrogeochemical role in the pond-peatland system similarly to other shallow boreal ponds (Ferone and Devito 2004). Although pools and ponds within peatlands can act as sources of CO₂ (Hamilton et al. 1994; Waddington and Roulet 2000), our study has shown that open water areas within a saline boreal fen can accumulate OM at the rates comparable to boreal and tundra shallow lakes and ponds. The mean organic content (as inferred from LOI) of the cores from studied ponds is 62.8±9.8% (Volik et al. 2017), which is higher than what has been reported for Alberta lakes (55.4%) (Campbell et al. 2000). Median OMAR in Pilsner and South Ponds (288 and 194 C g m⁻² yr⁻¹, respectively) are higher than in boreal and tundra ponds and shallow lakes that can accumulate from 7 to 72 C g m⁻² yr⁻¹ (e.g., Campbell et al. 2000; Dean 1999; Macrae et al. 2004). In contrast, Lager Pond is characterized by lower OMAR with median value of 8 g m⁻² yr⁻¹. High OMAR in Pilsner and South Ponds can be attributed to the high productivity of the ponds as the mean chlorophyll-*a* concentration of 65 µg L⁻¹ in studied ponds that has been reported by Volik et al. (2017) is much higher than what has been observed in eutrophic boreal shallow lakes (e.g., Bayley and Prather 2003). In addition, studied sediment cores contain sediments with abundant poorly decomposed plant remains (Figures 3.4 and 3.5) suggesting high inputs of organic matter from terrestrial vegetation and low decay rates associated with saline anoxic conditions. Low OMAR in Lager Pond seems to be associated with a low sediment accumulation rate and high decomposition of sediments as inferred from poorly preserved macrofossils in core Lager-1 (Figure 3.3). Median OMAR (181 g m⁻² yr⁻¹) of all studied ponds suggests that ponds situated within saline boreal fens can accumulate OM similarly to freshwater boreal ponds, and the estimated salinity levels (3–21 ppt) did not severely affect OMAR. Indeed, the highest OMAR in the ponds was associated with DI-salinity of 10–15 ppt (Figures. 3.3–3.5); moreover, Lager Pond has been characterized by lower DI-salinity than Pilsner and South Pond over last 100 years and has had the lowest OM accumulation rates.

Although salinity can affect wetland productivity (Cooper and Wissel 2012), and thus can affect OM accumulation, results here show that salinity was not the main driver of changes in

OMAR in the studied ponds. Weak and strong, positive and negative correlations between OMAR and DI-salinity (Figure 3.6) were observed here suggesting that relations between salinity and OMAR are not straightforward. No strong correlation between OMAR and DI-salinity was found in core Pilsner-1. A strong negative correlation between OMAR and DI-salinity in core South-1 was consistent with several studies (Wollheim and Lovvorn 1996; Herbst 2001; Cooper and Wissel 2012) that have shown that waterbody productivity, and thus OM accumulation, tends to decline under increasing salinity. However, a strong positive correlation between OMAR and DI-salinity was found in core Lager-1, and a similar positive correlation has been found in Mono Lake (California, USA) where rises in OMAR were attributed to decreased decomposition of organic matter by benthic microbial assemblages under increased salinity (Jellison et al. 1996). Consequently, it can be assumed that OMAR in studied ponds could change in conjunction with changes in salinity, but links between OM accumulation and salinity level are complicated by other factors.

Distinct differences between rates of OM accumulation estimated for peaty and gyttja samples (Figures 3.3–3.5) suggests that OMAR was mainly influenced by water level and type of primary producers. Our paleoecological data suggests that before 1953 the basin of Pilsner Pond was occupied by terrestrial vegetation and accumulated peat; similar conditions were observed in South Pond before 1932. Shifts from macrofossil assemblages dominated by *Atriplex*, which has moderate tolerance to waterlogged conditions (Asad 2002), to assemblages dominated by *waterlogging-tolerant T. maritima* (Fogel et al. 2004) and aquatic *Schoenoplectus* spp. (Figure 3.5) record a rise in water level and transition from peatland to inundated pond-like areas. Currently, such inundated depressions vegetated with *T. maritima* are abundant in the northern part of Saline. Notably, in the core from South Pond, diatoms were found in poorly decomposed peat sediments dated to 1931–1932 indicating relatively high and stable water levels that allow the survival of algae, while in Pilsner Pond fluctuating water levels in 1953–1966, recorded in the sediment core by peaty gyttja, hindered the expansion of diatoms. During the transition from peatland to inundated areas, the water levels in the Pilsner and South Pond basins were low enough to allow the existence of terrestrial peatforming vegetation, but high enough to create anoxic conditions. Consequently, the input of terrestrial vegetation composed of relatively to decay-resistant high-molecular-weight compounds rich in C (Meyers and Ishiwatari 1993) coupled with waterlogging resulted in the highest OMAR in 1946–1953 and 1931–1933 in

Pilsner and South Ponds, respectively. The increase in water level and transition to open waterbody stage is recorded by the presence of macrophytes (*Potamogeton* spp.) and diatoms, and disappearance of terrestrial vegetation in sediment cores (Figures 3.4, 3.5). This shift caused a decrease in OMAR as Pilsner and South Ponds became dominated by aquatic vegetation and algae that are known to be composed of less decay-resistant proteins with low-molecular-weight compounds high in N (Meyers and Ishiwatari 1993).

Studied ponds are sensitive to changes in precipitation, and precipitation can control pond salinity by dilution of salt content in water or by recharge of the saline aquifer (Volik et al. 2017). However, no relations between OMAR, precipitation, and cumulative departure from long-term mean precipitation (CDLM) in the Fort McMurray area (Volik et al. 2017) was found. This contrasts with Canada's Boreal Shield ecozone, where increases in precipitation and snowmelt intensify surface runoff to lakes and stimulate organic matter accumulation (Schindler et al. 1996). Within the Western Boreal Plains, rises in precipitation do not cause much increases in water input from the watershed into shallow lakes due to low topography, high evapotranspiration and high water storage capacity (Ferone and Devito 2004; Cobbaert et al. 2014). Consequently, increases in precipitation do not lead to increases in nutrient and organic matter input to the lakes (Sass et al. 2008), and OMAR in studied ponds is not directly influenced by precipitation. However, fluctuations in precipitation can cause shifts in the regime of shallow lakes (Cobbaert et al. 2014), and changes in OMAR and macrofossil assemblages in the core from Lager Pond reveal that pond regimes (macrophyte or algae-dominated) have an effect on OM accumulation. The highest OMAR was during 1909–1932 when Lager Pond had the highest salinity (15–16 ppt) and was vegetated with macrophytes as recorded by remains of *Potamogeton* spp. and *Schoenoplectus* spp. in the sediment core (Figure 3.3). After 1932, a shift to algae-dominated regime is evident from increase in total diatom concentration, coupled with abundance of remains of filamentous cyanobacteria and disappearance of *Potamogeton* spp. and *Schoenoplectus* spp. in sediments dated to 1932–1975. During that period OMAR was low and relatively stable despite salinity change.

3.4.2. Implications for fen construction in the Athabasca Oil Sands Region

An abundance of shallow small (up to 1.2 ha) ponds is a distinct feature of saline boreal fens that were suggested as appropriate natural analogs for landscape reclamation in the

Athabasca Oil Sands Region (AOSR) (Wells and Price 2015a). Our study shows that saline ponds located within the fens have accumulated organic matter at the rate comparable to boreal and subarctic freshwater ponds. Moreover, salinity up to 20 ppt did not reduce the potential to accumulate OM in saline ponds.

OMAR in studied ponds seem to be driven by factors that control decomposition rather than primary productivity, and positive relations between OMAR and salinity probably result from decreased mineralization due to the decline in microbial activity associated with the increase in osmotic value (Setia et al. 2011; Brouns et al. 2014). Moreover, several studies (Cebrian and Duarte 1995; Kortelainen et al. 2013) have shown that controls on decay have stronger impact on organic carbon sequestration than controls on productivity. Thus, reclamation efforts should focus on decreasing decomposition rates to achieve the highest OMAR in constructed ponds. In particular, attention should be paid to vegetation within riparian areas around ponds as litter quality has strong effect on decay rates (Vitt et al. 2009), and the input of terrestrial organic matter into waterbodies has an impact on stratification, light penetration, and oxygen availability driving decomposition (del Giorgio et al. 1997; Bastviken et al. 2004; Kankaala et al. 2006; Juutinen et al. 2009; Anas et al. 2015). Resistance to decomposition of each species should be taken into account and careful consideration made towards the choice of plant species to be plated around constructed ponds. In studied cores, high OMAR was associated with samples containing abundant remains of *T. maritima* and *Schoenoplectus* spp. This is in agreement with findings of Trites and Bayley (2009a) suggesting that *T. maritima* and some species of genus *Schoenoplectus* have slower decomposition rates, and thus can be suggested for planting within constructed saline fens.

Pond regime (macrophyte-dominated or algae-dominated) has had an influence on the rates of OM accumulation and should be taken into account while developing constructed pond design. Changes in macrofossil and diatom assemblages in studied cores recorded shifts in regimes of the ponds that were related to variation in OMAR; macrophyte-dominated regime was associated with higher OMAR while decline in OMAR under algae-dominated regime was found. Thus, planting macrophytes such as *Potamogeton* spp. can help increase OM accumulation in constructed ponds. However, open water areas within western boreal forests are characterized by high evaporative losses (Devito et al. 2012), and increased macrophyte cover

can lead to more intense evapotranspiration and reduction of water volume in waterbodies (Xu et al. 2014). Given this, rational macrophyte control through planting and harvest can be crucial for OM accumulation in constructed ponds.

Our estimations of OMAR were done for naturally saline ponds dominated by chlorides (Volik et al. 2017). The observed high OMAR in studied ponds may not hold in constructed wetlands dominated by sulphates (Ketcheson et al. 2016). In contrast to chlorides, sulphates are known to stimulate anaerobic decomposition (Canavan et al. 2006; Brouns et al. 2014), and thus a better understanding of the effects of brine composition and total salt concentration on microbial activity in pond sediments is necessary to predict OMAR in constructed waterbodies. In addition, restored fens are known to have altered nutrient turnover rates (Cabezas et al. 2014), and long-term carbon cycling in boreal lakes is driven by nitrogen (Kortelainen et al. 2013), so in-depth studies revealing differences in N-cycling within natural and constructed saline fens is necessary to anticipate changes in OMAR in constructed ponds.

3.5. Conclusion

This study of OM accumulation in open-water areas within a saline boreal fen has showed that although fluctuations in salinity is linked to changes in OMAR in studied ponds, a stronger influence on OM accumulation was observed by water level, type of primary producers and pond regime. The highest OMAR was found during a shift from terrestrial to open-water areas, which can be attributed to low decomposition rates due to high input of terrestrial plant litter, coupled with onset of anaerobic conditions. A macrophyte-dominated pond regime was characterized by higher OMAR relative to algae-dominated regime. Because OMAR in the studied saline ponds seems to be more influenced by environmental variables that drive decomposition rather than by controls on primary productivity, development of a constructed fen design will require careful consideration of factors promoting low decay rates. In particular, attention should be paid to vegetation within open-water areas and within riparian areas around ponds as litter quality has strong effect on the decomposition rates. The observed relation between OMAR and environmental factors in natural chloride-dominated saline wetlands may not hold in constructed sulphate-dominated fens, and better understanding of the effect of the chloride to sulphate ratio on microbial activity and OM accumulation in saline ponds may be required.

3.6. Acknowledgements

We wish to thank Matthew Elmes, Meaghan Quanz, Volodymyr Sivkov and Kate Jamieson for help with core collection and field extraction; Jessica Williamson, Casey Remmer and Eva Mehler for help with lab work; Johan Wiklund for Pb²¹⁰ dating and valuable comments. Funding provided by the Natural Science and Engineering Research Council (NSERC) of Canada, Collaborative Research and Development Program, co-funded by Suncor, Energy Inc., Imperial Oil Resources Limited and Shell Canada Energy (Price, Petrone); NSERC Discovery Grant Program (Petrone, Price, Macrae); NSERC Northern Supplement (Petrone); and Northern Studies Training Program (Volik).

4. Impact of salinity, hydrology and vegetation on long-term carbon accumulation in a saline boreal peatland and its implication for peatland reclamation in the Athabasca Oil Sands Region

4.1. Introduction

Growing anthropogenic pressure resulting in the disappearance and degradation of boreal peatlands has been documented over the last few decades (Turetsky 2002; Turetsky and St. Louis 2006). One of the biggest disturbances causing the total transformation of peatland ecosystems in the boreal region is surface mining of oil sands in north-eastern Alberta. Since the beginning of commercial development of the Athabasca Oil Sands Region in the 1960–70's, more than 700 km² of natural landscapes have been stripped up to 100 m deep to access oil bearing sands (Alberta Environment 2008). After ceasing mining operations, oil sands companies are obligated by the Government of Alberta to reclaim disturbed areas to self-sustaining boreal ecosystems that have equivalent ecological capacity to the pre-disturbance systems. As peatlands occupy a considerable portion of the natural boreal landscape (Vitt et al. 2009), approximately one-third of post-mined area should be reclaimed back to wetlands for restoring pre-disturbance landscape diversity (Alberta Environment 2008).

Peatland reclamation is a complex and multifaceted process with unpredictable final outcomes over shorter time scales (Ketcheson et al. 2016). Moreover, salinization has become an additional drawback for reclamation as open-pit mining disturbed originally isolated saline rocks overlaying oil sands (Purdy et al. 2005) and tailings associated with bitumen extraction have high salt contents. Further, the use of these saline tailings and rock mixture for peatland construction has caused excessive salt input into manmade ecosystems, and the first attempts to build peatlands (fens) have been affected by salinization (Biagi 2015; Kessel 2016; Simhayov 2017). Given the scale of potential salinization in constructed wetlands, naturally saline wetlands have been considered as possible models for reconstruction (Purdy et al. 2005; Wells and Price 2015a), and recently saline fens have been recognized as targets for reclamation (Environment and Parks 2015).

Despite current research attempts to understand saline peatland hydrology, geochemistry, and ecology (Purdy et al. 2005; Trites and Bayley 2009a; 2009b; Wells and Price 2015a; 2015b; Phillips et al. 2016; Wells and Price 2015a), geochemistry (Steward and Lemay 2011; Scarlett

and Price 2013; Wells and Price 2015b), and vegetation (Purdy et al. 2005; Trites and Bayley 2009a; 2009b), knowledge about saline fens is still limited, especially in terms of their carbon storage function. A study by Trites and Bayley (2009b) focused on the current production and decomposition rates of naturally saline and industrial wetlands and show an ability of natural saline peatlands to accumulate organic matter. However, no research has been carried out on the long-term rates and patterns of carbon accumulation with respect to climatic variability and salinity gradients.

There are several ways of estimating the long-term rate of carbon accumulation (Yu 2012), and long-term apparent rate of carbon accumulation (LARCA (Yu 2006) or LORCA (Clymo et al. 1998)) is one of the measures that has been widely used to characterized carbon accumulation in freshwater peatlands in the boreal region (Yu 2012). LARCA can be calculated by dividing total carbon content in a peat core by core age (single age point) (Tolonen and Turunen 1996) or by using multiple age determinations and carbon content measurements throughout a peat core (Yu 2012). LARCA is an apparent value because it does not account peat decomposition within a peat column, and it differs from the true or actual carbon accumulation rate (TRACA or ARCA (Clymo et al 1998)) that can only be calculated using peat accumulation models considering organic matter addition rate and the decay coefficient (Yu 2012). Despite such limitation, LARCA, coupled with paleoecological approach can help to recognize links between the carbon storage function of peatland ecosystems and environmental changes (e.g., Campbell et al. 2000; Vitt et al. 2000; Yu 2006; Roulet et al. 2007; Holmquist and MacDonald 2014; Yu et al. 2014).

Understanding of long-term carbon accumulation in saline peatlands is important for several reasons. First, although some mosses can tolerate elevated salt contents (up to 500 mg L⁻¹ of NaCl and 400 mg L⁻¹ of Na₂SO₄ (Pouliot et al. 2013)), in general, salinization hinders moss growth. As a result, an establishment of moss-dominated peatlands in the post-mined landscape will be challenging, and the usage of salt-tolerant wetland species will be necessary to construct sustainable wetland communities (Trites and Bayley 2009b). Such a shift from more recalcitrant moss assemblages (Vitt et al. 2009) to more labile graminoid assemblages (Trites and Bayley 2009a) can significantly affect peat accumulation in constructed wetlands (Chymko 2000; Rooney et al. 2012), and comparison of carbon accumulation rates in freshwater moss-dominated fens and saline graminoid-dominated fens is necessary to assess possible reduction in

carbon sequestration in constructed saline fens. Moreover, a better understanding of the controls on long-term carbon storage in naturally saline graminoid-dominated peatlands is required for establishing environmental conditions (i.e., topography, water table depth) that can compensate the increased decomposition rate and promote peat accumulation. Second, there is growing concern about peatland response to global climate change and anthropogenic pressure (Turetsky and Louis 2006; Bu et al. 2011), so understanding millennia-scale dynamics of carbon accumulation in naturally saline peatlands under various environmental conditions is essential for predicting future feedbacks of constructed saline peatlands to natural and human-induced disturbances. Finally, although saline fens were considered as targets for reclamation (Environment and Parks 2015), the maximum acceptable salinity level that would not severely affect long-term carbon accumulation at constructed saline wetlands is not yet known. Thus, an understanding of variations in carbon accumulation associated with differences in levels of dissolved salts in naturally saline fens should provide an answer to these questions.

In this study, we assessed the long-term apparent rate of carbon accumulation (LARCA) within a naturally saline fen situated in the Athabasca Oil Sands Region to identify temporal patterns in carbon accumulation with respect to salinity. We used plant macrofossil analysis to reconstruct paleoenvironmental conditions of the fen that helped us to infer a role of salinity, hydrology and vegetation in determining the rate of carbon accumulation. Current vegetation – hydrology – soil relationships along a salinity gradient were assessed for a better understanding of links between salinity levels, hydrological conditions and vegetation assemblages as well as for the understanding of ecological preferences of plant species that is crucial for paleoecological reconstruction. The following questions are addressed in this manuscript: 1) What is the degree of variability in carbon accumulation rates in less and more saline parts of a saline fen, and the roles of hydrology and vegetation in governing the changes in carbon accumulation? 2) How does carbon accumulation rate in a saline fen differ from the rates in freshwater western boreal fens? 3) What environmental settings are the most appropriate for long-term carbon storage under saline conditions and can these be considered future habitat goals for fen reclamation?

4.2. Methods

4.2.1. *Study site*

Saline fen (known as Saline Fen) is situated approximately 10 km south of Fort McMurray, Alberta (56°34'28.84" N, 111°16'38.39" W) (Figure 4.1) within the Salt Creek watershed, which is a part of the McMurray lowlands subdivision of the Dover Plains (Andriashek 2003). The region has a subhumid continental climate with mean annual precipitation of ~460 mm and mean annual temperature of 0.2°C (Environment Canada 2015). Saline Fen covers ~27 ha and has an irregular shape and elongated northwest-southeast orientation. The elevation varies from 401 m asl at the southern end to 397 m asl at the northern end (Wells and Price 2015a). The thickness of peat varies across the peatland from 1.5 m in the northern part to almost zero at the southwestern part (Wells and Price 2015a). Groundwater and surface water are dominated by Na⁺ and Cl⁻ while Ca²⁺, Mg²⁺ and SO₄²⁻ are also present; electrical conductivity of near-surface groundwater ranges from more than 60 mS cm⁻¹ in the southern part to 19 mS cm⁻¹ in the northern part (Wells and Price 2015b) (Figure 4.1(c)). pH of near-surface groundwater within the fen had a range of 6.5–7.5 (Wells and Price 2015a). The site is characterized by a well-developed ridge-depression patterned surface and by a presence of numerous shallow ponds in the southern and central parts of the peatland. Baltic rush (*Juncus balticus*), sweetgrass (*Hierochloa hirta* ssp. *arctica*), reed grass (*Calamagrostis inexpansa*), and foxtail barley (*Hordeum jubatum*) are a dominant within ridges while seaside arrow grass (*Triglochin maritima*) is the dominant species within depressions; areas with the highest salinity are occupied by halophyte vegetation (e.g., sea plantain (*Plantago maritima*), samphire (*Salicornia rubra*), horned seablite (*Suaeda calceoliformis*)).

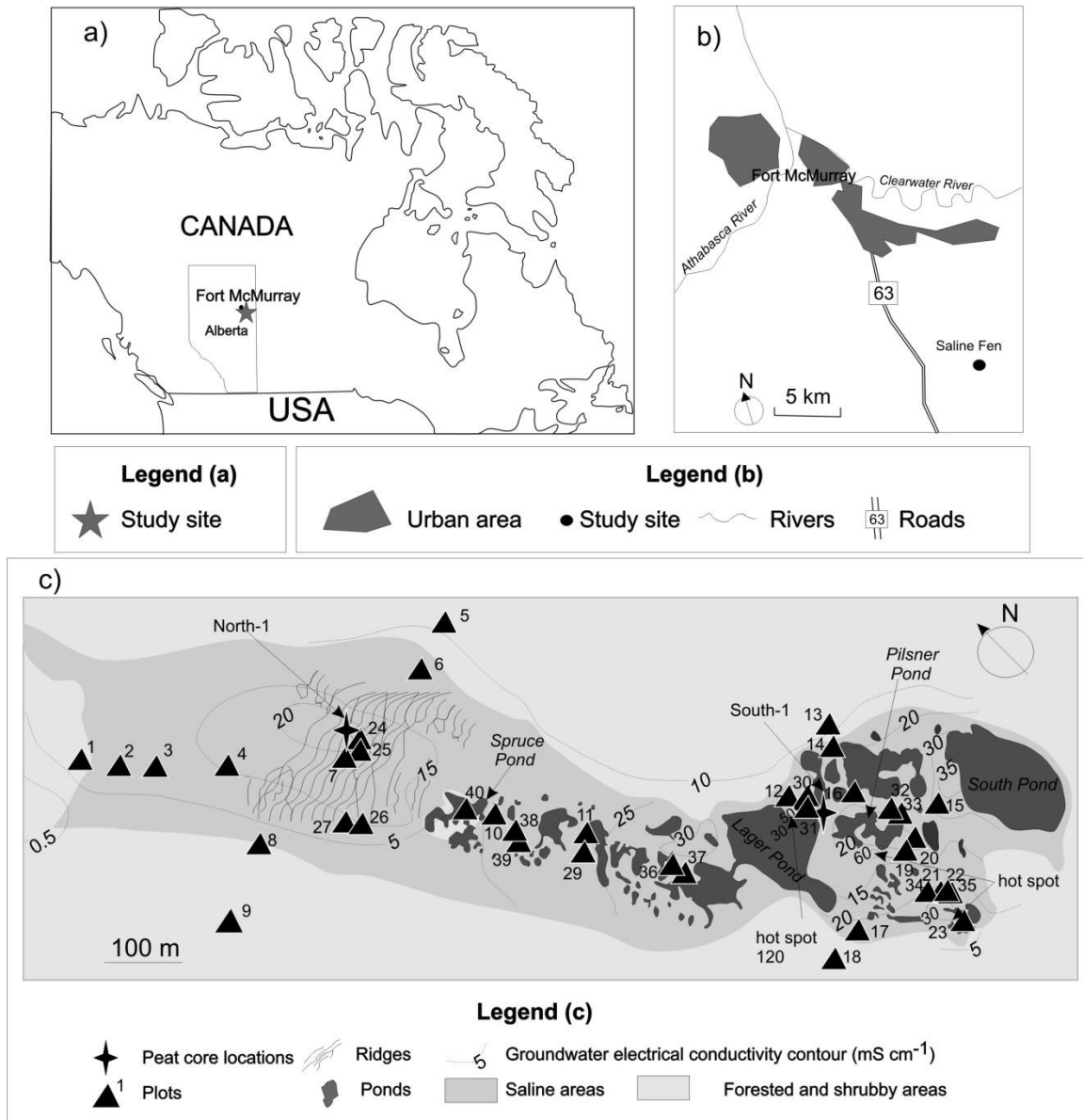


Figure 4.1 (a) regional map showing the location of the study area within Alberta; (b) map showing locations of study site near Fort McMurray, Alberta; (c) map of the study site including locations of peat cores (North-1, South-1) and vegetation plots

4.2.2. Collection of peat cores

A 128-cm core (North-1) and a 69-cm core (South-1) were collected from depression areas dominated by *T. maritima* in the northern ($56^{\circ}34'24.56''\text{N}$; $111^{\circ}16'29.57''\text{W}$) and southern ($56^{\circ}34'9.18''\text{N}$; $111^{\circ}16'10.14''\text{W}$) parts of Saline Fen respectively (Figure 4.1(c)) on August 11 2015. Both coring locations are characterized by mean water table depth of 1 cm below the soil

surface (see Appendix B and Figure 4.1 for details). The cores were taken using stainless steel tubes (wall thickness – 0.5 mm, diameter – 7.5 cm) with a sharpened edge, pushed into the peat. The tubes were transported to the laboratory and after cutting the tubes lengthwise, the cores were extracted and humification level was assessed using the von Post scale based on a squeeze test (von Post and Granlund 1926).

4.2.3. Laboratory analyses

The cores were sectioned in 1-cm intervals, and subsamples of 1 cm³ were taken every 1 cm using a 1-cm-diameter brass cylinder sampler and processed for loss on ignition (LOI) following Heiri et al. 2001). Subsamples were heated at temperatures of 90°C and 550°C for 24 and 4 hours, respectively, and dry bulk density, moisture and organic contents were estimated. Eight samples from North-1 and seven samples from South-1 were sent to A.E. Lalonde AMS Facility, University of Ottawa for radiocarbon dating (see Appendix B for details). Age – depth models for North-1 and South-1 were developed using linear interpolation between the dated samples (mid-points of the calibrated 2σ distribution range of the ¹⁴C dates).

LARCA was calculated as a product of the organic carbon content (OC) of each peat sample and the peat accumulation rate (AR) for each particular horizon derived from the age – depth curves (Yu et al. 2003; Holmquist and MacDonald 2014):

$$\text{LARCA}=\text{OC}\times\text{AR} \quad (4.1)$$

Organic carbon content (OC) was calculated as a product of organic matter content (OM) and the average carbon percent (51.8%) of peat organic matter reported from peatlands in Western Canada (Vitt et al. 2000; Yu et al. 2003; 2014):

$$\text{OC}=\text{OM}\times 0.518 \quad (4.2)$$

Although direct measurement of carbon is the most accurate way of carbon content determination (Nelson and Sommers 1996), quantification of organic carbon based on converted estimates of organic matter also can be used (Pribyl 2010). In our study, carbon content was estimated based on LOI because we followed method of Yu et al. (2003; 2014) and Yu (2006) to make our results comparable with estimations of LARCA of fresh fens in western boreal region. Moreover, because temporal changes in carbon accumulation rate rather than absolute

measurements of carbon storage are of interest here, we feel confident using a converting factor for carbon content estimation.

Samples of 5 cm³ were taken every 4 cm from each core and gently washed through a 125 µm sieve. Plant macrofossils were identified at x40 magnification using an herbarium collected at the study site and photo plates in Carrière (2002), Mauquoy et al. (2010). Macrofossils were counted at x10 magnification using a 100-cell grid graticule as a quadrat. Abundance of macrofossils in each sample was estimated as absolute number of objects, and then relative abundance was calculated. All parts of plants (leaves, stems, flowers, fruits, seeds) that belong to the same species were counted together; unrecognizable debris and roots were counted as well. Macrofossil diagrams were made using C2 by Juggins (2003).

4.2.4. Environmental and plant community data

During June – August, 2014, the vegetation – salinity – hydrology relationships were studied at 40 plot (1x1 m) along a salinity gradient (Figure 4.1(c)), and vegetation sampling was conducted in August, 2014 (all species were identified and percent cover was estimated), but only species with an abundance more than 1% in at least 2 plots were accounted for in this study. Two groups, mosses (predominantly *Tomenthypnum* sp.) and shrubs (predominantly *Salix* spp., *Betula* spp., and *Alnus* spp.), were recognized without further identification because of their absence in macrofossil records. Measurements of water table depth, soil moisture (HH2 Meter, Delta-T Devices), and temperature (at 0, 5, 10 cm) (Type K thermocouple probe and meter; HH200, Omega Scientific, USA) were taken in the field twice per month during June – August, 2014. Electrical conductivity (EC) was measured in the field by EC1:5 tests for which 1 part peat (taken from the rooting zone) was mixed with 5 parts distilled water, and the EC of the solution was tested using handheld probe (YSI ProPlus, YSI Incorporated, USA); soil EC was calculated by applying the EC1:5 conversion factor with respect to peat moisture content and texture (Rayment and Higginson 1992). Correlation between vegetation assemblages and 12 environmental variables (soil moisture (minimal, maximal, average), soil electrical conductivity (minimal, maximal, average), soil temperatures (minimal, maximal, average), and water table depth (minimal, maximal, average)) were determined using canonical correspondence analysis (CCA). Positively skewed data were log transformed, and negatively skewed data were square root transformed prior to analyses; a significance of ordination axes and individual variables was

explored using Monte Carlo permutation tests. All ordinations were performed using PAST 3.06 (Hammer et al. 2001).

4.3. Results

4.3.1. Chronology, macrofossils and long-term apparent rate of carbon accumulation

Both studied cores are composed of clay sediments and peat (see Appendix B for details). The basal peat is dated to 4590–4240 cal. yr BP in core North-1 and to 5270–4830 cal yr BP in core South-1 (Figure 4.2). The age – depth and cumulative peat mass – age models for cores North-1 and South-1 are characterized by near-concave curve and near-linear profiles, respectively (Figure 4.2). Mean LARCA of core North-1 ($29.67 \text{ gm}^{-2} \text{ yr}^{-1}$ (SD=14.53)) is higher than mean LARCA of core South-1 ($9.79 \text{ gm}^{-2} \text{ yr}^{-1}$ (SD=3.49)).

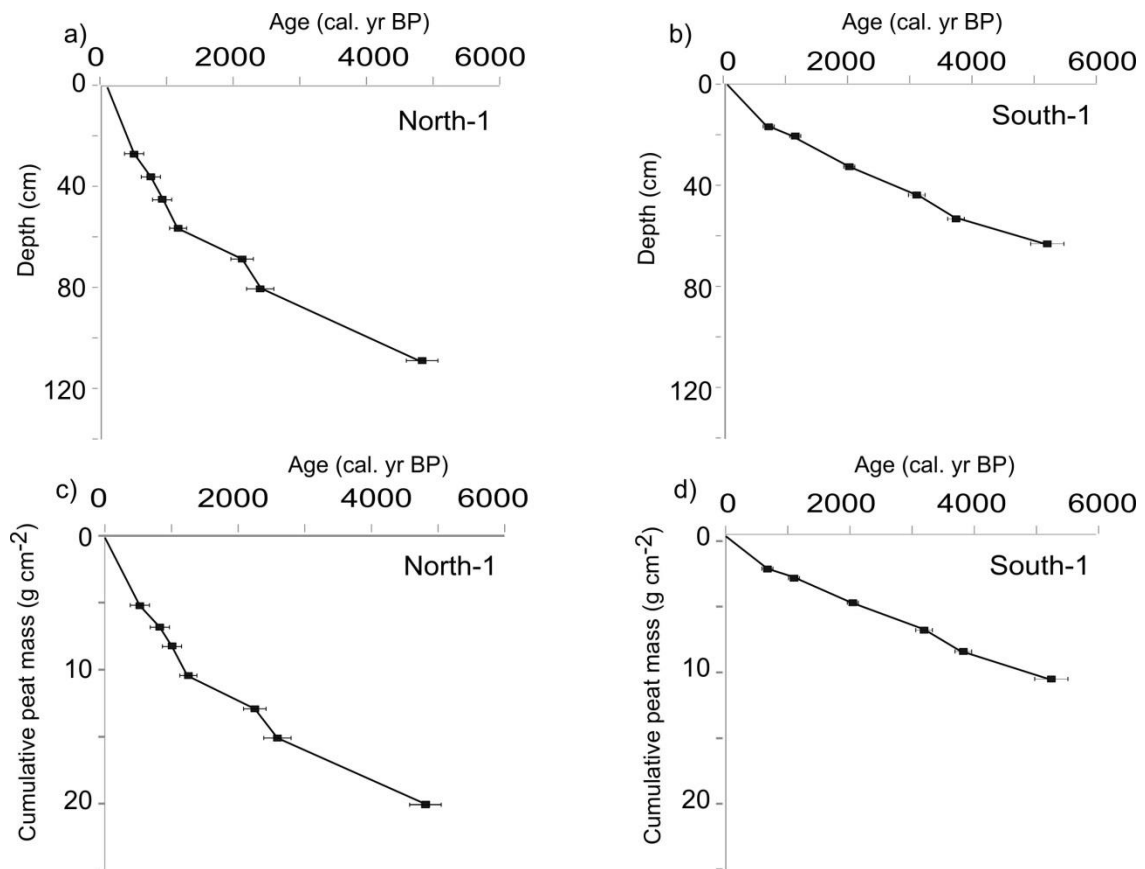


Figure 4.2. Age – depth models of the cores North-1 (a) and South-1 (b) and cumulative peat mass – depth models of the cores North-1 (c) and South-1 (d). The error range (2σ) is represented by horizontal bars.

The lower part of core North-1 (dated to 4500–2750 cal. yr BP) (Figure 4.3) consists of roots, unrecognizable debris and occasional remnants of *Juncus balticus* and Poaceae and is characterized by relatively stable LARCA (11–13 gm⁻² yr⁻¹). A sharp increase in LARCA (up to 37 gm⁻² yr⁻¹) coincides with a shift to assemblages dominated by *Triglochin maritima* in a portion of the core dated to 2400–2100 cal. yr BP. Following decline in LARCA (to 13–15 gm⁻² yr⁻¹) corresponds to a rise in unidentifiable debris and remnants of *J. balticus*, Poaceae and *Aster* spp. in a portion of the core dated to 2250–1500 cal. yr BP. Part of the core dated to 1225–1000 cal. yr BP contains well-preserved remnants of *T. maritima* and *Atriplex prostrata* and is characterized by the highest LARCA (up to 55 gm⁻² yr⁻¹). Peat accumulated during last ~1000 years is composed of roots and remnants of *T. maritima*, Poaceae, and *Aster* spp.; this part of the core is characterized by LARCA varying from 24 to 50 g m⁻² yr⁻¹ (Figure 4.3).

The lower part of core South-1 (dated to 5200–4000 cal. yr BP) (Figure 4.4) is composed of unidentifiable debris and occasional remnants of *Sonchus arvensis*, *Aster* spp., *Hordeum jubatum*, *Puccinellia nuttalliana* and has the lowest LARCA (5–8 gm⁻² yr⁻¹). The part of the core dated to 3750–3250 cal. yr BP contains remnants of *T. maritima*, *P. maritima*, *Salicornia rubra*, *Suaeda calceoliformis* and is characterized by increased LARCA (10–13 g m⁻² yr⁻¹). The portion of the core dated to 3000–750 cal. yr BP has relatively stable LARCA (8–10 gm⁻² yr⁻¹) although two transitions from macrofossil assemblages dominated by *J. balticus*, *H. jubatum*, *P. nuttalliana*, *Aster* spp. to assemblages dominated by *T. maritima*, *A. prostrata*, *P. maritima*, *S. rubra*, and *S. calceoliformis* are visible. Peat deposited during the last ~650 years is composed of remnants of *T. maritima*; LARCA within this portion of the core is the highest (13 to 15 g m⁻² yr⁻¹).

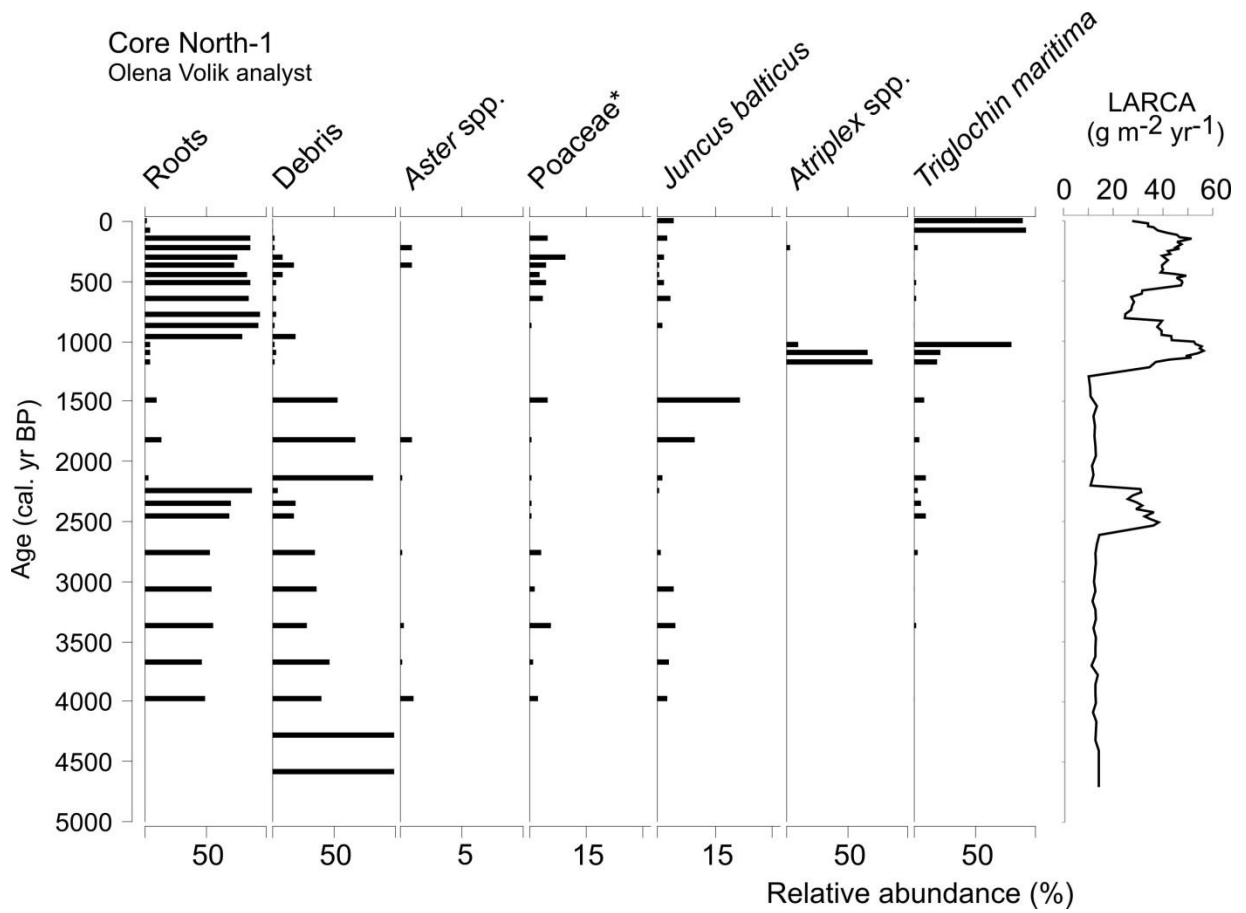


Figure 4.3. Macrofossil assemblages and LARCA in core North-1. * Poaceae includes *Calamagrostis* spp. and *Hierochloe* sp.

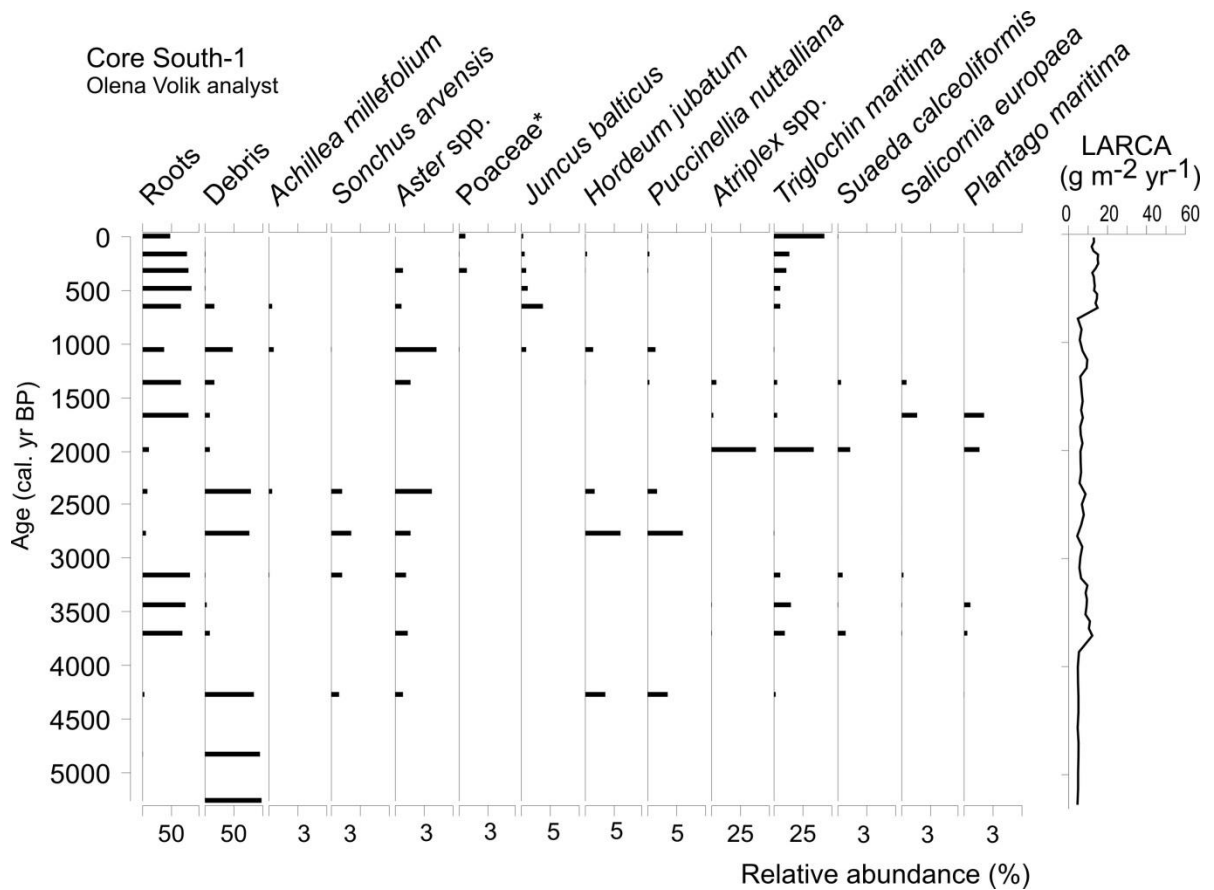


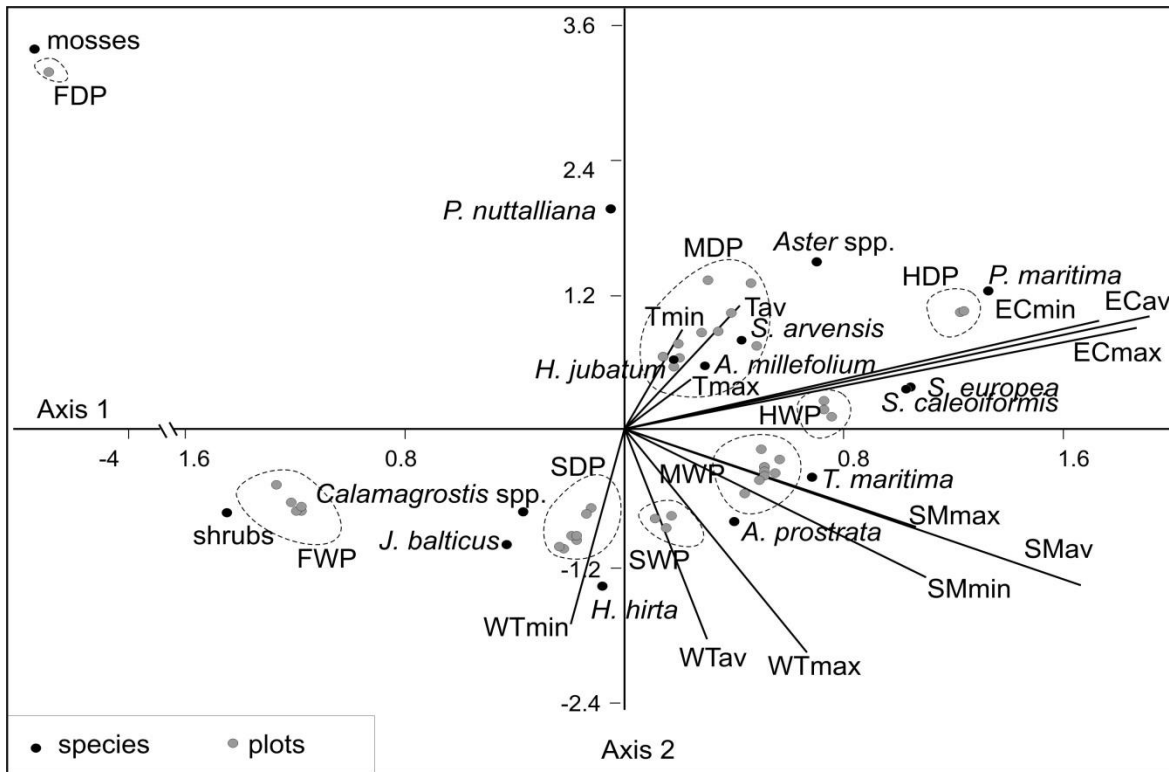
Figure 4.4. Macrofossil assemblages and LARCA in core South-1. * Poaceae includes *Calamagrostis* spp. and *Hierochloe* sp.

4.3.2. Recent environmental gradients and vegetation

Mean soil EC of combined dataset of 40 sample plots has a notable gradient varying from 1.4 to 24.9 mS cm⁻¹ (see Appendix B for details). CCA shows that Axis 1 ($\lambda=0.81$, $p=0.002$) and Axis 2 ($\lambda=0.60$, $p=0.006$) account for 31.9 % and 23.3 % of cumulative variance in the vegetation, respectively. Axis 1 represents a gradient of electrical conductivity and soil moisture that have the strongest effect on vegetation assemblages, and Axis 2 is largely a gradient of water table depth and soil temperature, but soil temperature has relatively weak effect on vegetation assemblages (Figure 4.5). Visual analysis of CCA biplot reveals eight distinct groups of sampling plots in terms of soil and moisture and EC (Figure 4.5).

Mosses and shrubs negatively correlate with soil EC and are dominant at fresh plots; however, shrubs prefer wet conditions while mosses are more abundant at dry plots. *J. balticus*,

Calamagrostis sp. and *Hierochloe* sp. correlate negatively with soil EC and are associated with slightly saline and dry plots. Distribution of *T. maritima* and *A. prostrata* is largely determined by soil moisture, and these two species are associated with moderately saline wet plots. *Aster* spp., *H. jubatum*, *P. nuttalliana*, *S. arvensis* and *A. millefolium* correlate positively with soil EC and temperatures and negatively with water table depth and are common at moderately saline dry plots. Soil EC has the strongest effect on distribution of *S. rubra*, *S. calceoliformis* and *P. maritima* and these species tend to occupy highly saline wet and dry plots (Figure 4.5).



Plots	ECav	SMav	WTav	Vegetation
Fresh & dry (FDP)	< 3	< 80	up to -30	Mosses
Fresh & wet (FWP)	< 3	> 80	-1.5 – 1	Shrubs
Slightly saline & dry (SDP)	3–5	< 80	1– - 15	<i>J. balticus</i> , <i>Calamagrostis</i> spp., <i>Hierochloe</i> sp.
Slightly saline & wet (SWP)	3–5	> 80	-5 – 0	<i>T. maritima</i> , <i>A. prostrata</i>
Moderately saline & dry (MDP)	5– 10	< 80	-23– -10	<i>H. jubatum</i> , <i>Aster</i> spp., <i>A.</i> <i>millefolium</i> , <i>P. nuttalliana</i>
Moderately saline & wet (MWP)	5– 10	> 80	-1 – 1	<i>T. maritima</i> , <i>A. prostrata</i>
Strongly saline & dry (HDP)	> 10	< 80	-24– -11	<i>P. maritima</i> , <i>S. calceoliformis</i>
Strongly saline & wet (HWP)	> 10	> 80	-7– -0.5	<i>T. maritima</i> , <i>S. rubra</i>

Figure 4.5. CCA ordination biplot based on soil electrical conductivity (average (ECav), maximal (ECmax), minimal (ECmin)), water table depth (average (WTav), maximal (WTmax), minimal (WTmin)), soil moisture (average (SMav), maximal (SMmax), minimal (SMmin)) and temperature (average (Tav), maximal (Tmax), minimal (Tmin)). Plant species and vegetation plots are shown as black and grey dots, respectively. Vegetation plots demonstrate distinct

grouping and following groups are identified: fresh & dry (FDP 2), fresh & wet (FWP), slightly saline & dry (SDP), slightly saline & wet (SWP), moderately saline & dry (MDP), moderately saline & wet (MWP), strongly saline & dry (HDP), strongly saline & wet (HWP). Average soil electrical conductivity (EC_{av}) ($mS\ cm^{-1}$), average soil moisture (SM_{av}) (%), average water table depth (WT_{av}) (cm) and vegetation of the plots are shown in a table below the CCA plot.

4.4. Discussion

4.4.1. Local-scale differences in LARCA within a saline fen

Our study shows remarkable differences in mean LARCA values and magnitude of LARCA fluctuation between the less saline and more saline parts of Saline Fen. Notably, changes in LARCA in the northern and the southern parts are not simultaneous, revealing the importance of differences in local conditions such as water table depth and salinity for peat accumulation rates.

The results suggest that changes in LARCA in the northern less saline part of the fen were tightly connected to water table fluctuation while salinity was relatively stable and had a little effect on LARCA. Low LARCA in 4500–2500 cal. yr BP, 2000–1250 cal. yr BP and decline in LARCA around 750 cal. yr BP corresponded to periods with decreased water table level that is evident from macrofossil assemblages dominated by *J. balticus* and Poaceae (*Calamagrostis* spp. and *Hierochloe* sp.) (Figure 4.3), species currently associated with slightly saline dry plots (Figure 4.5). Based on modern analogs, mean water table depth during these periods was ~10 cm below ground, soil moisture was lower than 80 %, and soil EC was lower than $5\ mS\ cm^{-1}$ (Figure 4.5). Abundance of *J. balticus*, a species that is not tolerant to prolonged waterlogging (Montemayor et al. 2015) and currently is dominant at ridges in Saline Fen (Phillips et al. 2016), indicates that area was not subjected to extended inundation. Most of increases in LARCA (around 2500 cal. yr BP, 1000 cal. yr BP and 500 cal. yr BP) (Figure 4.3) corresponded to periods with increased water level inferred from shifts to macrofossil assemblages composed of *T. maritima* and *Atriplex* sp., species that can tolerate waterlogging (Cooper 1982; Egan and Ungar 2000; Necajeva and Ievinsh 2008) and are dominant at wet inundated plots with soil EC of $3\text{--}5\ mS\ cm^{-1}$, mean water table of $-5\text{--}0\ cm$, and soil moisture of more than 80% (Figure 4.5). Although inundation probably occurred during these periods, waterlogging was not prolonged as

J. balticus, *Calamagrostis* spp., *Hierochloa* sp. were able to survive.

In the southern part of the fen, considerable variations in salinity and moisture conditions were recorded, and relationships between LARCA and water table depth seem to be influenced by salinity. LARCA was low during periods with decreased water table levels (~10–20 cm in average below ground) in 5200–3750 cal. yr BP, 3250–2250 cal. yr BP and around 1000 cal. yr BP that are evident from macrofossil assemblages composed of *H. jubatum*, *P. nuttalliana*, *S. arvensis*, *Aster* spp. preferring moderately saline dry conditions (Figure 4.5). However, following rises in water table levels (up to 1 cm above ground on average) during the time periods 3750–3000 cal. yr BP and 2250–1250 cal. yr BP inferred from macrofossil assemblages dominated by *T. maritima* and *A. prostrata* were not associated with pronounced increases in LARCA. This discrepancy probably resulted from the combined effect of inundation and elevated soil EC (>10 mS cm⁻¹) inferred from the presence of *S. rubra*, *S. calceoliformis* and *Plantago maritima*, species common at strongly saline plots (Figure 4.5). Such conditions are known to have negative impact on the growth of *T. maritima* (Cooper 1982; Phillips et al. 2016) and salt-tolerant graminoids (Montemayor et al. 2008; 2010; Israelsen et al. 2011), and thus can significantly affect net primary productivity, resulting in a decline in LARCA. Negative effect of high salinity on carbon accumulation is also evident from the rise in LARCA during the last ~750 years. This increase corresponds to declined salinity (EC<5 mS cm⁻¹) coupled with increased water table level as suggested by macrofossil assemblages composed of *T. maritima*, *J. balticus* and Poaceae. Such strengthening of links between water table depth and LARCA under decreased EC suggest that the influence of salinity on LARCA is determined by actual salt concentration, and there is a threshold value (probably 10 mS cm⁻¹), after which salinity can affect LARCA – hydrology relationships.

4.4.2. Carbon accumulation in a saline fen versus freshwater western continental fens

Although peat accumulation in western continental Canada started around 9000 cal. yr BP (Halsey et al. 1998), the Saline Fen began to accumulate peat around 5000–4400 cal. yr BP, and the mid-Holocene drought documented in the region (e.g., Hutton et al. 1994; Yu et al. 2014), is the most probable explanation of this lag. Low LARCA in Saline Fen around 4000 cal. yr BP can be related to region-wide decline in peat accumulation in western continental Canada due to Neoglacial cooling (Vitt et al. 2000; Yu et al. 2003; 2014). Sharp rises in LARCA around 3600

cal. yr BP (core South-1) and 2500 cal. yr BP (core North-1) (Figs. 3 and 4) coincide with peaks in LARCA in freshwater continental fens (Yu et al. 2003; 2014), that have been attributed to a wetter climate that caused an increase in water table (Yu et al. 2014). Although peat accumulation in Saline Fen seems to be sensitive to climate fluctuation similar to freshwater peatlands, the uncertainty about changes in LARCA under wetter or drier, warmer or cooler climatic conditions (e.g., Loisel and Garneau 2010), and the discrepancy in timing of LARCA changes in the northern and the southern parts of Saline Fen (see above), reveals the superiority of the local setting (including water table position and salinity) for carbon accumulation.

The mean value of 0.155 g cm^{-3} in organic matter density in Saline Fen is close to the average organic matter density (0.158 g cm^{-3}) reported from continental fens in western Canada (Yu et al. 2014). Despite the high organic matter density, mean LARCA of the site ($19.7 \text{ gm}^{-2} \text{ yr}^{-1}$ (SD=15.1)) is lower than what was observed in western continental fens ($32.5 \text{ gm}^{-2} \text{ yr}^{-1}$ by Yu et al. (2014)), but is comparable to the average rate reported for other western Canadian peatlands ($19.4 \text{ gm}^{-2} \text{ yr}^{-1}$) (Vitt et al. 2000). The northern part of the fen tends to have higher LARCA ($29.67 \text{ gm}^{-2} \text{ yr}^{-1}$ (SD=14.53)) that is close to LARCA in continental fens ($12.1\text{--}32.4 \text{ gm}^{-2} \text{ yr}^{-1}$ (Yu et al. 2014)), but LARCA in the southern part ($9.79 \text{ gm}^{-2} \text{ yr}^{-1}$ (SD=3.49)) is considerably lower. Carbon storage of the fen ranges from 89.03 in the southern part to 181.2 kg m^{-2} in the northern part, and is much lower than mean carbon storage of 264 kg m^{-2} observed in continental fens (Yu et al. 2014). Low carbon storage in the studied saline fen is not surprising as the fen has low LARCA, and is younger than the fens studied by Yu et al. (2014), which dated between 5000–11000 cal. yr BP.

4.4.3. Implications for wetland reclamation in the Alberta Oil Sands Region

This study shows notable and abrupt shifts in LARCA in response to variations in salinity and groundwater level, suggesting that saline fens, potential targets for reclamation, are dynamic systems sensitive to environmental change, and site-scale differences can transform the effect of region-wide changes, especially climatic fluctuations. This should be kept in mind to ensure that constructed saline fens will be able to persist and accumulate peat in spite of the changing climate. Ideally, constructed saline fens should be designed in a way that will allow regulation of some local settings (e.g., water input, drainage, connectivity with adjacent wetlands and waterbodies) and promote the adaptation of constructed system to new conditions.

Decreased mean LARCA in the southern, more saline part of Saline Fen, coupled with a weaker response of peat accumulation rates to rises in groundwater level, suggests that carbon accumulation is negatively affected by high salinity (soil EC >10 mS cm⁻¹). In the northern, less saline part of the fen, mean LARCA is comparable to LARCA in continental fens showing that carbon accumulation is not severely affected by low salinity (soil EC <5 mS cm⁻¹). Thus, for constructed saline fens it is essential to maintain slightly saline conditions with EC less to 5 mS cm⁻¹ to best support the carbon storage function of the fens.

Paleoecological reconstructions suggest that under slightly saline conditions (soil EC <5 mS cm⁻¹), the highest LARCA is associated with relatively high water table (-5–0 cm on average) and assemblages dominated by *T. maritima* and *A. prostrata*. This can be explained by reduced decomposition due to fast transition of plant litter from the acrotelm to the catotelm, coupled with increased decay resistance of *T. maritima* tissue (Trites and Bayley 2009a). Thus, our study confirms importance of high and stable groundwater level not only for successful initiation of peat accumulation at constructed fens, but also for long-term carbon storage.

T. maritima, a species that has been already considered appropriate for establishing peat accumulation in constructed wetlands (Trites and Bayley 2009a; Pouliot et al. 2012), and *A. prostrata* seem to be the most useful for achieving the highest rates of carbon accumulation in depressed areas with mean water table at -5–0 cm. In the elevated areas with deeper water table (~ -15 cm) *T. maritima* seems to have lower productivity, and *J. balticus*, *Calamagrostis* and *Hierochloa* are more useful for supporting relatively high LARCA.

Prolonged inundation (mean water table level above ground), especially coupled with high salinity (soil EC >10 mS cm⁻¹) appear to have negative effect on peat accumulation and should be avoided at constructed fens.

4.5. Acknowledgments

We wish to thank Meaghan Quanz for help with field work; Volodymyr Sivkov, Tristan Gingras-Hill, and Adam Green for help with core collection; Carley Crann (A.E. Lalonde AMS Facility, University of Ottawa) for radiocarbon dating. We thank the editors of Wetlands and anonymous reviewers for comments on an early draft of this work. Funding provided by the Natural Science and Engineering Research Council (NSERC) of Canada, Collaborative Research

and Development Program, co-funded by Suncor Energy Inc., Imperial Oil Resources Limited and Shell Canada Energy (Price, Petrone); NSERC Discovery Grant Program (Petrone); NSERC Northern Supplement (Petrone); and Northern Studies Training Program (Volik).

5. Environmental controls on CO₂ exchange along a salinity gradient in a saline boreal fen in the Athabasca Oil Sands Region

5.1. Introduction

Peatlands play an important role in global carbon, water, and nutrient cycles (Roulet 2000; Limpens et al. 2008) and have been exploited by humans over many centuries for fuel, agriculture and forestry. However, anthropogenic disturbance has increased dramatically in the 20th century as demand for mineral resources in the world economy has risen (Dubiński 2013). Large areas of the boreal zone have been affected by the growing mining industry. In particular, one of the world's largest mining-induced boreal peatland losses is occurring in the Athabasca Oil Sands Region (AOSR) (Alberta, Canada) where vegetation and surficial deposits have been completely removed for the development of open-pit mines from more than 700 km² of boreal land (Rooney et al. 2011), of which peatlands comprise 50% (Vitt et al. 1996).

After mine closure, oil companies are obligated by the Government of Alberta to reclaim disturbed areas to lands with “equivalent land capability”, which means that “the land is to have the same ability to support various land uses after conservation and reclamation, but the individual land uses do not have to be identical” (Province of Alberta 2003). About one third of post-mined lands must be reclaimed back to wetlands to restore pre-disturbance landscape diversity (Alberta Environment 2008). As reclamation requires total reconstruction of a whole ecosystem at the landscape scale (Johnson and Miyanishi 2008), a firm grasp on environmental processes in boreal ecosystems is essential for the reclamation success (Environment and Parks 2015). Consequently, there is a growing interest in better understanding natural ecosystems that can provide suitable targets for reclamation. In particular, saline boreal fens, groundwater fed peatlands with increased salt content, have been suggested as appropriate models for reclamation of areas with elevated salinity (e.g., Purdy et al. 2005; Wells and Price 2015a, b), which is commonly caused by salts derived from saline tailings and reclamation materials in the AOSR (Kessel 2016).

Saline fens are rare ecosystems that have been reported from Western Boreal Plains (Grasby and Betcher 2002; Purdy et al. 2005; Trites and Bayley 2009a; 2009b). These fens are slightly acid to neutral chloride dominated peatlands (Steward and Lemay 2011; Volik et al.

2017) with notable salinity gradients associated with the discharge of saline groundwater (Wells and Price 2015a; 2015b). Salinity has a strong effect on fen vegetation (Trites and Bayley 2009a) and control the distribution of plant communities, which in turn govern ecohydrological processes (e.g., evapotranspiration (Phillips et al. 2015)) and nutrient transformation (Trites and Bayley 2009b). Ridge-depression patterns, coupled with an abundance of depressed open-water areas (ponds), are common features of saline fens (Wells and Price 2015a), and water cycling within fens is influenced by such microtopography (Wells and Price 2015a; Phillips et al. 2015). Microtopographical heterogeneity and increased salinity may have an effect on carbon cycling in saline fens because microtopography can modify carbon dioxide (CO₂) fluxes (e.g., Waddington and Roulet 1996; Petrone et al. 2011), and notable differences in magnitude and direction of CO₂ exchange between ponded and vegetated areas within peatlands have been reported (Pelletier et al. 2015). In addition, elevated salt content can affect plant productivity and litter decomposition (Trites and Bayley 2009b). Despite some improvement in our understanding of the ecohydrological and biochemical functioning of saline fens, there is a paucity of information about CO₂ exchange within the fens. Carbon uptake, coupled with its long-term storage is one of the primary ecological services provided by peatlands including fens, so a better understanding of the carbon dynamics of saline fens is necessary to ensure that these ecosystems targeted by reclamation plans provide equivalent ecosystem services to those destroyed by mining.

Currently, it has been suggested that evaluation of functional characteristics of constructed fens (functional-based approach) can better reflect the state of the fens comparatively to assessment of their vegetation community structure (indicator species approach), and rates of gross photosynthesis and ecosystem respiration have been recognized as variables that are useful for assessment of functioning of the fens (Nwaishi et al. 2015). Consequently, better understanding of the relationship between salinity, vegetation and CO₂ fluxes in saline fens is necessary to set carbon storage benchmarks against which reclaimed fens can be evaluated (Environment and Parks 2015). In addition, the main drivers of saline fen productivity would allow reclamation plans to target environmental conditions that maximize the rate of carbon sequestration despite the negative effect of salinity stress on plant growth. Further, evaluation of variability in productivity and CO₂ exchange in saline boreal fens under different environmental conditions will help to predict how constructed saline fens will respond to natural and anthropogenic changes. Thus, this study aims to characterize the environmental controls on CO₂

fluxes in a saline boreal fen in the AOSR using community-scale measurements along a salinity gradient. The main objectives are: 1) to determine how electrical conductivity (EC), water table depth (WTD), soil moisture (SM) and temperature (ST), peat hydrophysical properties, nutrient availability, and vegetation influence net ecosystem exchange (NEE), ecosystem respiration (R), and gross primary productivity (GEP) within different microtopographic forms within the peatland; 2) to assess effect of changes in vegetation, water depth (WD), EC, pH, water temperature (WT), dissolved oxygen (DO) and nutrient concentrations on NEE, GEP and R within open-water areas (ponds); and 3) to identify key features of CO₂ exchange under saline conditions that can be useful for improvement of saline fen construction in the post-mined setting in the AOSR.

5.2. Materials and methods

5.2.1. Study site

This study was conducted at a saline peatland (hereafter, Saline Fen) 10 km south of the city of Fort McMurray (56°34'28.84" N, 111°16'38.39" W), Alberta, Canada (Figure 5.1). The site is situated within the Boreal Plain Ecozone, which is characterized by a subhumid continental climate. At Fort McMurray, mean annual temperature and mean annual precipitation based on 1981–2010 normals, are 0.2°C and 460 mm respectively (Environment Canada 2015). Saline Fen is a 27 ha elongated fen with a prominent ridge-depression pattern in the northern portion, and abundant shallow ponds in the central and southern portions of the peatland. The fen, with an average pH of 6.5–7.5 demonstrates a notable range of salinity; electrical conductivity of sodium chloride-dominated groundwater varies from more than 60 mS cm⁻¹ in the southern part to 19 mS cm⁻¹ in the northern part (Wells and Price 2015b) (Figure 5.1(c)). According to soil salinity classification (Abrol et al. 1988), the northern part of the fen is characterized by slightly (2–4 mS cm⁻¹) and moderately saline (4–8 mS cm⁻¹) conditions while the southern part has strongly (8–16 mS cm⁻¹) to very strongly saline (>16 mS cm⁻¹) conditions (Figure 5.1). The distribution of plant communities closely follows this salinity gradient. Slightly saline areas are dominated by mosses and shrubs (*Alnus* spp., *Salix* spp., *Betula* spp.) regardless of topographic position. Ridges with moderately saline conditions are dominated by baltic rush (*Juncus balticus*), sweetgrass (*Hierochloa hirta* ssp. *arctica*) and narrow reed grass (*Calamagrostis stricta*) while moderately saline depressions are dominated by seaside arrow grass (*Triglochin maritima*) and hastate-leaved orache (*Atriplex prostrata*). Strongly saline areas

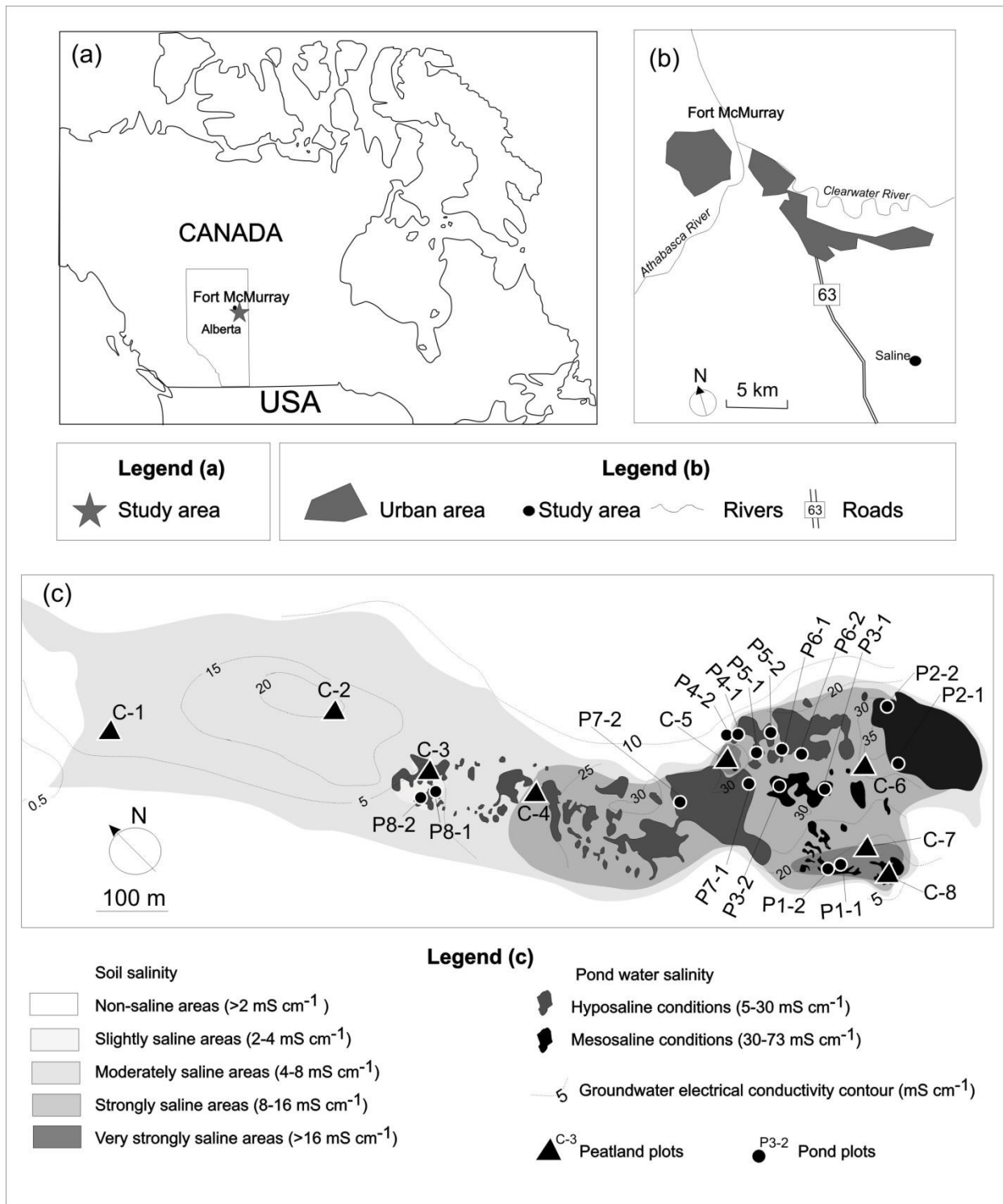


Figure 5.1 (a) Regional map showing the location of the study site within Alberta, Canada; (b) map showing location of Saline Fen near Fort McMurray, Alberta; (c) map of the study site, including locations of peatland and pond plots

are dominated by foxtail barley (*Hordeum jubatum*), *Puccinellia nuttalliana* and sea plantain (*Plantago maritima*) on the ridges, or by *T. maritima* in the depressions. Very strongly saline areas are dominated by *P. maritima* and horned seablite (*Suaeda calceoliformis*) on ridges, or *T. maritima* and samphire (*Salicornia rubra*) on depressions.

Numerous open-water areas (ponds) with salinity from 2 to 50 ppt are situated predominantly in the southern and central parts of the fen. The ponds are shallow (average depths of 0.4–0.5 m) and small (surface area from 1 m² to 1.2 ha). Most of the large ponds have irregular shapes, while small ponds are typically circular and located in deep depressions with steep margins. Some ponds have a semi-permanent regime and dry out during the late summer. According to limnological salinity classification scheme (Last and Ginn 2005; Herbert et al. 2015), ponds situated in the northern part of the fen can be characterized as hyposaline (5–30 mS cm⁻¹) whereas ponds in the southern part are mesosaline (30–73 mS cm⁻¹) (Figure 5.1). Eight ponds with mean EC ranging from 5 to 44 mS cm⁻¹ were selected for this study (Figure 5.1). Hyposaline ponds are dominated by diatoms such as *Staurosira construens* var. *venter*, *Staurosirella pinnata*, *Cocconeis placentula* var. *lineata*, *Navicula cryptocephala*, *Cyclotella meneghiniana* while *Anomoeoneis sphaerophora* fo. *costata*, *Navicula salinarum*, *Amphora coffeaeformis*, *Navicymbula pusilla*, *Diploneis stroemii*, and *Parlibellus cruciculus* are dominant in mesosaline ponds. *Triglochin maritima* occurs around hypo- and mesosaline ponds while *Salicornia rubra* grows around mesosaline ponds only. Emergent vegetation is more abundant in hyposaline ponds and includes *Typha* spp., *Scripus* spp., and *Schoenoplectus* spp. while mesosaline ponds are lacking emergent vegetation. Submergent vegetation in hypo- and mesosaline ponds is presented by *Potamogeton* spp. and *Ruppia* spp.

5.2.2. Community-scale CO₂ fluxes

Community-scale CO₂ fluxes were measured using enclosed dynamic Plexiglas chambers following the method of Petrone et al. (2011). In May 2015, eight peatland sites (see Figure 5.1 and Table 5.1 for details) were selected along a salinity gradient for CO₂ flux measurements, and semi-permanent polyvinyl chloride collars (height of 15 cm and inside diameter of 19 cm) were inserted 10 cm into the peat. Of these eight sites, six were equipped with two collars (one on a ridge and a second in a paired depression), and the remaining two sites (C-3 and C-6) were equipped with just one collar because they did not demonstrate ridge-depression patterns. In

addition, eight ponds were selected for measurements of CO₂ flux along a salinity gradient using a floating chamber at two plots per pond; no collars were installed, but each of the sixteen plots were marked with a stake. Six plots were dominated by *Potamogeton* spp.; no macrophytes were present in eight plots, and two plots had an extensive microbial mat but no macrophytes (see Table 5. 2 for details). Peatland collars and pond plots were used for measuring fluxes associated with the gross photosynthesis of the plants (full sun) and dark respiration of the aboveground vegetation, coupled with soil respiration (with non-transparent cover). During flux measurements at the peatland sites, a chamber was placed in a 3 mm channel on the top side of the collar and sealed with water to prevent air exchange (Brown et al. 2010). In the pond sites, the chamber was equipped with a Styrofoam float and placed directly on the water surface (ponds) reaching approximately 3 cm into the water column. A fan was placed inside the chamber for cooling and mixing of air inside the chamber (McLeod 2006; Brown et al. 2010). CO₂ concentration, air temperature, photosynthetically active radiation (PAR) and relative humidity within the chamber were measured using an EGM-2 Infrared Gas Analyzer (IRGA) for two minutes, with a 1 second sampling period and 30 second recording interval. The measurements at each peatland plot were made from May to August 2015 and for each pond plot measurements were taken from June to August. All measurements were collected between 9 am and 4 pm under PAR ranging between 1300 and 1700 μmol m⁻²s⁻¹. CO₂ flux (net ecosystem exchange, NEE) was calculated as,

$$NEE = \frac{\Delta M}{N} \frac{V}{A} CF \quad (5.1)$$

where Δ is change in the chamber headspace CO₂ concentration over time (ppm s⁻¹), M is the molar mass of CO₂ (44.01 g mol⁻¹), N is the molar volume of a CO₂ at standard temperature and pressure (0.022414 m³mol⁻¹), V is the corrected volume of the chamber and collar (m³), A is the area of the chamber (m²), and CF is the conversion factor from ppm to mol (1 ppm=10⁻⁶) (Petroni et al. 2011).

Gross ecosystem production (GEP) was calculated as,

$$NEE=GEP-R \quad (5.2)$$

where NEE is net CO₂ flux and R is flux associated with respiration of the aboveground vegetation and soil respiration (Kutzbach et al. 2007). CO₂ fluxes in this study represent point samples of midday fluxes and cannot be extrapolated to diurnal or seasonal carbon balances

(Heijmans et al. 2001), but to provide representation of average mid-day fluxes to compare relative fluxes across the salinity gradient (Petroni et al. 2011).

Table 5.1. Plant assemblages, percent cover, soil organic matter (SOM) in %, bulk density (BD) in gcm^{-3} , porosity (P), specific yield (Sy), aboveground biomass (AB) in gcm^{-3} , seasonal increase in belowground biomass (BBI) in gcm^{-3} , belowground biomass (BB) in gcm^{-3} at studied peatland plots. Ridge and depression plots are indicated by –R and –D in names, respectively.

Plots	SOM	BD	P	Sy	AB	BBI	BB	Vegetation cover (%)	Vegetation (% of vegetated area)
1	2	3	4	5	6	7	8	9	10
C1-R	83.5	0.11	0.26	0.05	2.34	0.86	1.72	92	<i>Juncus balticus</i> - 82, <i>Calamagrostis</i> sp. – 15, <i>Triglochin maritima</i> - 3
C1-D	83.7	0.12	0.19	0.04	2.21	0.79	1.59	95	<i>T. maritima</i> – 86, <i>J. balticus</i> – 14
C2-R	84.1	0.13	0.27	0.04	2.31	0.87	1.71	89	<i>J. balticus</i> - 81, <i>Calamagrostis stricta</i> – 10, <i>T. maritima</i> - 9
C2-D	82.9	0.13	0.22	0.04	2.23	0.80	1.64	93	<i>T. maritima</i> – 69, <i>Atriplex prostrata</i> – 22, . <i>J balticus</i> –9
C-3	92.1	0.09	0.46	0.91	2.01	0.74	1.39	100	Mosses – 93, <i>Vaccinium oxycoccos</i> – 6, <i>T. maritima</i> – 1
C4-R	85.2	0.12	0.20	0.04	2.58	1.01	1.97	100	<i>Hordeum jubatum</i> – 94, <i>J. balticus</i> - 3, <i>T. maritima</i> - 3
C4-D	74.9	0.15	0.21	0.06	2.48	1.00	1.91	100	<i>Hordeum jubatum</i> – 92, <i>T. maritima</i> – 5, <i>Puccinellia nuttalliana</i> - 3
C5-R	78.6	0.21	0.11	0.03	2.01	0.58	1.41	81	<i>Plantago maritima</i> – 78, <i>P. nuttalliana</i> – 11, <i>T. maritima</i> –9, <i>Suaeda calceoliformis</i> – 2
C5-D	73.7	0.22	0.12	0.02	2.50	0.05	1.28	80	<i>T. maritima</i> –84, <i>Salicornia rubra</i> – 11, <i>S. calceoliformis</i> - 4
C6	85.7	0.21	0.17	0.02	2.59	1.01	1.91	100	<i>P. nuttalliana</i> – 88, <i>H. jubatum</i> – 5, <i>P. maritima</i> – 5, <i>T. maritima</i> – 2

1	2	3	4	5	6	7	8	9	10
C7-R	78.2	0.17	0.16	0.04	2.04	0.05	1.45	79	<i>P. maritima</i> – 84, <i>S. calceoliformis</i> - 14, <i>S. rubra</i> – 2
C7-D	73.5	0.21	0.14	0.03	1.98	0.04	1.16	75	<i>T. maritima</i> – 65, <i>A. prostrata</i> – 22, <i>S. calceoliformis</i> – 13
C8-R	75.6	0.21	0.21	0.02	2.01	0.05	1.40	71	<i>T. maritima</i> – 100
C8-D	72.1	0.25	0.12	0.02	1.96	0.02	1.14	70	<i>T. maritima</i> – 95, <i>S. rubra</i> – 5

Table 5.2. Average depth and electrical conductivity (EC) in June-August, vegetation density (VD) and macrophyte assemblages at pond plots.

Pond name	Plots	EC (mS cm ⁻¹)	D (m)	VD	Dominant taxa
Long Pond	P-1-1	43.9	0.37	Sparse	<i>Ruppia</i> spp., <i>Potamogeton</i> spp.
	P-1-2	44.45	0.37	Moderate	<i>Ruppia</i> spp.
South Pond	P-2-1	30.1	0.38	None	No macrophytes, microbial mat
	P-2-2	31.1	0.33	None	No macrophytes, microbial mat
Pilsner Pond	P-3-1	38.2	0.27	None	No macrophytes
	P-3-2	23.8	0.25	None	No macrophytes
Round Pond	P-4-1	17.0	0.29	Dense	<i>Potamogeton</i> spp.
	P-4-2	17.9	0.30	Dense	<i>Potamogeton</i> spp.
Willow Pond	P-5-1	16.1	0.29	Sparse	<i>Potamogeton</i> spp.
	P-5-2	15.7	0.32	Sparse	<i>Potamogeton</i> spp.
Red Pond	P-6-1	21.0	0.22	Sparse	<i>Potamogeton</i> spp.
	P-6-2	20.4	0.19	Sparse	<i>Potamogeton</i> spp.
Lager Pond	P-7-1	20.2	0.40	Moderate	<i>Potamogeton</i> spp.
	P-7-2	19.6	0.29	Sparse	<i>Potamogeton</i> spp.
Spruce Pond	P-8-1	5.8	0.33	None	No macrophytes
	P-8-2	8.6	0.37	Sparse	<i>Potamogeton</i> spp., <i>Lemna</i> sp.

5.2.3. Environmental variables

To assess the relations between environmental variables and CO₂ fluxes, measurements of water table depth (WTD), soil moisture (SM) (HH2 Meter, Delta-T Devices), and temperature (ST) (at 0, 5 10 cm) (Type K thermocouple probe and meter; HH200, Omega Scientific, USA) were taken adjacent to collars simultaneously with flux measurements. Electrical conductivity (EC) was measured in the field by EC_{1:5} tests for which 1 part peat was mixed with 5 parts distilled water, and the EC of the solution was tested using handheld probe (YSI ProPlus, YSI Incorporated, USA); peat EC was calculated by applying the EC_{1:5} conversion factor with respect to peat moisture content and texture (Rayment and Higginson 1992). To quantify the availability of major anions and cations plant root simulator probes (PRS Probes; Western Ag. Innovations, Canada) were buried 10 cm below the peat surface for three weeks in July and August 2015. Within 24 to 72 hours after the field incubation, each probe was cleaned with distilled water, placed in a polyethylene bag and stored in a cool, dry location until shipped to Western Ag Innovations for analysis.

Pond water EC, water temperature, pH, dissolved oxygen (DO) and chlorophyll *a* concentrations were measured simultaneously with flux measurements using a handheld probe (YSI Professional Plus; YSI Incorporated, USA). Surface water (from ~ 20 cm) samples from each plot were collected simultaneously with flux measurements. The water samples were filtered (0.45 µm cellulose acetate filters) within 24 hours of collection and frozen (for major ion analysis and soluble reactive phosphorus (SRP), NO₃⁻ and NH₄⁺) or acidified (for total N and P). Samples were analyzed in the Biogeochemistry Lab at the University of Waterloo (major ions on DIONEX ICS3000; nutrients on Bran Luebbe AA3, Seal Analytical, Seattle, U.S.A., Methods G-102-93 (NH₄⁺), G-109-94 (NO₃⁻ and NO₂⁻), G-103-93 (SRP)).

5.2.4. Vegetation sampling

All species at each peatland collar were identified and percent cover was estimated, but only species with an abundance > 1% are considered in this study. The leaf area index (LAI) of each vegetated collar was measured after flux measurements using AccuPAR LP-80 Ceptometer (Decagon Devices, Inc). In September 2015, vegetated collars were harvested to a depth of 20 cm to quantify above and belowground biomass. Aboveground vegetation was clipped and oven dried at 60 °C for 2 days and then weighed to estimate aboveground biomass (AB). Coarse roots

were removed manually while fine roots were separated by washing through a 1 mm mesh sieve. The roots were oven dried at 60 °C for 2 days and weighed to estimate belowground biomass (BB). Seasonal increase in belowground biomass (BBI) was accessed using the soil core in-growth method (Neill 1992). In May 2015, peat cores (height of 10 cm and diameter of 5 cm) were taken near each vegetated collar; all live plant roots were removed and the peat was put back in the original hole. After recollecting the cores in September 2015, all live roots were removed, oven dried at 60 °C for 2 days and weighed to estimate BBI. Short (20 cm) peat cores were taken near vegetated collars and analysed for soil organic matter (SOM), bulk density (BD), porosity (P) and specific yield (Sy).

For pond sites, a survey of the vegetation under the floating chamber was conducted along with flux measurements. Emergent, floating, and submergent plants were identified to genus level; the relative density of the vegetation (macrophytes) (VD) was assessed based on 5-point scale (0 – no plants; 1 – sparse coverage (1 to 25 % of surface area covered with vegetation); 2 – moderate coverage (>25 to 50 %); 3 – dense (>50 to 75 %); 4 – very dense (>75 to 100 %).

5.2.5. Statistical analyses

The Mann–Whitney U-tests was used to detect differences in environmental variables and CO₂ fluxes between ridges and depression. Differences in CO₂ fluxes between plots along a salinity gradient were determined by the Kruskal–Wallis test. Probability values obtained from nonparametric tests were alpha corrected using a Bonferroni correction. Spearman's rank correlation was used to determine relations between NEE, GEP, R and environmental variables. All statistical analyses were performed using PAST 3.06 (Hammer et al. 2001).

5.3. Results

5.3.1. Spatial variability in CO₂ fluxes

Significant differences ($p < 0.05$) in NEE, GEP, and R between slightly to moderately saline, strongly saline, and very strongly saline sites were observed. The mean GEP of peatland sites ranged from 0.1 mg CO₂ m⁻² s⁻¹ (SD 0.02) within depressions with very strongly saline conditions to 0.35 mg CO₂ m⁻² s⁻¹ (SD 0.07) within strongly saline ridges (Figure 2a). The highest mean R (0.39 mg CO₂ m⁻² s⁻¹ (SD 0.1)) was observed within strongly saline ridges

(Figure 2a). Overall, ridge sites had significantly higher ($p < 0.05$) NEE, GEP, and R than depressions (Figure 5.2).

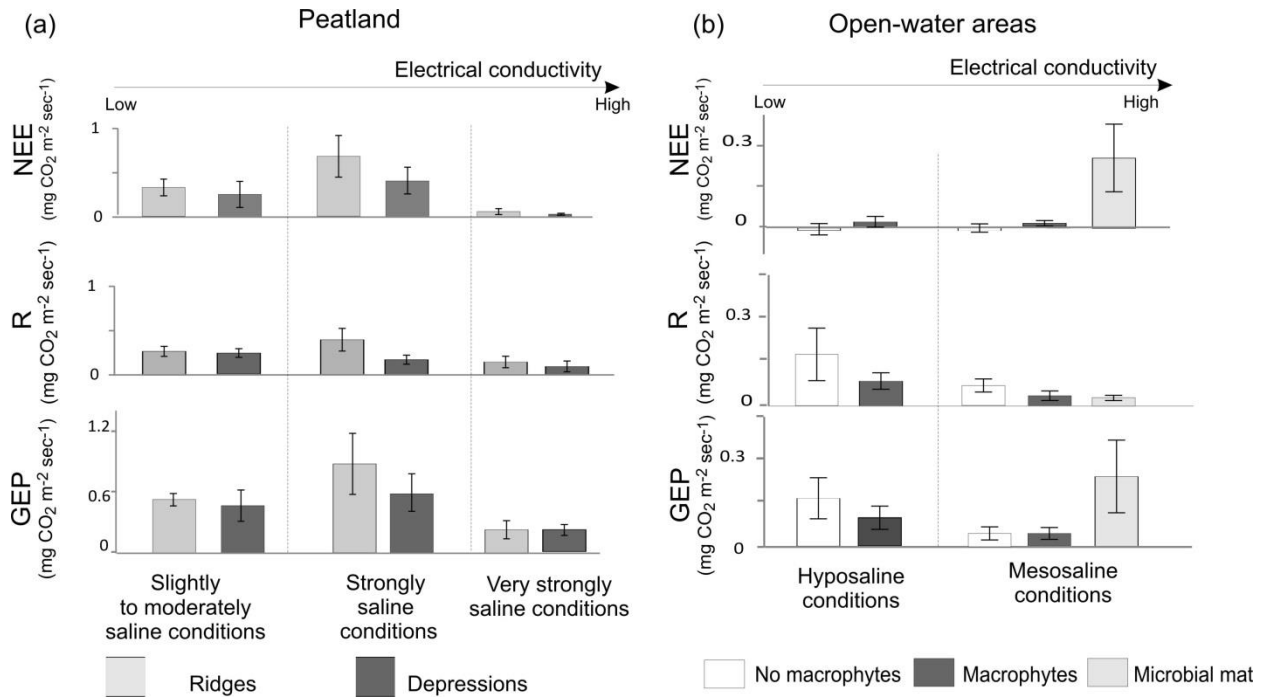


Figure 5.2. Net ecosystem exchange (NEE), gross ecosystem productivity (GEP) and ecosystem respiration (R) within peatland (a) and open-water areas (b). Positive NEE values indicate CO₂ uptake. The error range (2σ) is represented by vertical bars.

Hyposaline and mesosaline ponds were characterized by significant differences ($p < 0.05$) in NEE, GEP, and R. Sites with microbial mats had significantly higher ($p < 0.05$) mean GEP ($0.21 \text{ mg CO}_2 \text{ m}^{-2} \text{ s}^{-1}$ (SD 0.05)) and NEE ($0.24 \text{ mg CO}_2 \text{ m}^{-2} \text{ s}^{-1}$ (SD 0.05)) compared to phytoplankton- and macrophyte-dominated sites while R ($0.18 \text{ mg CO}_2 \text{ m}^{-2} \text{ s}^{-1}$ (SD 0.05)) was significantly higher ($p < 0.05$) within phytoplankton-dominated sites compared to macrophyte-dominated sites and sites with microbial mat (Figure 5.2(b)).

5.3.2. Controls on CO₂ fluxes within peatland

Variability in NEE, GEP, and R with respect to EC, WTD, SM, ST, LAI, and PAR within the peatland is shown in Figure 5.3. Significant differences ($p < 0.05$) in EC, WTD, SM, and LAI between ridges and depressions were found while ST was comparable between microtopographic forms. GEP and NEE were positively correlated ($r_s > 0.6$, $p < 0.05$) with LAI within both ridges

and depressions whereas NEE, R, and GEP were all negatively correlated ($r_s < -0.5$, $p < 0.05$) with EC in both depressions and ridges (Appendix C). Both WTD and SM showed negative correlations ($r_s < -0.5$, $p < 0.05$) with NEE and GEP within depressions; however, within ridges only WTD demonstrated a negative correlation ($r_s < -0.5$, $p < 0.05$) with NEE, GEP and R (Appendix C).

Soil properties (BD, Po, Sy) were generally similar along a salinity gradient and between microtopographical forms, and only SOM of very strongly saline plots was significantly lower ($p < 0.05$) than at less saline plots; moreover, mean SOM was also significantly higher ($p < 0.05$) within ridges than depressions (Appendix C). Strong positive correlations ($r_s > 0.7$, $p < 0.05$) between NEE, GEP, R, and SOM and were observed within ridges (Appendix C), and a strong positive correlation ($r_s > 0.7$, $p < 0.05$) between R and SOM was found within depressions. No strong significant correlation between NEE, GEP, R, and soil properties (BD, P, Sy) was evident.

No significant differences in mean aboveground biomass (AB), belowground biomass (BB) between ridges and depressions were found; however, differences in BB were significant ($p < 0.05$) along a salinity gradient. Increases in belowground biomass (BBI) were significantly higher ($p < 0.05$) within ridges (Table 5.1), and also BBI was significantly different ($p < 0.05$) along a salinity gradient. Within ridges, NEE and GEP were, positively correlated ($r_s > 0.6$, $p < 0.05$) with both aboveground and belowground biomass, as well as the increase in below ground biomass (Appendix C). Within depressions, NEE, GEP and R all demonstrated positive correlations ($r_s > 0.6$, $p < 0.05$) with BB and BBI, but only NEE was significantly positively correlated ($r_s > 0.6$, $p < 0.05$) with AB (Appendix C).

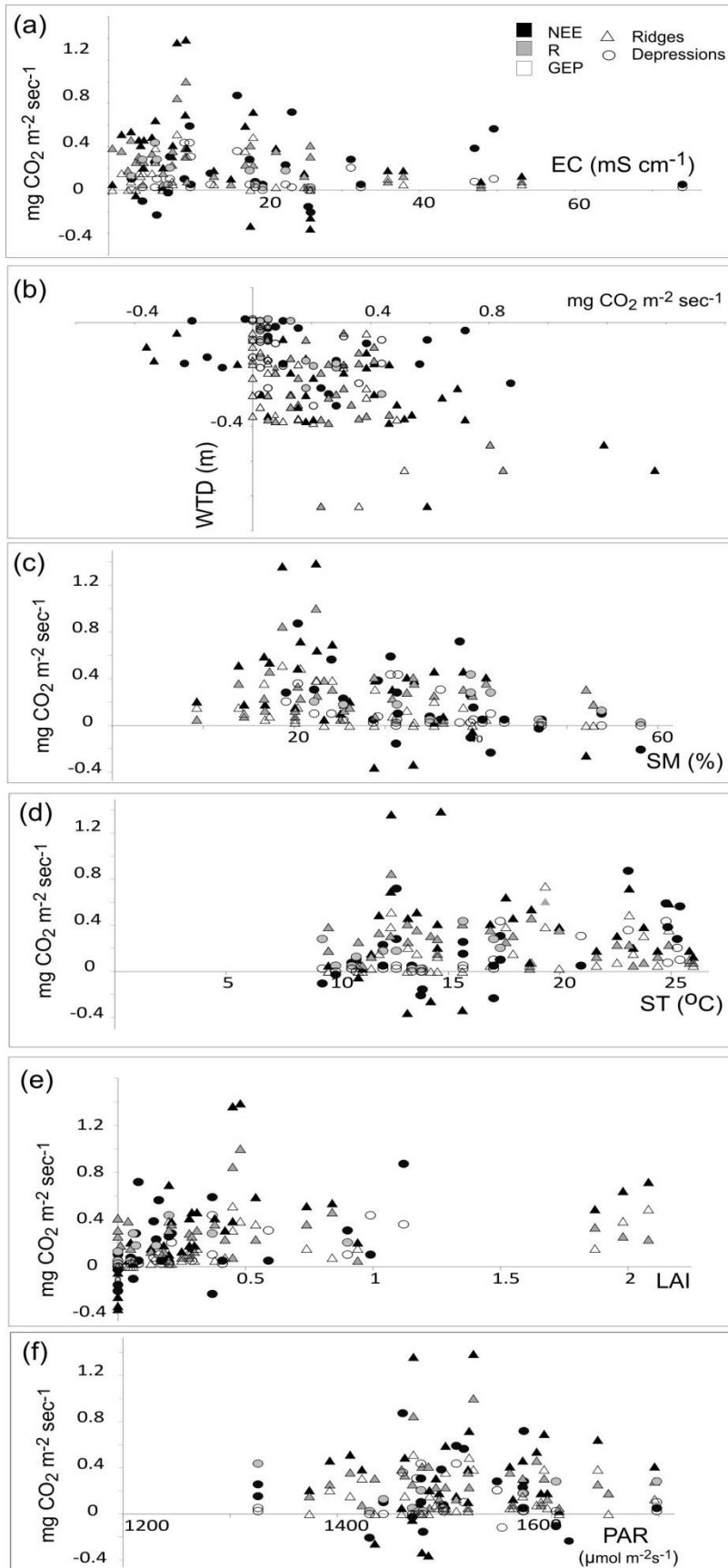


Figure 5.3. Variations in net ecosystem exchange (NEE), gross ecosystem productivity (GEP) and ecosystem respiration (R) with (a) electrical conductivity (EC), (b) water table depth (WTD), (c) soil moisture (SM), (d) soil temperature (ST), (e) leaf area index (LAI), and (f) photosynthetically active radiation (PAR) within ridges and depressions. Positive NEE values indicate CO₂ uptake

Nutrient availability within ridges and depressions is shown on Figure 5.4. Ridges were characterized by significantly higher ($p < 0.05$) availability of total nitrogen (TN), NH_4^+ , NO_3^- , K^+ , P, Fe, Mn, S, Zn, Ca^{2+} , and Mg^{2+} . Along a salinity gradient, significant differences ($p < 0.05$) in the availability of TN, NH_4^+ , K^+ , Fe, Al, S, Ca^{2+} were observed (Figure 5.4). Depressions were characterized by positive correlations ($r_s > 0.6$, $p < 0.05$) between all R, NEE, GEP and Mn, Ca^{2+} , Mg^{2+} availability though these elements were also negatively correlated ($r_s < -0.5$, $p < 0.05$) with EC (Appendix C). No significant correlations between nutrient availability and the response variables NEE, GEP or R was evident in ridges, however.

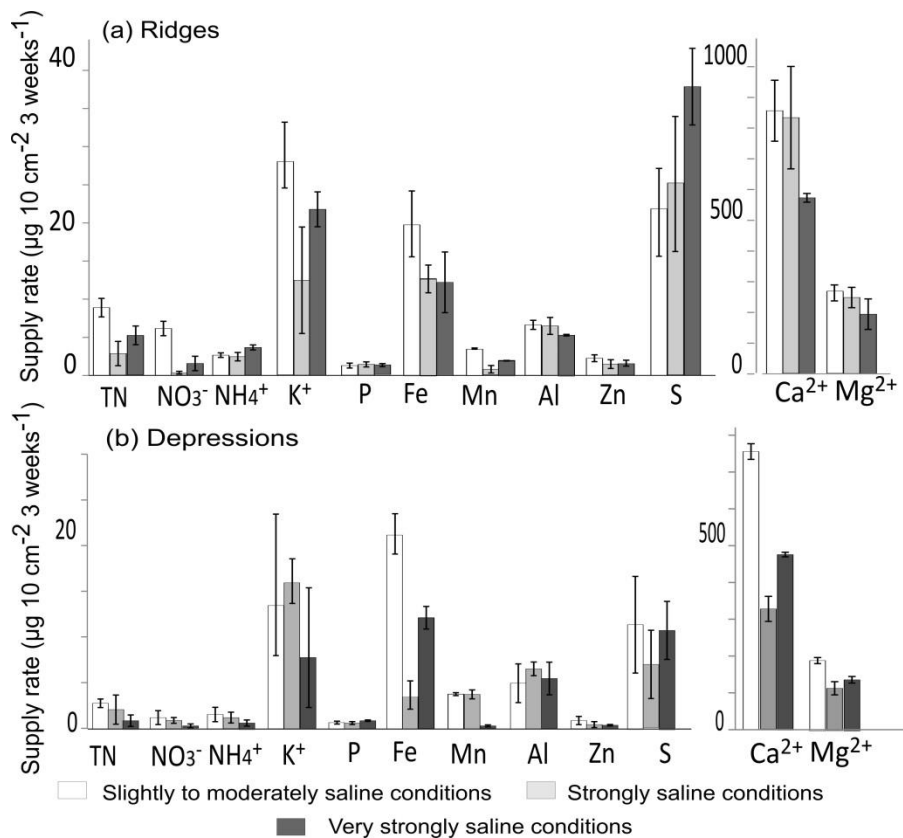


Figure 5.4. Nutrient availability (measured by PRS Probes) within ridges (a) and depressions (b) along a salinity gradient. The error range (2 SD) is represented by vertical bars.

5.3.3. Controls on CO_2 fluxes within open-water areas

Variability in NEE, GEP, and R with respect to pond water EC, WD, WT, pH, DO and chlorophyll *a* concentrations, and VD within open-water areas is shown on Figure 5.5. Notable spatial variability in pond water EC, was observed throughout the study site, and significant

differences ($p < 0.05$) in EC and chlorophyll *a* concentration between hyposaline and mesosaline ponds were found. However, WD, WT, DO, pH, and VD were not significantly different in hyposaline and mesosaline ponds. WD, EC WT, DO, and pH were comparable within unvegetated, macrophyte-dominated plots and plots with a microbial mat, but significant differences ($p < 0.05$) in vegetation density and chlorophyll *a* concentrations between these ponds were observed.

Nutrient concentrations in hyposaline and mesosaline ponds are shown on Figure 5.6. Mesosaline ponds had significantly higher ($p < 0.05$) concentration of SO_4^{2-} , K^+ , Mg^{2+} , Ca^{2+} , Na^+ , Cl^- , NH_4^+ , NO_3^- , PO_4^{3-} . No significant differences in SO_4^{2-} , K^+ , Mg^{2+} , Ca^{2+} , Na^+ , Cl^- between non-vegetated, macrophyte-dominated plots and plots with a microbial mat were found, but plots with a microbial mat had significantly higher ($p < 0.05$) NO_3^- and PO_4^{3-} concentrations and significantly lower NH_4^+ concentration compared to non-vegetated, macrophyte-dominated plots. In ponds, over the study season, both GEP and R correlated positively ($r_s > 0.5$, $p < 0.05$) with vegetation density and phosphate concentration (Appendix C).

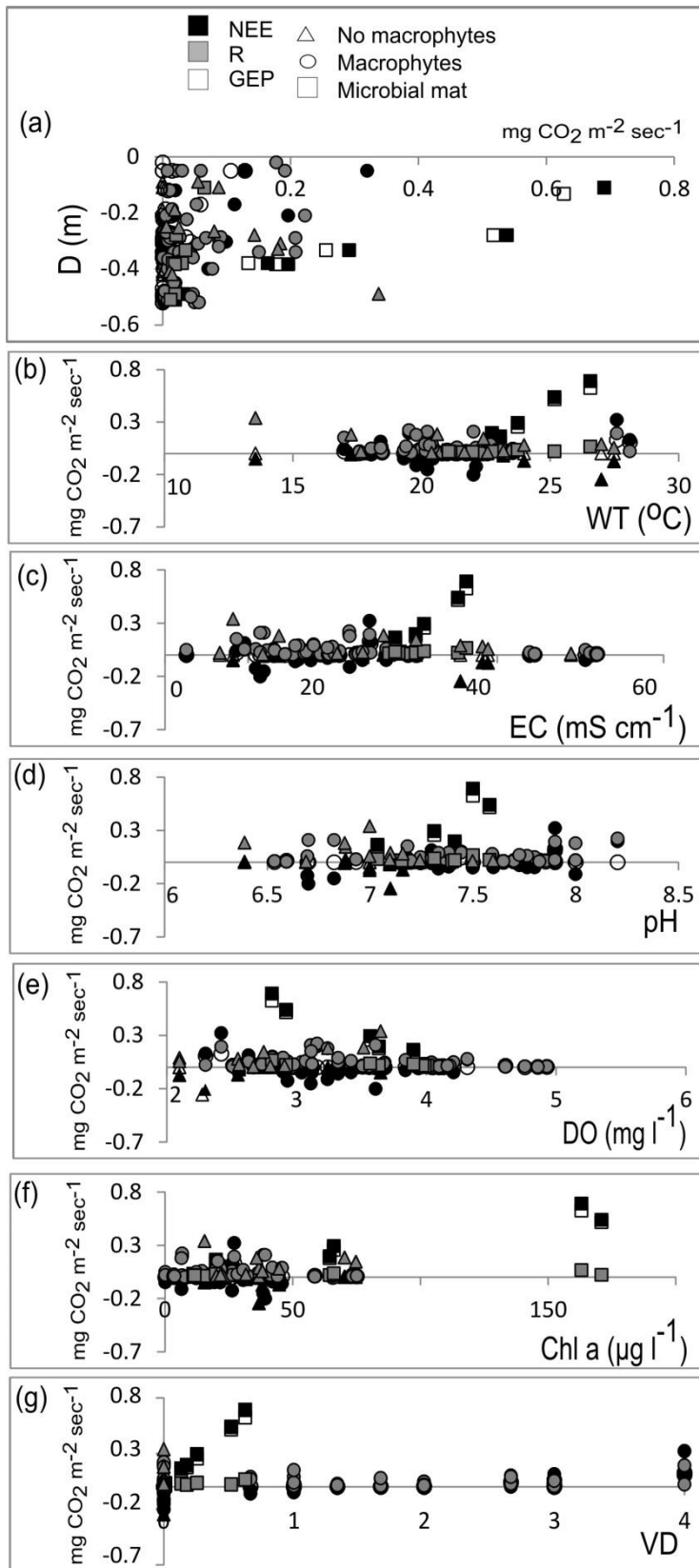


Figure 5.5. Variation in net ecosystem exchange (NEE), gross ecosystem productivity (GEP) and ecosystem respiration (R) with (a) water depth (D), (b) water temperature (WT), (c) electrical conductivity (EC), (d) pH, (e) dissolved oxygen concentration, (f) chlorophyll a concentration, and (g) vegetation density (VD) within open-water areas. Positive NEE values indicate CO₂ uptake

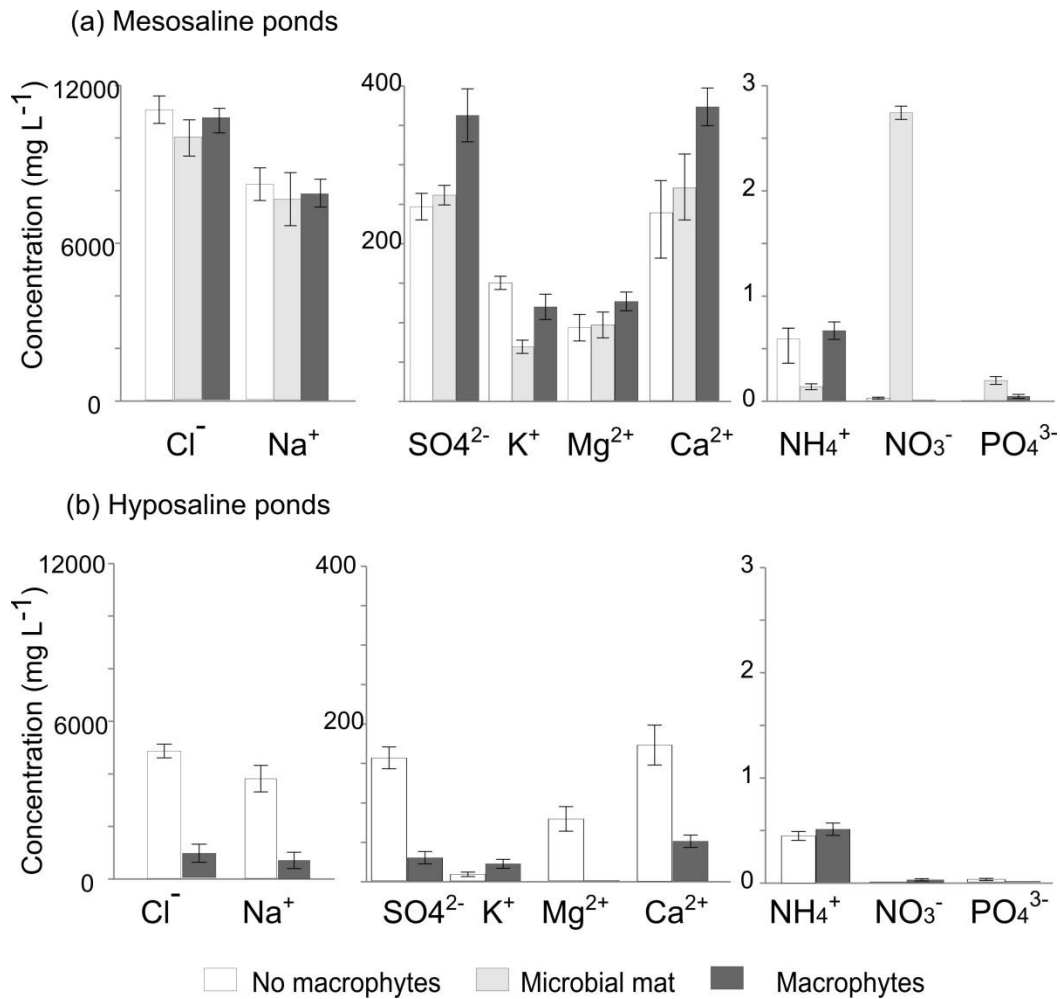


Figure 5.6. Nutrient concentrations in mesosaline (a) and hyposaline (b) ponds in the studied saline fen. Pond classification is based on biological classification scheme where hyposaline waterbodies have salinity of 3–20 ppt (EC 5.5–23 mS cm^{-1}), and mesosaline waterbodies is characterized by salinity of 20–50 ppt (EC 23–72 mS cm^{-1}) (Last and Ginn 2005). The error range (2 SD) is represented by vertical bars

5.4. Discussion

Construction of sustainable peatlands in post-mined oil sands landscapes is a multifaceted task that requires the re-establishment of key ecosystem functions including carbon capture and storage through biological processes, primarily photosynthesis. The results presented in this

study show that CO₂ uptake in a natural saline fen depends on the complex interactions between plant communities and environmental variables (primarily, WTD, EC, and nutrient availability) (Figure 5.7). Moreover, the data illustrate that peatland microtopographic heterogeneity has a strong influence on the relationship between CO₂ exchange and environmental conditions.

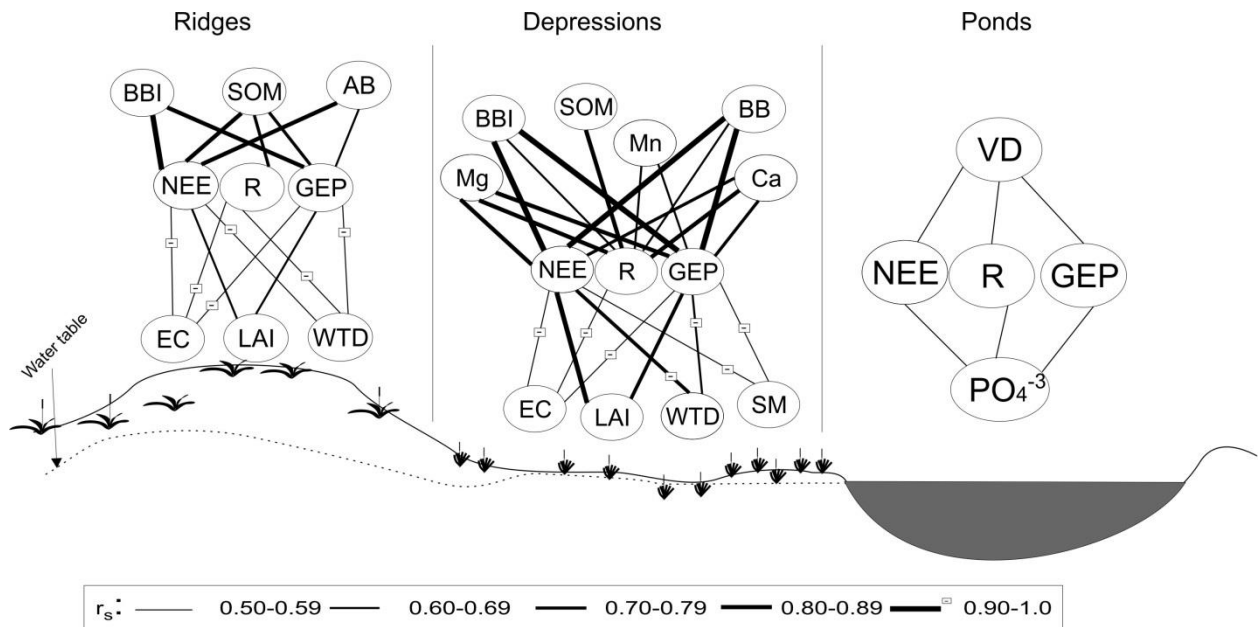


Figure 5.7. Correlations between net ecosystem exchange (NEE), gross primary productivity (GEP), ecosystem respiration (R) and environmental variables (electrical conductivity (EC), water table depth (WTD), soil moisture (SM), leaf area index (LAI), aboveground biomass (AB), belowground biomass (BB), seasonal increase in belowground biomass (BBI), soil organic matter (SOM), availability of calcium (Ca²⁺), manganese (Mn) and magnesium (Mg²⁺) (measured by PRS Probes), concentration of phosphates (PO₄³⁻), vegetation density (VD)) within depressions, ridges and ponds in the studied saline fen. Only strong significant correlations are shown. Strength of the relationship (r_s) has been shown as the width of a line. Negative correlation is indicated by “-” sign. Negative correlation between NEE, GEP, R, and WTD indicates higher NEE, GEP, and R associated with shallower water table.

5.4.1. CO₂ fluxes in peatland areas

Vegetation has been repeatedly shown to influence carbon fluxes (e.g., Andrews et al. 2013; Koelbener et al. 2010; Picek et al. 2007; Strilesky and Humphreys 2012). In our study, strong positive correlations between CO₂ fluxes and vegetation biomass suggest that vegetation properties are important for CO₂ exchange; moreover, LAI was positively correlated with NEE and GEP (Figure 5.7), and was found to explain a substantial portion of the variation in GEP and NEE within both ridges and depressions as revealed by semi-partial correlation (Appendix C). This is consistent with the findings of Lund et al. (2010), Humphreys et al. (2006) and Goud et al. (2017) suggesting that increased CO₂ uptake is often associated with increased LAI.

Negative correlations between NEE, GEP, R and EC (Figure 5.7), coupled with higher GEP in the less saline part of the fen is consistent with previous findings that salinity is one of the most important factors that can affect plant productivity and CO₂ exchange (Neill 1993; Curco et al. 2002; Willis and Hester 2004; Trites and Bayley 2009a, b; Neubauer 2013). Notably, in the studied saline fen, LAI was negatively correlated with EC within ridges and depressions, and this is consistent with a negative effect of elevated salt content on plant growth (Sperling et al. 2014; Sutter et al. 2014); moreover, the strong negative correlation between EC and LAI is consistent with previous work (Phillips et al. 2016) that reported a negative relationship between salinity and LAI, even within the same species (*T. maritima*). A negative correlation between R and EC within ridges and depressions (Figure 5.7) in this study is consistent with the negative impact of elevated salt content on microbial activity that has been previously documented (e.g., Rejmánková and Houdkova 2006; Tripathi et al. 2006).

Wetland productivity is known to be tied tightly to the moisture regime, as driven by the WTD (Wallen et al. 1988; Hilbert et al. 2000). Several field studies have shown a positive correlation between primary productivity and WTD (Szumigalski and Bayley 1996). Notably, the relationship between productivity and WTD can be influenced by microtopography: within hummocks and ridges elevated above the water table, higher primary productivity is associated with a lower water table, whereas in depressions (lawns and hollows) primary productivity is higher during wet conditions (Alm et al. 1997; Strack et al. 2006). In contrast, in this study, a strong negative correlation between GEP and WTD was observed in both ridges and depressions (Figure 5.7). Such negative correlation between WTD and GEP within ridges can be explained by the dominance of flood-sensitive species (e.g., *J. balticus*, *H. jubatum*) (Cooper 1982; Montemayor et al. 2015), so the higher water table can reduce GEP. A negative correlation between GEP and WTD within depressions can be associated with prolonged flooding that hinders oxygen diffusion into roots from soil, causing a shift from aerobic respiration to energy-inefficient anaerobic respiration in flood-tolerant species (Reddy and DeLaune 2008). Such increased energy demand often results in an energy deficit affecting photosynthetic activity, water and nutrient adsorption and distribution, and thus overall plant growth (Pezeshki and DeLaune 2012). Consequently, although inundation-tolerant species such as *T. maritima* can survive within depressions, their productivity can be reduced due to energy depletion.

Carbon exchange is known to be linked to nutrient dynamics, and increased nutrient availability is often associated with increased productivity (Bonan and VanCleve 1992; Mack et al. 2004). In this study, we observed strong positive correlation between magnesium, manganese, and calcium availability and GEP, NEE and R within depressions (Figure 5.7; Appendix C). Although these cations can be confounded with EC semi-partial correlation suggested significant

contribution of magnesium, manganese, and calcium availability to GEP, NEE and R (Appendix C). Such correlation can be expected as magnesium, manganese, and calcium play important role in photosynthesis, nitrogen and phosphorous assimilation, and cell formation (Rydin and Jeglum 2013), and thus are tightly connected to plant productivity and respiration. Moreover, Mg, Ca, and Mn availability can be limiting for plant productivity within depressions, as their availability is decreased under anaerobic conditions, and salinity coupled with higher pH can also yield reductions in Mg, Ca, and Mn supply (Cooper 1984; Stueben et al. 2004; Rydin and Jeglum 2013).

5.4.2. CO₂ flux within open-water areas (ponds)

Our results suggest that CO₂ flux in ponds is more strongly influenced by vegetation properties (such as vegetation density) and community composition than by environmental variables. While CO₂ uptake rates were notably higher in ponds with macrophyte cover, low CO₂ uptake was observed in ponds lacking submergent vegetation, and this can be expected due to the absence of photosynthetic macrophytes that coincides with what was reported from salt marshes (Miller et al. 2001; Moseman-Valtierra et al. 2016). Although phytoplankton productivity and respiration are important components of carbon cycling in aquatic ecosystems (Kobayashi et al. 2013), microalgae are not likely the main contributors to CO₂ uptake within ponds as suggested by the low productivity of plankton-dominated ponds and the weak. The highest CO₂ uptake was observed in a mesosaline pond (South Pond) that had excessive benthic microbial mats (Figure 2b). Such photosynthetic microbial mats are known from saline environments (Ley et al. 2006; Kunin et al. 2008; Burow et al. 2013), and have high primary production rates that are comparable to rates of tropical rain forests (Guerrero and Mas 1989). Our findings suggest that microbial mats are likely important contributors to CO₂ fluxes, but further detailed studies of

community composition and the main pathway of carbon through the microbial community are required for better understanding of role of microbial mats in carbon cycling within open-water areas in saline boreal fens.

Positive correlations between GEP, R, and phosphates observed in this study (Figure 5.7) was expected as P is a key nutrient in aquatic ecosystems, and increased ecosystem production is often associated with P load (Wetzel 2001; Elser et al. 2007). However, this is in contrast to saline prairie lakes and wetlands that are often N-limited (Sahm et al. 2009). Although our study has shown that EC had a strong effect on primary productivity within peatlands, EC was not a controlling parameter for CO₂ fluxes; moreover mesosaline ponds had higher GEP than hyposaline ponds.

5.4.3. Implications for fen construction in AOSR

Microtopography plays an important role in the regulation of water drainage, water table position and salinity within constructed wetlands (BGC Engineering Inc. 2010); in addition, our study revealed that microtopography plays an important role in regulation of CO₂ fluxes within peatland areas. Because topographic heterogeneity is one of the desired features of constructed wetlands (Wylynko and Hrynyshyn 2014), development of appropriate planting scheme (a construction document that shows the position, variety and quantity of plants to be planted within constructed wetlands) that will support the highest possible CO₂ uptake within different microtopographic forms is of paramount importance. Our results suggest that *J. balticus*, *C. stricta* and *H. jubatum* support high CO₂ uptake within ridges while *T. maritima* and *A. prostrata* are the most productive in depressions. However, a more detailed study with a wide range of

plant species is required to determine the most appropriate species composition with respect to the height, slope, aspect and general shape of microtopographical forms.

The EC gradient across the studied fen had a strong impact on biologically dependent carbon sequestration (Figure 5.2), with decreasing biomass production from more saline to less saline parts of the fen. Within peatland plant productivity varied greatly due to differences in WTD, and a strong negative effect of elevated EC ($>15 \text{ mS cm}^{-1}$) coupled with prolonged flooding on primary productivity and respiration was found. Consequently, although the accumulation of organic matter under saline conditions depends mainly on the presence of a high water table (Trites and Bayley 2009a), continuous waterlogging especially in areas with $\text{EC} > 15 \text{ mS cm}^{-1}$ should be avoided in constructed fens, as it can reduce CO_2 sequestration.

This study suggests that vegetation cover is of paramount importance for CO_2 exchange within ponds, and ponds with dense macrophyte cover had higher GEP comparatively to phytoplankton-dominated ponds. Given this, fen design should ensure pond construction is favourable for vegetation establishment. Salt-tolerant *S. pectinata* seems to be useful for increasing carbon uptake within open-water areas in constructed fens, but further studies are required to determine the most suitable species composition under different salinity levels. Because aquatic areas within western boreal forests have increased evaporative losses (Devito et al. 2012), and dense macrophyte cover can result in more intense evapotranspiration and a consequent decline in water level (Xu et al. 2014), macrophyte control through planting and harvest seems to be necessary for achieving the highest possible GEP that would not affect water balance in constructed ponds. Although productivity of planktonic algae seem to be low in the studied ponds, benthic microbial mats were associated with the highest GEP suggesting possible usefulness of the microbial mats for increasing productivity in constructed open-water areas.

Microbial mats may be suitable for mesosaline ponds where growth of macrophytes is limited due to salt content; however, detailed study of role of the mats in carbon transformation in ponds is necessary to determine their usefulness for wetland construction in AOSR.

5.5. Conclusion

Notable differences in CO₂ fluxes between ridges, depressions, and ponds reveal obvious spatial heterogeneity in saline fen carbon dynamics. Vegetation properties, WTD, and EC were identified as the main controlling factors on CO₂ fluxes within peatland. Microtopography was important for CO₂ fluxes, largely through its alteration of relations between CO₂ exchange and environmental factors, and more complex relationships between NEE, GEP, R and environmental variables were observed within depressions. Within open water areas (ponds), changes in CO₂ fluxes were mostly associated with vegetation density and phosphate concentration. This study illustrated importance of appropriate choice of vegetation communities for open-water areas within constructed fens; moreover, the results suggested that development of planting schemes with respect to microtopographical differences will help to support carbon capture within constructed fens.

In this study, differences in NEE, R, and GEP between hyposaline and more mesosaline parts of the peatland were observed, and were primarily associated with vegetation LAI, WTD, and EC. Moreover, the data illustrate that microtopography has a strong influence on the relationship between CO₂ exchange and environmental conditions, and depressions are characterized by more complex relationships between NEE, GEP, R and environmental variables (Figure 5.7).

5.6. Acknowledgements

We wish to thank Adam Green, Corey Wells, George Sutherland, Eric Kessel, Dr. Scott Ketcheson, Matthew Elmes, Kate Jamieson, Greg Carron, Tristan Gingras-Hill, and Volodymyr Sivkov for help with field work; Kishari Sooriya Arachchilage (Western Ag Innovations Inc., Saskatoon, Canada) for help with PRS Probes; Vito Lam for chemical analyses. Funding provided by the Natural Science and Engineering Research Council (NSERC) of Canada, Collaborative Research and Development Program, co-funded by Suncor, Energy Inc., Imperial Oil Resources Limited and Shell Canada Energy (Price, Petrone); NSERC Discovery Grant Program (Petrone, Price); NSERC Northern Supplement (Petrone); and Northern Studies Training Program (Volik).

6. Summary

Saline boreal fens (minerotrophic peat-forming wetlands) have been considered as appropriate natural analogs for reclamation in areas affected by salinization in the Athabasca Oil Sands Region (AOSR). Because an understanding of the main drivers of carbon uptake and storage within the fens can provide insights into biogeochemical functioning of constructed wetlands under saline conditions, this thesis presented the first time assessment of environmental controls on carbon sequestration in a saline boreal fen near Fort McMurray (Alberta, Canada). General characteristic of saline wetlands, introduction into carbon sequestration in peat-forming wetlands as well as into the main challenges associated with fen construction in AOSR were discussed in chapter one.

Chapter two presented paleolimnological study that investigated salinity change in three ponds (Lager, Pilsner, and South Ponds) within the fen using weighted-averaging transfer functions based on diatoms and an environmental dataset from 32 saline boreal ponds. This study showed that diatom-inferred (DI) salinity fluctuation in the fen were associated with changes in cumulative departure from mean precipitation (CDLM) in Fort McMurray area, but relations between precipitation and DI-salinity were complicated by pond hydrologic functioning. While in a precipitation-fed pond, declines in salinity were associated with rises in precipitation resulted in dilution of salt content in pond water, in ponds located within a saline groundwater discharge zone, increases in salinity coincided with increases in precipitation due to intensification of saline ground water input from the saline aquifer. Pond connectivity with adjacent freshwater wetlands was also important for explanation of salinity changes because of input of fresh water into ponds associated with increases in precipitation. The results emphasized the need to consider notable salinity fluctuation within natural saline fens, coupled with complexity of “salinity – precipitation – groundwater” relationships, while developing design of constructed fens and predicting constructed fen potential resilience under climate change.

Chapter three sought to determine relations between organic matter accumulation rates (OMAR) estimated from ^{210}Pb - age model and organic matter content (as measured by loss-on-ignition), DI-salinity, and changes in hydrological conditions and vegetation inferred from macrofossils in three studied ponds. Estimated salinity levels (3–21 ppt) did not reduce rates of

organic matter accumulation because median OMAR in three cores was close to rates observed in freshwater boreal and subarctic ponds. Results from this study showed that relationships between organic matter accumulation and salinity level are intricate because strong and weak, positive and negative correlations between OMAR and DI-salinity were found in pond sediment cores. Thus, it was concluded that salinity was not the main driver of changes in OM, and OMAR was more influenced by changes in water level, pond regime and primary produces as revealed by macrofossil data. As high OMAR in studied ponds were associated with low decomposition rates rather than with high primary productivity rates, it seems that development of future fen design should be based on attentive analysis of factors that can reduce decay rates (e.g., litter quality, water level fluctuation).

Chapter four presented paleoecological study of effect of salinity, vegetation cover, and hydrological conditions on long-term apparent rate of carbon accumulation (LARCA) in terrestrial parts of the fen. In the less saline part of the study site, variations in LARCA were associated with macrofossil-inferred changes in water table depth (WTD), and high LARCA values corresponded to periods with high water table. In contrast, in more saline part of the fen, no increases in LARCA in response to rises in water table were observed. From this, it was concluded that low salinity ($EC < 5 \text{ mScm}^{-1}$) did not affect “carbon accumulation – hydrology” links while high salinity ($EC > 10 \text{ mScm}^{-1}$) altered links between LARCA and water table depth possibly via the negative effect on the plant productivity. Observed mean LARCA in the less saline part of the site ($29.67 \text{ gm}^{-2} \text{ yr}^{-1}$) suggested that under low salinity saline fens can accumulate carbon at the rates comparable to rich fens, but under high salinity carbon accumulation is notably lower as revealed by mean LARCA of $9.79 \text{ gm}^{-2} \text{ yr}^{-1}$ in more saline part of the fen. This study showed that maintaining high and stable water table, coupled with a proper choice of vegetation with respect to microtopography is of paramount importance not only for successful initiation of peat accumulation, but also for long-term carbon storage within constructed fens. However, continuous waterlogging, coupled with high salinity ($EC > 10 \text{ mS cm}^{-1}$) affect carbon accumulation and should not be allowed at constructed fens. Results from this study indicated that *Triglochin maritima* and *Atriplex prostrata* are proper candidates for planting within depressions in constructed fens while *Juncus balticus*, *Hordeum jubatum*, *Calamagrostis* spp. and *Hierochloe* spp. are more suitable for planting within ridges for supporting long-term carbon storage in constructed fens.

The assessment of net ecosystem exchange (NEE), ecosystem respiration (R), and gross primary productivity (GEP) within open-water and terrestrial areas within the fen was presented in chapter five. Notable differences in CO₂ fluxes between both aquatic and terrestrial, elevated and depressed areas were observed that reveal obvious spatial heterogeneity in saline fen carbon dynamics. Vegetation properties, water table depth, and electrical conductivity were identified as the main controlling factors for CO₂ fluxes within terrestrial areas. Microtopography was important for CO₂ fluxes, largely through its alteration of relations between CO₂ exchange and environmental factors, and more complex relationships between NEE, GEP, R and environmental variables were observed within depressions. Within open water areas, changes in CO₂ fluxes were mostly associated with vegetation density and phosphate concentration. This study illustrated importance of appropriate choice of vegetation communities for open-water areas within constructed fens; moreover, the results suggested that development of planting schemes with respect to microtopographical differences for terrestrial areas will help to support carbon capture within constructed fens.

7. General conclusions and recommendations

In conclusion, the main findings of this study are:

- The studied saline fen is a dynamic system, and notable fluctuations in salinity in response to environmental changes on regional and local scale have occurred over time. Precipitation constitutes the primary driver of salinity in open-water areas, but hydrological functioning of ponds, coupled with connectivity to regional saline aquifers and adjacent freshwater wetlands can alert links between salt concentration and input of meteoric water.
- Although vegetation is the primary control on carbon sequestration, other factors that have an effect on carbon uptake do not always coincide with the drivers of long-term carbon accumulation; moreover, combination and importance of controls on carbon sequestration can differ between open-water and terrestrial areas, ridges and depressions (Figure 7.1).
- Vegetation properties, water table depth, and electrical conductivity were identified as the main controlling factors on carbon capture and long-term accumulation within terrestrial areas. Additional drivers of carbon uptake (e.g., soil moisture, availability of magnesium, manganese and calcium) were found within depressions suggesting that microtopographical differences can modify relations between CO₂ exchange and environmental variables.
- Water table depth was positively related to long-term carbon accumulation and negatively to current carbon uptake. Carbon sequestration was not severely affected by low salinity (EC < 5 mS cm⁻¹), but high salinity (EC > 10 mS cm⁻¹) had an extremely negative effect on long-term carbon storage and carbon uptake within terrestrial areas of the fen.
- Terrestrial areas accumulated carbon at the overall rate lower than in western continental fens, and one of the causes of such a lower rate can be a decreased rate of primary productivity under increased salinity as suggested by assessment of current carbon uptake in the fen.
- Within open-water areas, carbon uptake was driven by vegetation density and phosphate concentration while water level and type of primary producers were the

most important factors determining rate of organic matter accumulation. Salinity was of secondary importance for explanation of changes in both carbon capture and storage in studied ponds.

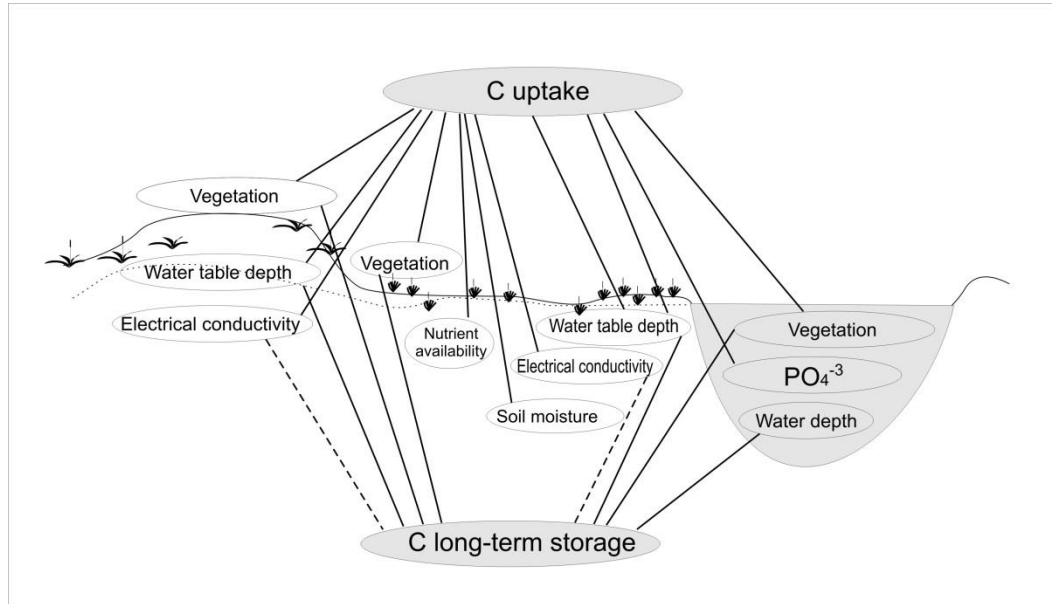


Figure 7.1. Conceptual diagram of controls on carbon uptake and long-term storage in a saline boreal fen. Broken lines indicate that $EC > 10 \text{ mS cm}^{-1}$ has an effect on carbon storage.

- Open-water areas have accumulated organic matter at rate comparable to freshwater boreal and subarctic ponds. Such relatively high rate of organic matter accumulation in ponds is a function of input and slow decay of terrestrial plant litter whereas contribution from aquatic primary producer is smaller as suggested by very low recent GEP in studied ponds.

Based on the above results, the following suggestions can be useful for future saline fen construction projects:

- It is essential to maintain slightly saline conditions with mean EC up to 5 mS cm^{-1} to support the carbon sequestration in constructed fens.
- High and stable groundwater level is important not only for the successful initiation of peat accumulation at constructed fens, but also for long-term carbon storage. However, prolonged inundation (mean water table level above ground), especially coupled with high salinity ($EC > 10 \text{ mS cm}^{-1}$) appear to have extremely negative

effect on carbon uptake and long-term accumulation within terrestrial areas and should be avoided at constructed fens.

- Incorporation of landscape connectivity into post-mined landscape design plans can be useful not only for maintaining the water balance of reclaimed area, but also for salinity control.
- Constructed saline fens should be designed in a way that will allow regulation of some local settings (e.g., water input, drainage, connectivity with adjacent wetlands and waterbodies) and promote the adaptation of manmade system to new conditions.
- Topographic controls can be used not only for the regulation of water drainage, water table position and salinity, but also for regulation of carbon uptake within terrestrial areas in constructed fens.
- Incorporating open-water areas into constructed fen design will make constructed system more complex and less predictable because manipulations of environmental characteristics (e.g., water table depth, nutrient load, EC) in order to improve functioning of the fens can have an opposite effect on CO₂ uptake within aquatic and terrestrial parts.
- Development of planting schemes for terrestrial areas within constructed fens should be based on microtopographic differences to supporting the highest possible CO₂ uptake within elevated and depressed forms.
- *J. balticus*, *Calamagrostis* spp. *H. jubatum* can support high CO₂ uptake and long-term accumulation within ridges while *T. maritima* and *A. prostrata* are more suitable for depressions.
- Attention should be paid to vegetation within riparian areas around constructed ponds as litter quality influence decay rates that in turn have stronger effect on rates of organic matter accumulation comparatively to primary productivity.
- Unvegetated ponds should not be included into constructed fen design. Planting macrophytes such as *Potamogeton* spp. can help increase rates of carbon uptake and organic matter accumulation in constructed ponds, but rational macrophyte control through planting and harvest is necessary to prevent intense evapotranspiration and reduction of water volume in the waterbodies.

- This study assessed controls on carbon uptake and carbon/organic matter accumulation within naturally saline fen dominated by chlorides while constructed fens are expected to be dominated by sulphates. Consequently, further studies of effects of brine composition and total salt concentration on carbon capture and accumulation are necessary to predict rates of carbon sequestration in constructed fens. In addition, more detailed study with a wide range of plant species is required to determine the most appropriate planting scheme to support the highest rates of carbon capture and accumulation. Finally, a study of role of benthic microbial mats in carbon transformation in ponds is necessary to determine their usefulness for increasing carbon sequestration in constructed wetlands in the Athabasca Oil Sands Region.

References

- Abrol IP, Yadav JSP, Massoud FI (1988) Salt-affected soils and their management. FAO Soil Bulletin 39. Rome: Food and Agriculture Organization of the United Nations 131 p. Available at <http://www.fao.org/docrep/x5871e/x5871e00.htm> (accessed 2016.05.19)
- Alberta Environment (2008) Guideline for wetland establishment on reclaimed oil sands leases (2nd edition). Prepared by Harris ML of Lorax Environmental for the Wetlands and Aquatics Subgroup of the Reclamation Working Group of the Cumulative Environmental Management Association. Fort McMurray, AB
- Alberta Environment and Parks (2015) Reclamation Criteria for Wellsites and Associated Facilities for Peatlands, October, 2015, Edmonton, Alberta, PP 142. <http://aep.alberta.ca> (accessed 2016.05.19).
- Alberta Landscape and Landuses (2015) Precipitation. <http://www.abll.ca/tables/Meteorology/Precipitation> (accessed 2016.05.01)
- Alm J, Talanov A, Saarnio S, Silvola J, Ikkonen E, Aaltonen H, Nykanen H, Martikainen PJ (1997) Reconstruction of the carbon balance for microsites in a boreal oligotrophic pine fen, Finland. *Oecologia* 110:423–431
- Anas MUM, Scott KA, Wissel B (2015) Carbon budgets of boreal lakes: state of knowledge, challenges and implications. *Environ Rev* 23:275–287.
- Andrews SE, Schultz R, Frey SD, Bouchard V, Varner R, Ducey MJ (2013) Plant community structure mediates potential methane production and potential iron reduction in wetland mesocosms. *Ecosphere* 4:1–17.
- Andriashek L (2003) Quaternary geological setting of the Athabasca oil sands (in situ) area, northeast Alberta. Alberta Energy and Utilities Board, EUB/AGS Earth Sciences Report, April.
- Appleby PG, Oldfield F (1978) The calculation of lead-210 dates assuming a constant rate of supply of unsupported ^{210}Pb to the sediment. *Catena* 5:1–8.
- Arzani A (2008) Improving salinity tolerance in crop plants: a biotechnological view. *In Vitro Cell Dev Biol Plant* 44:373–383
- Asad A (2001) Adaptation trials of *Atriplex* and *Maireana* species and their response to saline waterlogged conditions in Pakistan. *Pak. J Biol Sci* 4:451–457.
- Baskaran M, Nix J, Kuyper C, Karunakara N (2014) Problems with the dating of sediment core using excess ^{210}Pb in a freshwater system impacted by large scale watershed changes. *J Environ Radioactiv* 138:355–363.
- Bastviken D, Persson L, Odham G, Tranvik L (2004) Degradation of dissolved organic matter in oxic and anoxic lake water. *Limnol Oceanogr* 49:109–116.
- Batjes NH (1996) Total carbon and nitrogen in the soils of the world. *Eur J Soil Sci* 47:151–163.

Battarbee RW, Jones VJ, Flower RJ, Cameron NG, Bennion H, Carvalho, Juggins S (2001) Diatoms. In: Smol JP, Birks HJB, Last W (eds) Tracking Environmental Change Using Lake Sediments. Vol. 3: Terrestrial, Algal, and Siliceous Indicators. Kluwer Academic Publishers, Dordrecht, pp 155–202.

Bayley SE, Prather CM (2003) Do wetland lakes exhibit alternative stable states? Submersed aquatic vegetation and chlorophyll in western boreal shallow lakes. *Limnol Oceanogr* 48:2335–2345.

Beilman DW, MacDonald GM, Smith LC, Reimer PJ (2009) Carbon accumulation in peatlands of West Siberia over the last 2000 years. *Global Biogeochem Cycles* 23:1012.

BGC Engineering Inc. (2010) Review of reclamation options for oil sands tailings substrates. Oil Sands Research and Information Network, University of Alberta, School of Energy and the Environment, Edmonton, Alberta. OSRIN Report No. TR-2

Biagi K (2015) Understanding flow pathways, major chemical transformations and water sources using hydrochemical data in a constructed fen, Alberta. M.Sc. Thesis, McMaster University

Binford MW (1990) Calculation and uncertainty analysis of ^{210}Pb dates for PIRLA project lake sediment cores. *J Paleolimnol* 3:253–267.

Blodau C (2002). Carbon cycling in peatlands: A review of processes and controls. *Environ Rev* 10:111–134.

Bonan GB, Van Cleve K (1992). Soil temperature, nitrogen mineralization and carbon source – sink relationships in boreal forests. *Can J For Res* 22:629–638.

Botch MS, Kobak KI, Vinson TS, Kolchugina TP (1995) Carbon pools and accumulation in peatlands of the Former Soviet Union. *Global Biogeochem Cycles* 9:37–46.

Bridgham SD, Pastor J, Janssens JA, Chapin C, Malterer TJ (1996) Multiple limiting gradients in peatlands: a call for a new paradigm. *Wetlands* 16:45–65.

Brouns K, Verhoeven JT, Hefting MM (2014) The effects of salinization on aerobic and anaerobic decomposition and mineralization in peat meadows: The roles of peat type and land use. *J Environ Management* 14:44–53

Brown S, Petrone R, Mendoza C, Devito K (2010) Surface vegetation controls on evapotranspiration from a sub-humid Western Boreal Plain. *Hydrol Process* 24:1072–1085.

Bu Z, Hans J, Li H, Zhao G, Zheng X, Ma J, Zeng J (2011) The response of peatlands to climate warming: A review. *Acta Ecologica Sinica* 31:157–162.

Bubier J, Crill P, Mosedale A, Frohling S (2003) Peatland responses to varying interannual moisture conditions as measured by automatic CO₂ chambers. *Glob Biogeochem Cycles* 17:1–15.

Burow LC, Woebken D, Marshall IP, et al (2013) Anoxic carbon flux in photosynthetic microbial mats as revealed by metatranscriptomics. *ISME J* 7:817–829.

Butcher JB, Nover D, Johnson TE, Clark CM (2015) Sensitivity of lake thermal and mixing dynamics to climate change. *Climatic Change* 129: 295.

Cabezas A, Pallasch M, Schönfelder I, Gelbrecht J, Zak D (2014) Carbon, nitrogen, and phosphorus accumulation in novel ecosystems: Shallow lakes in degraded fen areas. *Ecol Eng* 66:63–71.

Cai T, Flanagan LB, Syed KH (2010) Warmer and drier conditions stimulate respiration more than photosynthesis in a boreal peatland ecosystem: analysis of automatic chambers and eddy covariance measurements. *Plant Cell Environ* 33:394–407.

Campbell ID, Campbell C, Vitt DH, Kelker D, Laird LD, et al. (2000) A first estimate of organic carbon storage in Holocene lake sediment in Alberta, Canada. *Paleolimnol* 24:395–400.

Campbell ID, Campbell C, Yu Z, Vitt DH, Apps MJ (2000) Millennial-scale rhythms in peatlands in the western interior of Canada and in the global carbon cycle. *Quat Res* 54:155–158.

Canavan RW, Slomp CP, Jourabchi P, Van Cappellen P, Laverman A M, Van den Berg GA (2006) Organic matter mineralization in sediment of a coastal freshwater lake and response to salinization. *Geochim Cosmochim Acta* 70:2836–2855.

Carrière S (2002) Photographic key for the microhistological identification of some Arctic vascular plants. *Arctic* 55:247–268.

Cebrian J, Duarte CM (1995) Plant growth-rate dependence of detrital carbon storage in ecosystems. *Science* 268:1606–1608.

Chapin FS, Woodwell GM, Randerson JT, Rastetter EB, et al. (2006) Reconciling carbon-cycle concepts, terminology, and methods. *Ecosystems* 9: 1041–1050.

Chymko N (2000) Guideline for wetland establishment on reclaimed oil sands leases. Oil Sands Wetlands Working Group, Alberta Environment, Environmental Service, Edmonton, Canada, Report #ESD/LM/00-1, T/517.

Clymo RS, Turunen J, Tolonen K (1998) Carbon Accumulation in Peatland. *Oikos* 81:368–388.

Cobbaert D, Wong A, Bayley S (2014) Precipitation-induced alternative regime switches in shallow lakes of the boreal plains (Alberta, Canada). *Ecosystems* 17: 535–549.

Colla G, Roupael Y, Cardarelli M, Tullio M, Rivera CM, Rea E (2008) Alleviation of salt stress by arbuscular mycorrhizal in zucchini plants grown at low and high phosphorus concentration. *Biol Fertil Soils* 44:501–509.

Cooper A (1982) The effects of salinity and waterlogging on the growth and cation uptake of salt marsh plants. *New Phytologist* 90:263–275.

Cooper A (1984) A comparative study of the tolerance of salt marsh plants to manganese. *Plant Soil* 81:47–59

Cooper RN, Wissel B (2012) Loss of trophic complexity in saline prairie lakes as indicated by stable-isotope based community-metrics. *Aquat Biosyst* 8:6.

Couwenberg J, Dommain R, Joosten H (2009) Greenhouse gas fluxes from tropical peatlands in south-east Asia. *Glob Change Biol* 16:1715–1732.

Cumming BF, Smol JP (1993) Development of diatom-based salinity models for paleoclimatic research from lakes in British Columbia (Canada). *Hydrobiologia* 269–270: 179–96.

Curco A, Ibanez C, Day JW, Prat N (2002) Net primary production and decomposition of salt marshes of the Ebre Delta (Catalonia, Spain). *Estuaries* 25:309–324

Dean WE, Gorham E (1998) Magnitude and significance of carbon burial in lakes, reservoirs, and peatlands. *Geology* 26:535–538.

Del Giorgio PA, Cole JJ, Cimperlis A (1997) Respiration rates in bacteria exceed phytoplankton production in unproductive aquatic systems, *Nature* 385:148–151.

Devito K, Mendoza C, Qualizza C (2012) Conceptualizing water movement in the boreal plains – implications for watershed reconstruction. Synthesis report prepared for the Canadian Oil Sands Network for Research and Development, Environmental and Reclamation Research Group, pp 164. Available at <https://era.library.ualberta.ca/downloads/6108vb631> (accessed 2015.11.22).

Devito KJ, Creed IF, Fraser CJD (2005) Controls on runoff from a partially harvested aspen-forested headwater catchment, Boreal Plain, Canada. *Hydrol Process* 19: 3–25. .

Dubiński J (2013) Sustainable Development of Mining Mineral Resources. *J Sustain Min* 12:1–6.

Egan TP, Ungar IA (2000) Mortality of the salt marsh species *Salicornia europaea* and *Atriplex prostrata* (Chenopodiaceae) in response to inundation. *Ohio Journal of Science* 100:24–27.

Elser JJ, Bracken MES, Cleland EE, et al (2007) Global analysis of nitrogen and phosphorus limitation of primary producers in freshwater, marine and terrestrial ecosystems. *Ecol Lett* 10:1135–1142.

Environment and Parks (2015) Reclamation Criteria for Wellsites and Associated Facilities for Peatlands, October, 2015, Edmonton, Alberta, PP 142. Available at <http://aep.alberta.ca> (accessed 2016.05.19)

Environment Canada (2015) Calculation Information for 1981 to 2010 Canadian Normals Data. Fort McMurray. Available http://climate.weather.gc.ca/climate_normals/station_metadata_e.html?StnId=2519 (accessed 2015.11.22)

Evelin H, Kapoor R, Giri B (2009) Arbuscular mycorrhizal fungi in alleviation of salt stress: a review. *Ann Bot* 104:1263–1280

Feng G, Zhang FS, Xi L, Tian CY, Tang C, Rengel Z (2002) Improved tolerance of maize plants to salt stress by arbuscular mycorrhiza is related to higher accumulation of soluble sugars in roots. *Mycorrhiza* 12:185–190

Ferone JM, Devito KJ (2004) Shallow groundwater-surface water interactions in pond-peatland complexes along a Boreal Plains topographic gradient. *J Hydrol* 292: 75–95.

Flanagan LB, Syed KH (2011) Stimulation of both photosynthesis and respiration in response to warmer and drier conditions in a boreal peatland ecosystem. *Glob Change Biol* 17:2271–2287.

Fogel BN, Crain CM, Bertness MD (2004) Community level engineering effects of *Triglochin maritima* (seaside arrowgrass) in a salt marsh in northern New England, USA. *J Ecol* 92:589–597.

Foster IDL, Mighall TM, Proffitt H, Walling DE, Owens PN (2006) Post-depositional ¹³⁷Cs mobility in the sediments of three shallow coastal lagoons, SW England. *J Paleolimnol* 35: 881–95.

Fritz SC (1990) Twentieth-century salinity and water-level fluctuations in Devils Lake, North Dakota: Test of a diatom-based transfer function. *Limnol Oceanogr* 35:1771–1781.

Fritz SC (2013) Salinity and climate reconstructions from continental lakes. In Elias SA, Mock CJ (eds) *Encyclopedia of Quaternary Science*, 2nd edition. Elsevier, pp 507–515.

Fritz SC, Cumming BF, Gasse F, Laird KR (2010) Diatoms as indicators of hydrologic and climatic change in saline lakes. In Stoermer EF, Smol JP (eds) *The Diatoms: Applications for the Environmental and Earth Sciences*, 2nd edition. Cambridge University Press, Cambridge, pp 186–208.

Fritz SC, Juggins S, Battarbee RW (1993) Diatom assemblages and ionic characterization of lakes of the northern Great Plains, North America: a tool for reconstructing past salinity and climate fluctuations. *Can J Fish Aquat Sci* 50: 1844–1856.

Frolking S, Roulet NT, Moore TR, Lafleur PM, Bubier JL, Crill PM (2002) Modeling seasonal to annual carbon balance of Mer Bleue Bog, Ontario, Canada. *Global Biogeochem Cycles* 16:1030–1050.

Gasse F, Barker P, Gell PA, Fritz SC, Chalié F (1997) Diatom-inferred salinity in palaeolakes: An indirect tracer of climate change. *Quaternary Sci Rev* 16: 547–563.

Gasse F, Juggins S, Khelifa LB (1995) Diatom-based transfer functions for inferring past hydrochemical characteristics of African lakes. *Palaeogeogr Palaeoclimat Palaeoecol* 117:31–54.

Gibberd MR, Colmer TD, Cocks PS (1999) Root porosity and oxygen movement in waterlogging-tolerant *Trifolium tomentosum* and -intolerant *Trifolium glomeratum*. *Plant Cell Environ* 22:1161–1168.

Gorham E (1991), Northern peatlands, role in the carbon cycle and probable responses to climatic warming. *Ecol Appl* 1:182–195

Government of Alberta Energy, 2017. Oil Sands: Facts and Statistics. <http://www.energy.alberta.ca/OilSands/791.asp> (accessed 2017.02.23).

Government of Canada (2017) Canadian Climate Normals 1981-2010 Station. Fort McMurray. http://climate.weather.gc.ca/climate_normals/results_1981_2010_e.html?searchType=stnProv&lstProvince=AB&txtCentralLatMin=0&txtCentralLatSec=0&txtCentralLongMin=0&txtCentralLongSec=0&stnID=2519&dispBack=0 (accessed 2017.02.22).

Grasby SE, Betcher RN (2002) Regional hydrogeochemistry of the carbonate rock aquifer, southern Manitoba. *Can J Earth Sci* 39:1053–1063.

Guerrero R, Mas J (1989) Multilayered microbial communities in aquatic ecosystems: growth and loss factors. In: Cohen Y, Rosenberg E (eds) *Microbial mats – physiological ecology of benthic microbial communities*. American Society for Microbiology, Washington, pp 37–51.

Halsey LA, Vitt DH, Bauer IE (1998) Peatland initiation during the Holocene in continental western Canada. *Climatic Change* 40:315–342.

Hamilton JD, Kelly CA, Rudd JW, Hesslein RH, Roulet NT (1994) Flux to the atmosphere of CH₄ and CO₂ from wetland ponds on the Hudson Bay lowlands (HBLs). *J Geophys Res* 99:1495–1510.

Hammer Ø, Harper DAT and Ryan PD (2001) PAST: Paleontological Statistics Software Package for Education and Data Analysis. *Palaeontologia Electronica* 4: 9.

Hayashi M, Farrow C (2014) Watershed-scale response of groundwater recharge to inter-annual and inter-decadal variability in precipitation (Alberta, Canada). *Hydrogeol J* 22: 1825–1839.

Heagle D, Hayashi M, Kamp G Van Der (2013) Surface-subsurface salinity distribution and exchange in a closed-basin prairie wetland. *J Hydrol* 478:1–14.

Heijmans MMPD, Arp WJ, Berendse F (2001) Effects of elevated CO₂ on vascular plants on evapotranspiration in bog vegetation. *Glob Change Biol* 7:817–827.

Heiri O, Lotter AF and Lemcke G (2001) Loss on ignition as a method for estimating organic and carbonate content in sediments: Reproducibility and comparability of results. *Journal of Paleolimnology* 25:101–110.

Herbert ER, Boon P, Burgin AJ, et al (2015) A global perspective on wetland salinization: ecological consequences of a growing threat to freshwater wetlands. *Ecosphere* 6:art206.

Herbst DB (2001) Gradients of salinity stress, environmental stability and water chemistry as a template for defining habitat types and physiological strategies in inland salt waters. *Hydrobiologia* 466: 209–219.

Hilbert DW, Roulet N and Moore T (2000) Modelling and analysis of peatlands as dynamical systems. *J Ecol* 88:230–242.

Hobbs WO, Fritz SC, Stone JR, Donovan JJ, Grimm EC, Almendinger JE (2011) Environmental history of a closed-basin lake in the US Great Plains: Diatom response to variations in groundwater flow regimes over the last 8500 cal. yr BP. *Holocene* 21: 1203–1216.

Holmquist J, MacDonald GM (2014) Peatland succession and long-term apparent carbon accumulation in central and northern Ontario, Canada. *The Holocene* 24:1075–1089.

Hughes PDM, Barber KE (2003) Mire development across the fen-bog transition on the Teifi floodplain at Tregaron Bog, Ceredigion, Wales, and a comparison with 13 other raised bogs. *J Ecol* 91:253–264.

Humphreys ER, Lafleur PM, Flanagan LC, et al. (2006) Summer carbon dioxide and water vapour fluxes across a range of northern peatlands. *J Geophys Res* 111: G04011.

Hutton MJ, MacDonald GM, Mott RJ (1994) Postglacial vegetation history of the Mariana Lake region, Alberta. *Can J Earth Sci* 31:418–425.

Israelsen KR, Ransom CV, Waldron BL (2011) Salinity tolerance of foxtail barley (*Hordeum jubatum*) and desirable pasture grasses. *Weed Sciences* 59:500–505.

Jahromi F, Aroca R, Porcel R, Ruiz-Lozano JM (2008) Influence of salinity on the in vitro development of *Glomus intraradices* and on the in vivo physiological and molecular responses of mycorrhizal lettuce plants. *Microb Ecol* 55:45–53

Jellison R, Anderson RF, Melack JM, Heil D (1996) Organic Matter accumulation in sediments of hypersaline Mono Lake during a period of changing salinity. *Limnol Oceanogr* 41: 1539–1544.

Johnson E, Miyanishi K (2008) Creating new landscapes and ecosystems: the Alberta Oil Sands. *Ann N Y Acad Sci* 1134:120–145

Juggins S (2011) C2 Version 1.7: software for ecological and paleoecological data analysis and visualisation. University of Newcastle, Newcastle upon Tyne. Available at <https://www.staff.ncl.ac.uk/stephen.juggins/software/code/C2.pdf> (accessed 2016.03.12).

Juszczak R, Humphreys E, Acosta M, et al (2013) Ecosystem respiration in a heterogeneous temperate peatland and its sensitivity to peat temperature and water table depth. *Plant Soil* 366:505–520.

Juutinen S, Rantakari M, Kortelainen P, Huttunen JT, Larmola T, Alm J, Silvola J, Martikainen PJ (2009) Methane dynamics in different boreal lake types. *Biogeosciences* 6: 209–223.

Kankaala, P., Huotari, J., Peltomaa, E., Saloranta, T., Ojala, A., 2006. Methanotrophic activity in relation to methane efflux and total heterotrophic bacterial production in stratified, humic, boreal lake. *Limnol. Oceanogr.* 51, 1195–1204.

Kessel E (2016) The Hydrogeochemistry of a Constructed Fen Peatland in a Post-Mined Landscape in the Athabasca Oil Sands Region, Alberta, Canada. M.Sc. Thesis, University of Waterloo.

Kessler S, Barbour SL, van Rees KCJ, Dobchuk. BS (2010) Salinization of soil over saline-sodic overburden from the oil sands in Alberta. *Can J Soil Sci* 90:637–647.

Ketcheson SJ, Price JS, Carey SK, Petrone RM, Mendoza C A, Devito KJ (2016) Constructing fen peatlands in post-mining oil sands landscapes: Challenges and opportunities from a hydrological perspective. *Earth-Science Reviews* 161:130–139.

Khadka B, Munir TM, Strack M (2015) Effect of environmental factors on production and bioavailability of dissolved organic carbon from substrates available in a constructed and reference fens in the Athabasca oil sands development region. *Ecol Eng* 84:596–606.

Kobayashi T, Ralph TJ, Ryder DS, Hunter SJ (2013) Gross primary productivity of phytoplankton and planktonic respiration in inland floodplain wetlands of southeast Australia: Habitat-dependent patterns and regulating processes. *Ecol Res* 28:833–843.

Koelbener A, Strom L, Edwards PJ, Venterink HO (2010) Plant species from mesotrophic wetlands cause relatively high methane emissions from peat soil. *Plant Soil* 326:147–158

Korhola A, Alm J, Tolonen K et al. (1996) Three-dimensional reconstruction of carbon accumulation and CH₄ emission during nine millennia in a raised mire. *J Quaternary Sci* 11:161–165.

Kortelainen P, Rantakari M, Pajunen H, Mattsson T, Juutinen S, Larmola T, Alm J, Silvola J, Martikainen PJ (2013) Carbon evasion/accumulation ratio in boreal lakes is linked to nitrogen. *Global Biogeochem Cycles* 27: 363–374.

Kunin V, Raes J, Harris JK, et al. (2008) Millimeter-scale genetic gradients and community-level molecular convergence in a hypersaline microbial mat. *Mol Syst Biol* 4: 198.

Kutzbach L, Schneider J, Sachs T, et al (2007) CO₂ flux determination by closed-chamber methods can be seriously biased by inappropriate application of linear regression. *Biogeosciences* 4:1005–1025.

Laan P, Berrevoets MJ, Lythe S, Armstrong W, Blom CWPM (1989) Root morphology and aerenchyma formation as indicators of the flood tolerance of *Rumex* species. *J Ecol* 77:693–703.

Lafleur PM, Moore TR, Roulet NT, Frolking S (2005) Ecosystem respiration in a cool temperate bog depends on peat temperature but not water table. *Ecosystems* 8: 619–629.

Laird KR, Fritz SC, Maasch KA, Cumming BF (1996) Greater drought intensity and frequency before AD 1200 in the Northern Great Plains, USA. *Nature* 384: 552–554.

Last WM, Ginn FM (2005) Saline systems of the Great Plains of western Canada: an overview of the limnogeology and paleolimnology. *Saline Systems* 1:10.

Ley RE, Harris JK, Wilcox J, et al. (2006). Unexpected diversity and complexity of the Guerrero Negro hypersaline microbial mat. *Appl Environ Microbiol* 72:3685–3695.

Limpens J, Berendse F, Blodau C, et al (2008) Peatlands and the carbon cycle: from local processes to global implications - a synthesis. *Biogeosciences* 5:1475–1491.

Loisel J, Garneau M (2010) Late Holocene paleoecohydrology and carbon accumulation estimates from two boreal peat bogs in eastern Canada: potential and limits of multi-proxy archives. *Palaeogeogr Palaeoclim Palaeoecol* 291:493–533.

Lund M, Lafleur PM, Roulet NT, et al. (2010) Variability in exchange of CO₂ across 12 northern peatland and tundra sites. *Glob Change Biol* 16:2436–2448.

Mack MC, Schuur EAG, Syndergaard B-HM, Shaver GR, Chapin FS (2004). Ecosystem carbon storage in arctic tundra reduced by long-term nutrient fertilization. *Letters to Nature* 431:440–443

Macrae ML, Bello RL, Molot L (2004) Long-term carbon storage and hydrological control of CO₂ exchange in tundra ponds in the Hudson Bay Lowland. *Hydrol Process* 18:2051–2069.

Malmer N, Johansson T, Olsrud M, Christensen TR (2005) Vegetation, climatic changes and net carbon sequestration in a North-Scandinavian subarctic mire over 30 years. *Glob Change Biol* 11:1895–1909.

Mauquoy D, Hughes P, Van Geel B (2010) A protocol for plant macrofossil analysis of peat deposits. *Mires and Peat* 7:1–5.

Mavi MS, Marschner P, Chittleborough DJ, Cox JW, Sanderman J (2012) Salinity and sodicity affect soil respiration and dissolved organic matter dynamics differently in soils varying in texture. *Soil Biol Biochem* 45:8–13.

McLeod MK, Daniel H, Faulkner R, Murison R (2004) Evaluation of an enclosed portable chamber to measure crop and pasture actual evapotranspiration at small scale. *Agric Water Manag* 67:15–34.

Meiggs D, Taillefert M (2011) The effect of riverine discharge on biogeochemical processes in estuarine sediments. *Limnol Oceanogr* 56:1797–1810.

Meyers PA, Ishiwatari R (1993) Lacustrine organic geochemistry – an overview of indicators of organic matter sources and diagenesis in lake sediments. *Org Geochem* 20:867–900.

Meyers PA, Ishiwatari R (1995) Organic matter accumulation records in lake sediments. In: Lerman A, Imboden DM, Gat JR (eds) *Physics and Chemistry of Lakes*, Springer, Berlin Heidelberg, Berlin, Heidelberg, pp. 279–328.

Miller WD, Neubauer SC, Anderson IC (2001) Effects of sea level induced disturbances on high salt marsh metabolism. *Estuaries* 24:357–367.

Montemayor MB, Price JS, Rochefort L (2015) The importance of pH and sand substrate in the revegetation of saline non-waterlogged peat fields. *J Env Management* 163:87–97.

Montemayor MB, Price JS, Rochefort L, Boudreau S (2008) Temporal variations and spatial patterns in saline and waterlogged peat fields. 1. Survival and growth of salt marsh graminoids. *Env Experiment Botany* 62:333–342.

Moseman-Valtierra S, Abdul-Aziz OI, Tang J, et al (2016) Carbon dioxide fluxes reflect plant zonation and belowground biomass in a coastal marsh. *Ecosphere* 7:e01560.

Murphy MT, Moore TR (2010) Linking root production to aboveground plant characteristics and water table in a temperate bog. *Plant Soil* 336:219–231.

National Wetlands Working Group (1997) *The Canadian Wetland Classification System*. 2nd edition. Wetlands Research Centre, University of Waterloo, Waterloo, Ontario.

Necajeva J, Ievinsh G (2008) Seed germination of six coastal plant species of the Baltic region: effect of salinity and dormancy-breaking treatments. *Seed Science Research* 18:173–177.

Neill C (1992) Comparison of Soil Coring and Ingrowth Methods for Measuring Belowground Production. *Ecology* 73:1918–1921.

Neill C (1993) Seasonal flooding, soil salinity and primary production in northern prairie marshes. *Oecologia* 95:499–505.

Nelson DW, Sommers LE (1996) Total carbon, organic carbon, and organic matter. In: Sparks DL, Page AL, Helmke PA, Loeppert RH, Soltanpour PN, Tabatabai MA, Johnston CT, Sumner ME (eds) *Methods of Soil Analysis. Part 3, Chemical Methods*. Soil Science Society of America– American Society of Agronomy, Madison, pp 961–1010.

Neubauer SC (2013) Ecosystem Responses of a Tidal Freshwater Marsh Experiencing Saltwater Intrusion and Altered Hydrology. *Estuaries and Coasts* 36:491–507.

Nwaishi F, Petrone RM, Price JS, Andersen R (2015) Towards developing a functional-based approach for constructed peatlands evaluation in the Alberta Oil Sands Region, Canada. *Wetlands* 35:211–225.

Pelletier L, Strachan IB, Roulet NT, et al (2015) Effect of open water pools on ecosystem scale surface-atmosphere carbon dioxide exchange in a boreal peatland. *Biogeochemistry* 124:291–304.

Pelletier L, Strachan IB, Roulet NT, Garneau M (2015) Can boreal peatlands with pools be net sinks for CO₂? *Environ Res Lett* 10:035002.

Petrone RM, Silins U, Devito KJ (2007) Dynamics of evapotranspiration from riparian pond complex in the Western Boreal Forest, Alberta, Canada. *Hydrol Process* 21: 1391–1401.

Petrone RM, Solondz DS, Macrae ML, et al (2011) Microtopographical and canopy cover controls on moss carbon dioxide exchange in a western Boreal Plain peatland. 129:115–129.

Pezeshki SR, DeLaune RD (2012) Soil oxidation-reduction in wetlands and its impact on plant functioning. *Biology (Basel)* 1:196–221.

Phillips T, Petrone RM, Wells CM, Price JS (2015) Characterizing dominant controls governing evapotranspiration within a natural saline fen in the Athabasca Oil Sands of Alberta, Canada. *Ecohydrology* 9: 817–829. DOI: 10.1002/eco.1685.

Phillips T, Petrone RM, Wells CM, Price JS (2016) Characterizing dominant controls governing evapotranspiration within a natural saline fen in the Athabasca Oil Sands of Alberta, Canada. *Ecohydrology* 9:817–829.

Picek T, Cizkova H, Dusek J (2007) Greenhouse gas emissions from a constructed wetland: plants as important sources of carbon. *Ecol Eng* 31:98–106.

Pienitz R, Walker IR, Zeeb BA, Smol JP, Leavitt PR (1992) Biomonitoring past salinity changes in an athalassic subarctic lake. *Int J Salt Lake Res* 1: 91–123.

Pouliot R, Rochefort L, Graf MD (2012) Impacts of oil sands process water on fen plants: Implications for plant selection in required reclamation projects. *Env Pollut* 167:132–137.

Pouliot R, Rochefort L, Graf MD (2013) Fen mosses can tolerate some saline conditions found in oil sands process water. *Environmental and Experimental Botany* 89:44–50.

Pribyl DW (2010) A critical review of the conventional SOC to SOM conversion factor. *Geoderma* 156: 75–83.

Price J (1990) Coastal salt marshes: hydrology and salinity. *Can Geographer* 34:83–85.

Price JS, McLaren RG, Rudolph DL (2010) Landscape restoration after oil sands mining: conceptual design and hydrological modelling for fen reconstruction. *Int J Mining, Reclam Environ* 24 :109–23.

Price JS, McLaren RG, Rudolph DL (2010) Landscape restoration after oil sands mining: conceptual design and hydrological modelling for fen reconstruction. *Int J Mining Reclam Environ* 24:109–123.

Province of Alberta (2003) Environmental Protection and Enhancement Act and Regulations. Revised Statutes of Alberta 2000 Chapter E-12, with amendments in force as of December 18 2003. Alberta Queen's Printer

Purdy BG, Macdonald SE, Lieffers VJ (2005) Naturally saline boreal communities as models for reclamation of saline oil sand tailings. *Restor Ecol* 13:667–677.

Raich JW, Schlesinger WH (1992) The global carbon dioxide flux in soil respiration and its relationship to vegetation and climate. *Tellus* 44B:81–99.

Rayment GE, Higginson FR (1992). Australian laboratory handbook of soil and water chemical methods. Inkata Press, Port Melbourne.

Reavie ED, Edlund MB (2013) Assessing the performance of a diatom transfer function on four Minnesota lake sediment cores: Effects of training set size and sample age. *J Paleolimnol* 50:87–104.

Reavie ED, Juggins S (2011) Exploration of sample size and diatom-based indicator performance in three North American phosphorus training sets. *Aquat Ecol* 45:529–38.

Reddy KR, Delaune RD (2008) *Biogeochemistry of wetlands: science and applications*. CRC, Taylor and Francis Group, Boca Raton.

Reed JM, Mesquita-Joanes F, Griffiths HI (2012) Multi-indicator conductivity transfer functions for Quaternary palaeoclimate reconstruction. *J Paleolimnol* 47: 251–275.

Reed JM, Roberts N, Leng MJ (1999) An evaluation of the diatom response to Late Quaternary environmental change in two lakes in the Konya Basin, Turkey, by comparison with stable isotope data. *Quat Sci Rev* 18:631–646.

Rejmankova E, Houdkova K (2006) Wetland plant decomposition under different nutrient conditions: what is more important, litter quality or site quality? *Biogeochemistry* 80:245–262.

Rooney RC, Bayley SE, Schindler DW (2012) Oil sands mining and reclamation cause massive loss of peatland and stored carbon. *Proc Natl Acad Sci* 109:4933–4937.

Roulet NT (2000) Peatlands, carbon storage, greenhouse gases, and the Kyoto Protocol: Prospects and significance for Canada. *Wetlands* 20:605–615.

Roulet NT, Lafleur PM, Richard PJH, Moore TR, Humphreys ER, Bubier J (2007) Contemporary carbon balance and late Holocene carbon accumulation in a northern peatland. *Global Change Biology* 13:397–411.

Rydin H, Jeglum JK (2013) *The biology of peatlands*, 2nd edition. Oxford University Press, Oxford

Ryves DB, Battarbee RW, Juggins S, Fritz SC, Anderson NJ (2006) Physical and chemical predictors of diatom dissolution in freshwater and saline lake sediments in North America and West Greenland. *Limnol Oceanogr* 51: 1355–1368.

Sahm CR, Saros JE, Fritz SC, et al. (2009) Phytoplankton productivity across prairie saline lakes of the Great Plains (USA): a step toward deciphering patterns through lake classification models. *Can J Fish Aquat Sci* 66:1435–1448.

Saros JE, Fritz SC (2000) Changes in the growth rates of saline-lake diatoms in response to variation in salinity, brine type and nitrogen form. *J Plankton Res* 22: 1071–83.

Sass GZ, Creed IF, Devito KJ (2008) Spatial heterogeneity in trophic status of shallow lakes on the Boreal Plain: Influence of hydrologic setting. *Water Resour Res* 44.

Scarlett SJ, Price JS (2013) The hydrological and geochemical isolation of a freshwater bog within a saline fen in north-eastern Alberta. *Mires and Peat* 12:1–12.

Schindler DW, Curtis PJ, Bayley SE, Parker BR, Beaty KG, Stainton MP (1997) Climate-induced changes in the dissolved organic carbon budgets of boreal lakes. *Biogeochemistry* 36:9–28.

Setia R, Marschner P, Baldock J, Chittleborough D, Smith P, Smith J (2011) Salinity effects on carbon mineralization in soils of varying texture. *Soil Biol Biochem* 43:1908–1916.

Simhayov R (2017) Chemical characterization of construction materials and solute transport in peat from the Nikanotee constructed fen watershed in the Athabasca oil sands region, Alberta, Canada. PhD Thesis, University of Waterloo

Smerdon BD, Devito KJ, Mendoza CA (2005) Interaction of groundwater and shallow lakes on outwash sediments in the sub-humid Boreal Plains of Canada. *J Hydrol* 314: 246–262.

Smith AJ, Donovan JJ, Ito E, Engstrom DR, Panek VA (2002) Climate-driven hydrologic transients in lake sediment records: Multiproxy record of mid-Holocene drought. *Quat Sci Rev* 21: 625–646

Smol JP, Briks HJB, Last WM (2001) Using biology to study long-term environmental change In: Smol JP, Birks HJB, Last W (eds) *Tracking Environmental Change Using Lake Sediments. Vol. 3: Terrestrial, Algal, and Siliceous Indicators*. Kluwer Academic Publishers, Dordrecht, pp 1–4.

Spaulding SA, Lubinski DJ, Potapova M (2010) Diatoms of the United States. Available at: <http://westerndiatoms.colorado.edu> (accessed 2015.07.21).

Sperling O, Lazarovitch N, Schwartz A, Shapira O (2014) Effects of high salinity irrigation on growth, gas-exchange, and photoprotection in date palms (*Phoenix dactylifera* L., cv Medjool). *Environ Exp Bot* 99:100–109.

Staats N, De Winder B, Stal LJ, Mur LR (1999) Isolation and characterization of extracellular polysaccharides from the epipelagic diatoms *Cylindrotheca closterium* and *Navicula salinarum*. *Eur J Phycol* 34: 161–169. DOI: 10.1080/09670269910001736212.

Stanek W, Silc T (1977) Comparisons of four methods for determination of degree of peat humification (decomposition) with emphasis on the von Post method. *Can J Soil Sci.* 57:109–117.

Stewart SA, Lemay TG (2011) Inorganic water chemistry of saline fens in northeastern Alberta (NTS 74D). Energy Resources Conservation Board, ERCB/AGS Open File Report, September

Stewart SA, Lemay TG (2011) Inorganic water chemistry of saline fens in northeastern Alberta (NTS 74D). Energy Resources Conservation Board, ERCB/AGS Open File Report, September.

Strack M, Waddington JM, Rochefort L, Tuittila E-S (2006) Response of vegetation and net ecosystem carbon dioxide exchange at different peatland microforms following water table drawdown. *J Geophys Res* 111:G02006.

Strilesky SL, Humphreys ER (2012) A comparison of the net ecosystem exchange of carbon dioxide and evapotranspiration for treed and open portions of a temperate peatland. *Agric For Meteorol* 153:45–53.

Stueben BL, Cantrelle B, Sneddon J, Beck JN (2004) Manganese K-edge XANES studies of Mn speciation in Lac des Allemandes as a function of depth. *Microchem J* 76:113-120

Stumm W, Morgan J (1996) *Aquatic chemistry: chemical equilibria and rates in natural waters*. Wiley, New York, New York, USA

Sulman BN, Desai AR, Saliendra NZ, Lafleur PM, Flanagan LB, Sonnentag O, Mackay DS, Barr AG, van der Kamp G (2010) CO₂ fluxes at northern fens and bogs have opposite responses to inter-annual fluctuations in water table. *Geophys Res Lett* 37: L19702.

Sutter LA, Perry JE, Chambers RM (2014) Tidal freshwater marsh plant response to low level salinity increases. *Wetlands* 34:167–175

Szumigalski AR, Bayley SE (1996) Decomposition along a bog to rich fen gradient in central Alberta, Canada. *Can J Bot* 74:573–581.

Telford RJ, Lamb HF, Mohammed MU (1999) Diatom-derived palaeoconductivity estimates for Lake Awassa, Ethiopia: Evidence for pulsed inflows of saline groundwater? *J Paleolimnol* 21: 409–421.

Tolonen K, Turunen J (1996) Accumulation rates of carbon in mires in Finland and implications for climate change, *Holocene* 6:171–178.

Tripathi S, Kumari S, Chakraborty A, Gupta A, Chakrabarti K, Bandyapadhyay BK (2006) Microbial biomass and its activities in salt-affected coastal soils. *Biol Fertil Soils* 42:273–277

Trites M, Bayley SE (2009a) Organic matter accumulation in western boreal saline wetlands: A comparison of undisturbed and oil sands wetlands. *Ecol Eng* 35: 1734–1742.

Trites M, Bayley SE (2009b) Organic matter accumulation in western boreal saline wetlands: A comparison of undisturbed and oil sands wetlands. *Ecol Eng* 35:1734–1742.

Turetsky M (2002) Current disturbance and the diminishing peatland carbon sink. *Geophysical Research Letters* 29:7–10.

Turetsky MR, St Louis VL (2006) Disturbance in Boreal Peatlands. In: Wieder RK, Vitt DH, (eds) *Boreal peatland ecosystems*. Springer Berlin Heidelberg, Berlin, Heidelberg, pp 359–379.

Turunen J, Tomppo E, Tolonen K, Reinikainen A (2002) Estimating carbon accumulation rates of undrained mires in Finland – application to boreal and subarctic regions. *Holocene* 12:69–80.

Van Bellen S, Garneau M, Booth RK (2011) Holocene carbon accumulation rates from three ombrotrophic peatlands in boreal Quebec, Canada: Impact of climate-driven ecohydrological change. *Holocene* 21:1217–1231.

Vance RE, Last WM, Smith AJ (1997) Hydrologic and climatic implications of a multidisciplinary study of Late Holocene sediments from Kenosee Lake, southeastern Saskatchewan, Canada. *J Paleolimnol* 18: 1–29.

Villa JA, Bernal B (2017) Carbon sequestration in wetlands, from science to practice: An overview of the biogeochemical process, measurement methods, and policy framework. *Ecol Eng.* doi: 10.1016/j.ecoleng.2017.06.037.

Vitt DH, Halsey LA, Bauer IE, Campbell C (2000) Spatial and temporal trends in carbon storage of peatlands of continental western Canada through the Holocene. *Canadian Journal of Earth Sciences* 37:683–693.

Vitt DH, Halsey LA, Thormann MN, Martin T (1996) Peatland Inventory of Alberta. Edmonton, AB: Alberta Peat Task Force, University of Alberta

Vitt DH, House M (2015) Establishment of bryophytes from indigenous sources after disturbance from oil sands mining. *Bryologist* 118:123–129.

Vitt DH, Wieder RK, Scott KD, Faller S (2009) Decomposition and peat accumulation in rich fens of boreal Alberta, Canada. *Ecosystems* 12:360–373.

Volik O, Petrone RM, Hall RI, Macrae ML, Wells CM, Elmes MC, Price JS (2017) Long-term precipitation-driven salinity change in a saline, peat-forming wetland in the Athabasca Oil Sands Region, Canada: a diatom-based paleolimnological study. *J Paleolimnol* 58:533–550.

von Post L, Granlund E (1926) Södra Sveriges Torvtillgångar I (Peat resources in southern Sweden I). *Sveriges Geologiska Undersökning C* 335 19:1–128.

Vose JM, Dougherty PM, Long JM, et al. (1994) Factors influencing the amount and distribution of leaf area of pines stands. *Ecological Bulletins* 43:102–114.

Waddington JM, Roulet NT (1996) Exchange on the Developmental Topography of a Peatland. *Global Biogeochem Cycles* 10:233.

Waddington JM, Roulet NT (2000) Carbon balance of a boreal patterned peatland. *Glob Change Biol* 6:87–97.

Wallen B, Falkengren-Grerup U, Malmer N (1988) Biomass, productivity and relative rate of photosynthesis of *Sphagnum* at different water levels on a south Swedish peat bog. *Holarct Ecol* 11:70–76.

Weber K, Stewart M (2004) A critical analysis of the cumulative rainfall departure concept. *Ground Water* 42:935–938.

Wells CM (2014) The hydrology and geochemistry of a saline spring fen peatland in the Athabasca Oil Sands Region of Alberta. MSc Thesis, University of Waterloo

Wells CM, Price JS (2015a) A hydrologic assessment of a saline-spring fen in the Athabasca Oil Sands Region, Alberta, Canada – a potential analogue for oil sands reclamation. *Hydrol Process* 29: 4533–4548.

Wells CM, Price JS (2015b) The hydrogeologic connectivity of a low-flow saline-spring fen peatland within the Athabasca oil sands region, Canada. *Hydrogeol J* 23:1799–1826.

Weston NB, Vile MA, Neubauer SC, Velinsky DJ (2011) Accelerated microbial organic matter mineralization following salt-water intrusion into tidal freshwater marsh soils. *Biogeochemistry* 102:135–151.

Wetzel PR, van der Valk AG, Toth LA (2001). Restoration of wetland vegetation on the Kissimmee River floodplain: potential role of seed banks. *Wetlands* 21:189–198.

Whiting GJ, Chanton JP (2001) Greenhouse carbon balance of wetlands: methane emission versus carbon sequestration. *Tellus Ser. B* 53:521–528.

Williams W, Sherwood J (1994) Definition and measurement of salinity in salt lakes. *Int J Salt Lake Res* 3: 53–63.

Williams WD, Boulton AJ, Taaffe RG (1990) Salinity as a determinant of salt lake fauna: a question of scale. *Hydrobiologia* 197: 257–266.

Willis JM, Hester MW (2004) Interactive effects of salinity, flooding, and soil type on *Panicum hemitomon*. *Wetlands* 24:43–50.

Wilson SE, Cumming BF, Smol JP (1994) Diatom-salinity relationships in 111 lakes from the Interior Plateau of British Columbia, Canada: the development of diatom-based models for paleosalinity reconstructions. *J Paleolimnol* 12: 197–221.

Wilson SE, Cumming BF, Smol JP (1996) Assessing the reliability of salinity inference models from diatom assemblages: an examination of a 219-lake data set from western North America. *Can J Fish Aquat Sci* 53:1580–1594.

Winter TC, Rosenberry DO (1998) Hydrology of prairie pothole wetlands during drought and deluge: a 17-year study of the Cottonwood Lake wetland complex in North Dakota in perspective to long term measured and proxy hydrological records. *Clim Chang* 40: 189–209.

Wollheim WM, Lovvorn JR (1996) Effects of macrophyte growth forms on invertebrate communities in saline lakes of the Wyoming High Plains. *Hydrobiologia* 323:83–96.

Wood ME, Macrae ML, Strack M, Price JS, Osko TJ, Petrone RM (2015) Spatial variation in nutrient dynamics among five different peatland types in the Alberta Oil Sands Region. *Ecohydrology* 9:688–699.

Wortley L, Hero JM, Howes M (2013) Evaluating ecological restoration success: A review of the literature. *Restor Ecol* 21:537–543.

Wylynko D, Hrynyshyn J (2014) Guidelines for wetlands establishment on reclaimed oil sands leases, 3rd ed. Cumulative Environmental Management Association. Fort McMurray, Alberta

Xu ZH, Yin XA, Yang ZF (2014) An optimisation approach for shallow lake restoration through macrophyte management. *Hydrol Earth Syst Sci* 18:2167–2176.

Yu Z (2006) Holocene carbon accumulation of fen peatlands in boreal western Canada: A complex ecosystem response to climate variation and disturbance. *Ecosystems* 9:1278–1288.

Yu Z, Campbell ID, Campbell C, Vitt DH, Bond GC, Apps MJ (2003) Carbon sequestration in western Canadian peat highly sensitive to Holocene wet-dry climate cycles at millennial timescales. *The Holocene* 13:801–808.

Yu Z, Vitt DH, Wieder RK (2014) Continental fens in western Canada as effective carbon sinks during the Holocene. *The Holocene* 24:1090–1104.

Yu ZC (2012) Northern peatland carbon stocks and dynamics: a review. *Biogeosciences* 9:4071–4085.

Zedler JB, Kercher S (2005) Wetland resources: status, trends, ecosystem services, and restorability. *Annual Rev Env Res* 30:39–74.

Zhang Z, Moon HS, Myneni SCB, Jaffé PR (2017) Effect of dissimilatory iron and sulfate reduction on arsenic dynamics in the wetland rhizosphere and its bioaccumulation in wetland plants (*Scirpus actus*). *J Hazard Mater* 321:382–389.

Appendix A. Environmental dataset and results of statistical analyses used for diatom-based transfer function development

Table A-1. List of sampled ponds including their coordinates (Coord), depth in m (D), major ion concentrations (mg L⁻¹), salinity (ppt) in May (Sal_May) and August (Sal_Aug), conductivity (mS cm⁻¹) in May (Cond_May), and August (Cond_Aug), pH, dissolved oxygen in mg L⁻¹ (DO), chlorophyll *a* concentration in ug L⁻¹ (Chl a)

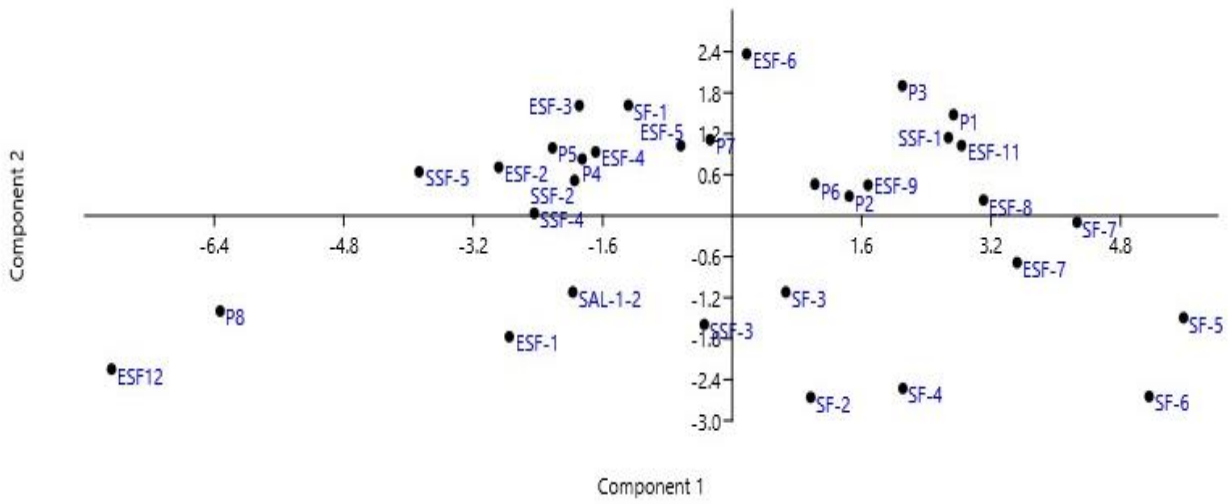
Pond name	Coord	D	Cl	SO ₄	Na	K	Mg	Ca	Sal_May	Cond_May	Sal_Aug	Cond_Aug	pH	DO	Chl a
ESF12	56°33'50.61"N 111°15'51.51"W	0.56	656.8	10.6	478.2	1.5	15.4	43.0	1.1	2.0	1.3	2.6	8.2	3.5	0.07
SSF-5	56°33'55.29"N 111°16'24.31"W	0.48	1679.9	44.2	1344.7	2.6	30.4	68.9	2.5	5.0	3.0	6.0	8.0	2.9	5.01
P8	56°34'17.86"N 111°16'28.88"W	0.49	920.4	29.5	697.4	0.1	21.6	50.2	3.3	5.0	6.2	9.5	7.2	2.5	21.75
P5	56°34'9.34"N 111°16'7.09"W	0.52	3842.5	126.9	3021.0	4.0	67.1	134.9	3.4	5.8	8.1	14.0	7.8	2.5	73.35
ESF-1	56°34'7.09"N 111°14'51.88"W	0.59	2224.2	31.4	1707.6	3.1	29.8	49.9	1.4	2.5	3.6	6.6	7.8	4.2	4.79
ESF-2	56°34'3.64"N 111°14'46.51"W	0.53	2245.5	72.6	1758.6	3.6	34.7	64.6	2.3	4.1	3.8	6.7	7.8	4.7	7.09
P4	56°34'9.37"N 111°16'9.03"W	0.5	4068.9	123.3	3199.1	6.8	70.1	143.9	6.2	6.3	4.2	10.6	7.9	2.3	26.3
SSF-4	111°16'23.15"W	0.45	2384.9	57.2	1909.9	3.5	38.0	82.6	3.2	6.2	4.3	8.4	7.6	4.4	9.02
ESF-5	56°33'50.57"N 111°14'36.88"W	0.41	4919.6	174.8	3911.4	6.5	73.4	137.1	3.2	6.4	5.3	10.5	7.5	5.8	19.39
ESF-3	56°34'3.75"N 111°14'43.84"W	0.51	3281.3	118.4	2631.9	4.7	50.4	93.9	3.5	6.9	5.4	10.7	7.9	2.6	18.1
SSF-2	56°33'53.84"N 111°16'23.01"W	0.49	2726.0	86.1	2176.7	5.3	41.5	84.0	3.9	6.5	5.7	9.4	7.3	4.7	15.52
ESF-4	56°33'59.56"N 111°14'40.77"W	0.39	3153.7	115.3	2467.1	3.9	47.9	90.4	4.0	7.3	5.8	10.5	8.1	4.6	9.13
SAL-1-2	56°34'19.71"N 111°16'28.51"W	0.45	3301.1	66.8	2573.6	3.5	62.4	130.0	4.8	8.5	5.9	10.6	7.5	2.7	9.15
P7	56°34'8.02"N 111°16'10.71"W	0.51	7106.2	206.1	5575.4	9.4	120.3	235.1	7.5	14.1	11.7	22.0	8.2	3.1	6.69
SF-1	56°34'16.09"N 111°16'23.48"W	0.47	4099.0	138.4	3283.8	4.5	71.0	146.5	5.0	7.3	8.0	11.8	8.1	3.6	14.3
P6	56°34'7.13"N 111°16'6.16"W	0.35	9571.2	284.9	7439.5	31.0	112.4	366.1	8.2	10.1	16.9	20.9	7.8	3.4	19.39

Pond name	Coord	D	Cl	SO ₄	Na	K	Mg	Ca	Sal_ May	Cond_ May	Sal_A ug	Cond_ Aug	pH	DO	Chl a
SSF-3	56°33'53.75"N 111°16'22.27"W	0.38	4923.5	81.4	3879.0	2.2	83.7	137.0	4.8	9.2	8.5	16.2	7.4	4.3	74.19
P2	56°34'3.62"N 111°16'1.19"W	0.49	9964.5	258.2	7779.7	42.6	98.1	277.6	11.3	15.8	27.7	30.8	7.6	2.9	170.9 3
ESF-6	56°33'50.42"N 111°14'35.29"W	0.51	6364.5	265.1	5099.2	10.6	91.2	158.6	8.3	15.0	11.8	21.3	7.9	4.1	29.15
ESF-9	56°34'14.22"N 111°16'22.03"W	0.46	9438.1	225.5	7432.3	23.7	84.4	210.0	9.6	15.7	14.0	22.8	8.0	4.9	72.43
SF-2	56°34'6.70"N 111°16'8.20"W	0.35	7884.0	150.2	6107.7	8.3	134.0	269.7	14.4	18.4	19.9	25.5	6.3	2.5	36.8
P3	111°16'21.04"W	0.41	11241. 9	374.9	8611.3	209.7	137.4	403.8	10.4	17.2	15.2	25.0	7.8	4.1	26.12
SF-3	56°33'49.69"N 111°14'34.10"W	0.52	8377.1	154.5	6489.3	6.7	140.0	292.4	10.5	18.3	16.5	28.7	7.5	2.9	12.02
SSF-1	56°33'52.46"N 111°16'20.42"W	0.47	10819. 6	231.4	8721.2	126.0	88.6	224.5	10.5	18.5	19.1	33.6	7.8	2.7	16.51
ESF-11	56°33'49.37"N 111°14'35.78"W	0.45	12574. 0	333.4	9935.0	75.3	103.8	289.0	16.3	27.5	22.1	37.2	7.9	4.6	17.32
P1	56°34'2.21"N 111°16'10.30"W	0.49	10936. 1	247.3	8639.6	198.6	97.4	249.0	22.6	27.3	35.5	43.0	7.9	3.5	3.69
SF-4	56°34'1.65"N 111°16'8.95"W	0.23	12901. 5	243.9	9802.1	0.1	134.4	444.0	17.0	28.9	22.8	38.7	7.8	4.3	60.94
ESF-8	56°33'49.99"N 111°14'34.27"W	0.39	13236. 9	331.7	10465. 4	54.7	131.3	239.6	17.9	31.6	23.3	41.1	7.7	4.2	13.23
ESF-7	56°33'49.95"N 111°14'35.38"W	0.24	14557. 0	278.6	11525. 2	38.2	160.3	253.7	18.1	30.3	26.0	43.5	8.0	2.5	14.05
SF-7	56°34'0.33"N 111°16'8.70"W	0.38	19388. 4	324.7	15568. 0	67.1	142.2	250.0	22.1	34.3	35.1	54.5	8.0	2.9	0.18
SF-5	56°34'1.59"N 111°16'7.97"W	0.15	23037. 9	358.4	18037. 5	237.1	125.2	264.6	35.1	56.1	41.5	66.2	7.3	4.1	5.39
SF-6	56°34'0.67"N 111°16'7.66"W	0.21	23583. 0	344.3	18021. 5	69.0	122.2	252.9	35.8	57.8	41.8	67.6	7.4	4.2	1.95

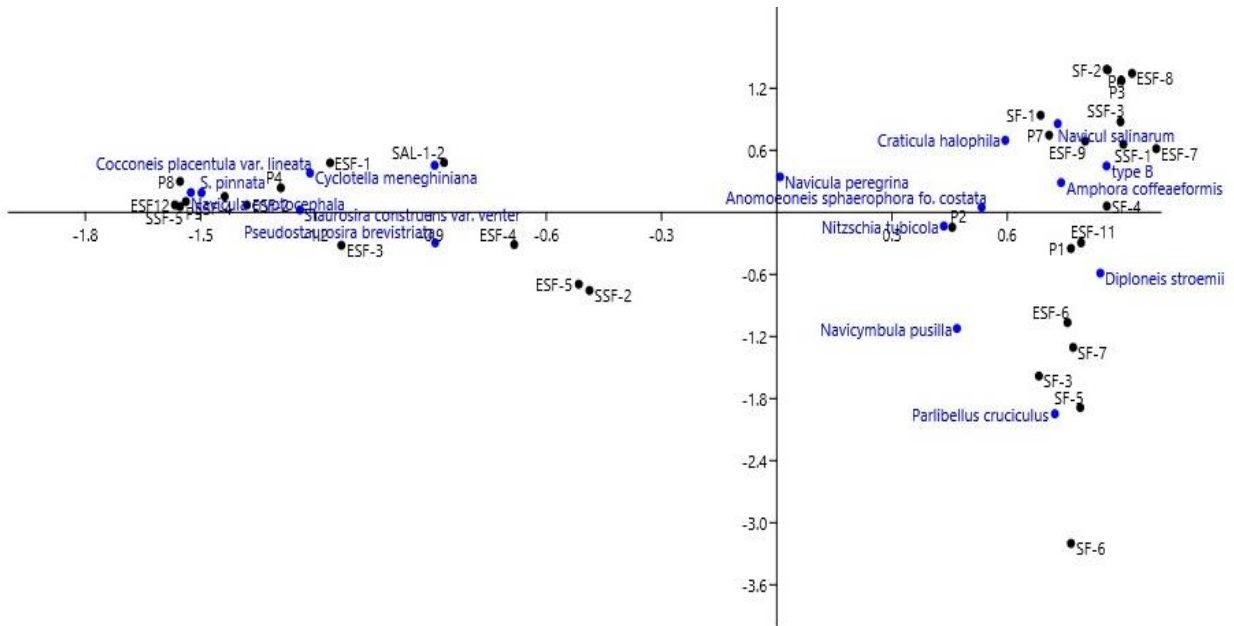
Table A-2. Eigenvalues, percent explained variance and loadings of the first two axes for principal component analysis (PCA), canonical analysis (CA), and canonical correspondence analysis (CCA)

	PCA		CA		CCA	
	Axis 1	Axis 2	Axis 1	Axis 2	Axis 1	Axis 2
Eigenvalue	9.6	2.1	0.80	0.39	0.70	0.26
% variance	56.4	12.1	30.5	14.8	43.45	16
Variables						
Salinity	0.31	-0.07	-	-	-0.84	0.15
Conductivity	0.31	-0.09	-	-	-0.87	0.25
pH	-0.04	0.36	-	-	0.08	-0.27
DO	0.04	0.05	-	-	-0.16	0.11
Depth	-0.22	0.29	-	-	0.55	-0.25
Cl ⁻	0.32	0.01	-	-	-0.88	0.13
SO ₄ ²⁻	0.30	0.21	-	-	-0.82	0.04
Na ⁺	0.32	0.02	-	-	-0.18	-0.60
K ⁺	0.24	0.23	-	-	-0.57	0.15
Mg ²⁺	0.29	0.03	-	-	-0.83	-0.08
Ca ²⁺	0.28	0.03	-	-	-0.81	-0.12
%Cl	0.14	-0.54	-	-	-0.20	0.46
%SO ₄	-0.10	0.54	-	-	0.16	-0.03
%Na	0.20	0.18	-	-	0.16	-0.44
%K	0.15	0.22	-	-	-0.37	-0.03
%Mg	-0.29	-0.06	-	-	0.70	-0.21
%Ca	-0.26	-0.09	-	-	0.54	-0.25
Species						
<i>Staurosira construens</i> var. <i>venter</i>			-1.39	0.04	1.36	0.04
<i>Staurosirella pinnata</i>			-1.68	0.30	1.60	0.40
<i>Pseudostaurosira brevistriata</i>			-1.00	-0.47	1.17	0.60
<i>Navicula cryptocephala</i>			-1.71	0.31	1.97	0.83
<i>Cocconeis placentula</i> var. <i>lineata</i>			-1.36	0.61	1.48	0.08
<i>Cyclotella meneghiniana</i>			-1.00	0.73	1.35	0.42
<i>Anomooneis sphaerophora</i> fo. <i>costata</i>			0.60	0.08	-0.45	-0.57
<i>Nitzschia tubicola</i>			0.49	-0.21	-0.57	-0.31
<i>Halamphora coffeaeformis</i>			0.83	0.46	-0.75	-0.55
<i>Craticula halophila</i>			0.67	1.12	-0.57	-1.70
<i>Navicul salinarum</i>			0.82	1.38	-0.73	-1.22
<i>Navicula peregrina</i>			0.01	0.55	0.09	-0.57
<i>Navicymbula pusilla</i>			0.53	-1.81	-0.67	1.33
<i>Diploneis stroemii</i>			0.94	-0.95	-1.24	0.72
<i>Parlibellus crucicula</i>			0.81	-3.13	-1.12	4.25
<i>Navicula</i> sp., type B			0.96	0.72	-1.07	0.31

	PCA		CA		CCA	
	Axis 1	Axis 2	Axis 1	Axis 2	Axis 1	Axis 2
Ponds						
ESF12	-7.67	-2.25	-1.40	0.04	1.38	0.07
SSF-5	-3.87	0.64	-1.39	0.03	1.35	0.04
P8	-6.33	-1.40	-1.39	0.19	1.42	0.18
P5	-2.22	0.99	-1.37	0.06	1.35	0.09
ESF-1	-2.75	-1.77	-1.04	0.30	1.10	0.03
ESF-2	-2.88	0.71	-1.23	0.04	1.20	0.03
P4	-1.85	0.83	-1.15	0.15	1.14	-0.06
SSF-4	-2.44	0.04	-1.28	0.10	1.26	-0.01
ESF-5	-0.63	1.02	-0.46	-0.43	0.42	0.34
ESF-3	-1.89	1.61	-1.01	-0.20	0.98	0.21
SSF-2	-1.95	0.52	-0.44	-0.47	0.42	0.37
ESF-4	-1.69	0.93	-0.61	-0.19	0.58	0.14
SAL-1-2	-1.97	-1.12	-0.77	0.30	0.85	-0.18
P7	-0.27	1.11	0.63	0.46	-0.54	-0.52
SF-1	-1.28	1.62	0.61	0.58	-0.52	-0.58
P6	1.02	0.46	0.77	0.86	-0.67	-0.93
SSF-3	-0.34	-1.59	0.80	0.54	-0.73	-0.59
P2	1.45	0.29	0.41	-0.09	-0.38	-0.07
ESF-6	0.18	2.37	0.68	-0.66	-0.73	0.45
ESF-9	1.68	0.45	0.72	0.43	-0.65	-0.51
SF-2	0.97	-2.66	0.77	0.86	-0.71	-0.90
P3	2.10	1.90	0.80	0.79	-0.72	-0.88
SF-3	0.66	-1.12	0.61	-0.98	-0.68	0.57
SSF-1	2.67	1.14	0.81	0.41	-0.74	-0.51
ESF-11	2.83	1.03	0.71	-0.18	-0.72	0.08
P1	2.74	1.48	0.68	-0.22	-0.70	0.11
SF-4	2.11	-2.53	0.77	0.04	-0.77	-0.27
ESF-8	3.11	0.23	0.83	0.83	-0.79	-0.61
ESF-7	3.52	-0.69	0.88	0.38	-0.95	0.07
SF-7	4.26	-0.10	0.69	-0.81	-0.75	0.63
SF-5	5.58	-1.50	0.71	-1.17	-0.82	1.07
SF-6	5.15	-2.65	0.68	-1.99	-0.88	2.14



(a)



(b)

Figure A-1. PCA ordination diagram of 32 ponds used for training set development (a), and CA ordination diagram of 32 ponds and 16 diatom species used for training set development (b)

Appendix B. Description and chronology of cores North-1 and South-1 and environmental dataset from 40 vegetation plots along salinity gradient at Saline Fen

Table B-1. Radiocarbon dates for cores North-1 and South-1*. Types of pre-treatment are identified as AAA – acid-alkali-acid pre-treatment, A – acid pre-treatment

Lab ID	Depth, cm	Material	Type of pre-treatment	¹⁴ C age BP	±	F ¹⁴ C	±	Calibrated range BP (2σ)	Mid-point cal. yr BP
Core North-1									
UOC-2176	28-29	Bulk Peat	AAA	433	22	0.9475	0.0026	520–470	497
UOC-2177	36-37	Bulk Peat	AAA	834	24	0.9014	0.0027	790–690	740
UOC-2178	44-45	Bulk Peat	AAA	988	25	0.8842	0.0027	960–900	930
UOC-2179	56-57	Bulk Peat	AAA	1165	21	0.8650	0.0022	1180–1050	1114
UOC-2180	68-69	Bulk Peat	AAA	2104	25	0.7695	0.0024	2140–2000	2073
UOC-2181	80-81	Bulk Peat	AAA	2466	26	0.7357	0.0024	2710–2430	2570
UOC-1058	106-107	Bulk Peat	AAA	3974	60	0.6098	0.0046	4590-4240	4412
Core South-1									
UOC-2182	16-17	Bulk Peat	AAA	597	24	0.9284	0.0028	650–580	616
UOC-2183	20-21	Bulk Peat	AAA	1083	21	0.8739	0.0022	1010–940	973
UOC-2184	32-33	Bulk Peat	AAA	1983	24	0.7813	0.0023	1990–1880	1937
UOC-2185	44-45	Bulk Peat	AAA	2931	26	0.6943	0.0022	3170–2990	3080
UOC-2186	52-53	Bulk Peat	AAA	3405	24	0.6545	0.0020	3700– 3580	3642
UOC-1060	63-64	Bulk Peat	AAA	4355	57	0.5815	0.0041	5270-4830	5048

* Eight samples from North-1 and seven samples from South-1 (see Table 4-1 for details) were sent to A.E. Lalonde AMS Facility, University of Ottawa for radiocarbon dating. After standard acid-alkali-acid pre-treatment (Brock et al. 2010), the samples were freeze dried overnight. Dry samples were combusted in a tin capsule using a Thermo Flash 1112 elemental analyzer in CN mode interfaced with an extraction line to trap the pure CO₂ in a pre-baked 6 mm pyrex tube. Samples of pure CO₂ were converted to elemental carbon in the presence of hydrogen using the semi-automated graphitization lines. Dating was performed on a 3MV accelerator mass spectrometer (AMS) by High Voltage Engineering. The measurements were normalized with respect to the reference material Oxalic II (F¹⁴C=1.34) and the ages were calculated using the Libby ¹⁴C half-life of 5568 years. OxCal v4.2.4 (Bronk 2009) was used for calibration, and calibrated results are presented with 2σ confidence limits 1 (Table B-1). The IntCal13 calibration curve (Reimer et al. 2013) was used for the samples with an F¹⁴C less than 1. Because dating was performed on peat at the bases of almost all stratigraphical units along the peat profiles and this allowed considering changes in peat accumulation rates (Telford et al. 2004), age – depth models for North-1 and South-2 were developed using linear interpolation between the dated samples (mid-points of the calibrated 2σ distribution range of the ¹⁴C dates). Radiocarbon dates in the two cores are internally consistent and suggest continuous accumulation from Middle – Late Holocene to the present.

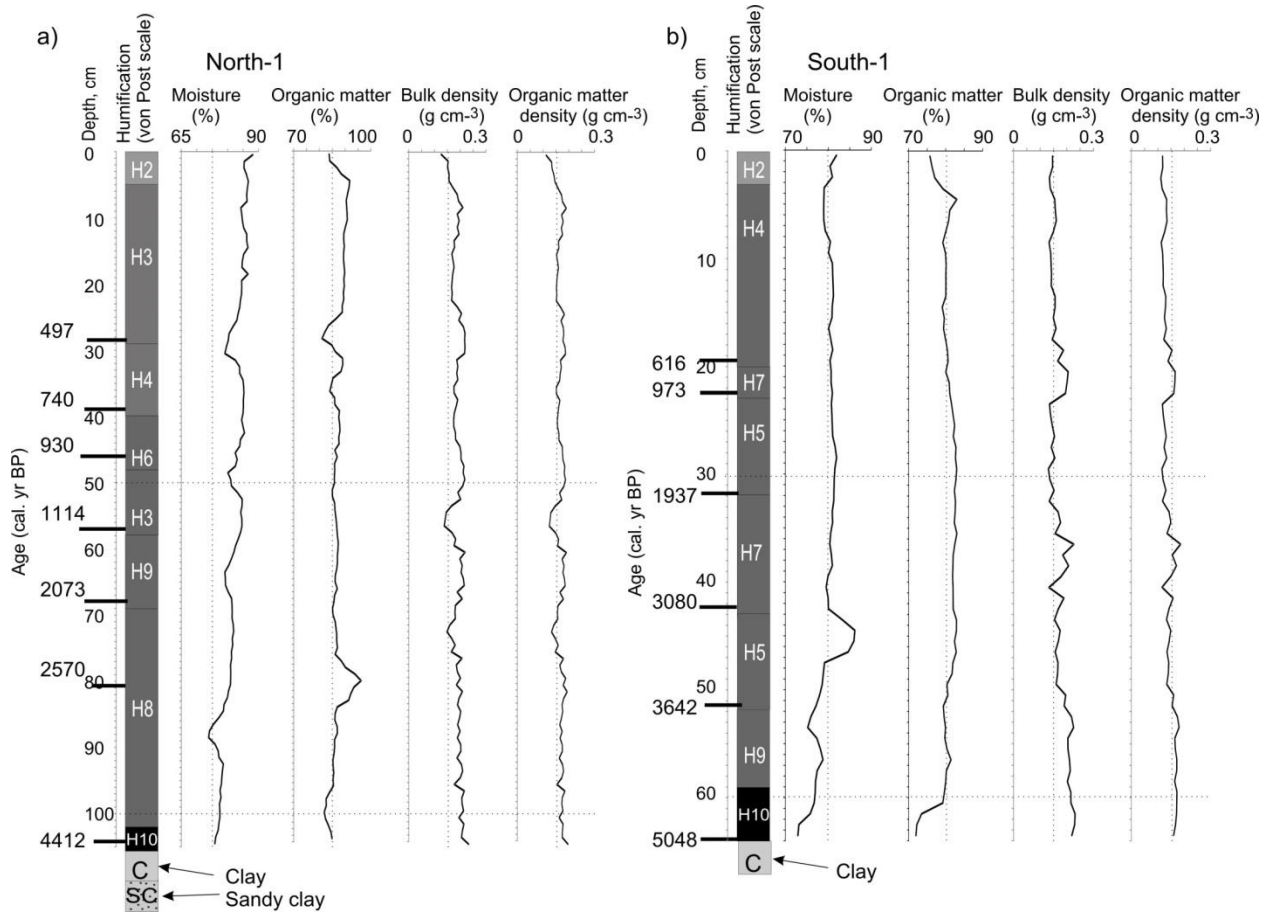
Brock F, Higham T, Ditchfield P, Ramsey CB (2010) Current pretreatment methods for AMS radiocarbon dating at the Oxford Radiocarbon Accelerator Unit. *Radiocarbon* 52: 103–112.

Bronk RC (2009) Dealing with outliers and offsets in radiocarbon dating. *Radiocarbon* 51: 1023–1045.

Reimer PJ, Bard E, Bayliss A, et al. (2013). IntCal13 and Marine13 Radiocarbon Age Calibration Curves 0-50,000 Years cal BP. *Radiocarbon* 55: 1869–1887.

Telford RJ, Heegaard E, Birks HJB (2004) All age–depth models are wrong: but how badly? *Quaternary Science Reviews* 23:1–5.

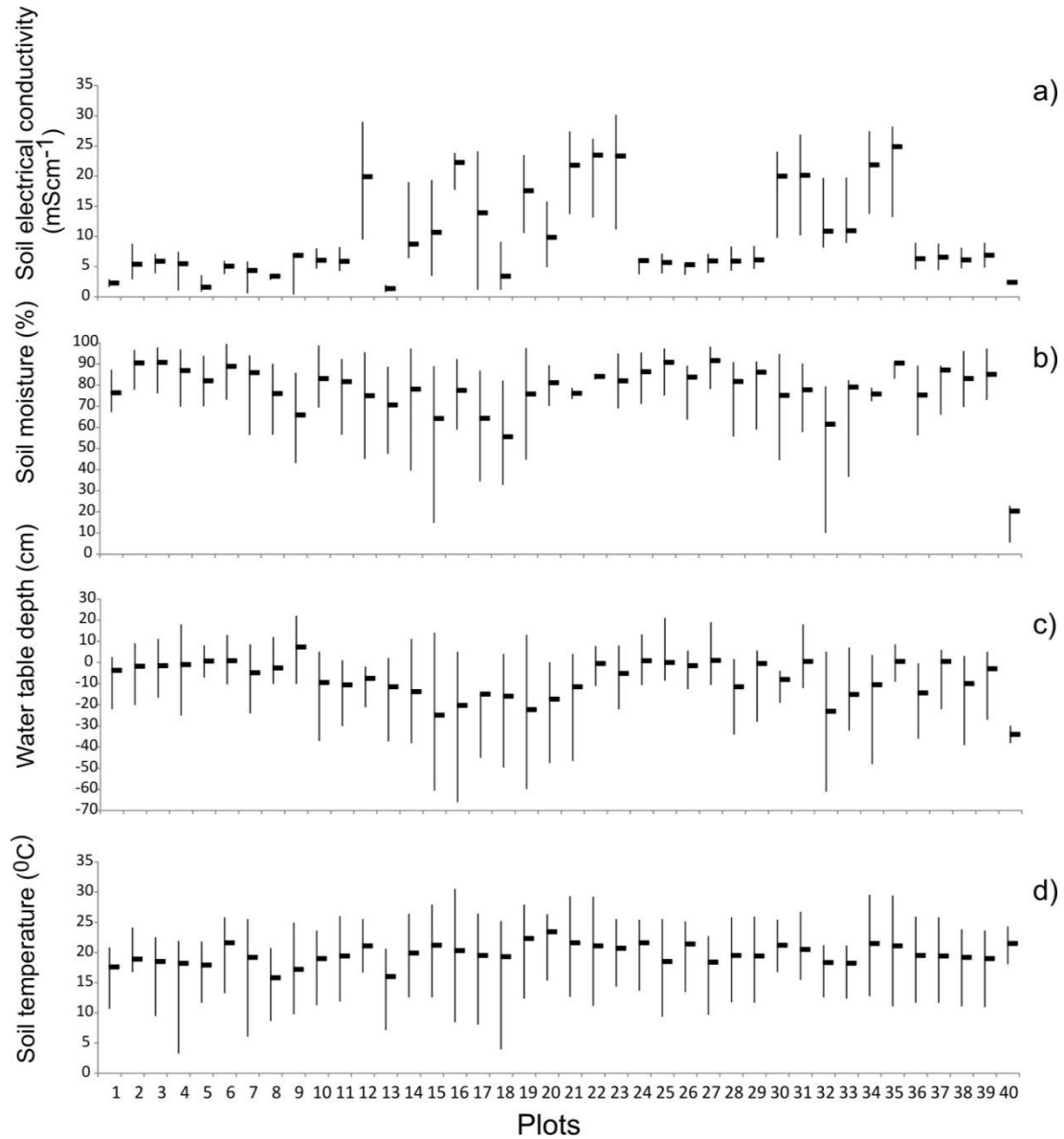
Figure B-1. Lithology of cores North-1 (a) and South-1 (b). Moisture and organic matter contents are shown as presents while bulk density and ash-free density are shown as g cm^{-3} . Humification (von Post scale (von Post and Granlund 1926)) and radiocarbon dates are shown on left side of each diagram. Clay sediments at the bottom of the cores are shown not to scale*.



*Clay sediments at the bottom parts of cores North-1 and South-1 have similar lithology and are characterized by low organic matter (1.7–3.2%) and moisture content (16–25%), and a high bulk density (1.8–2.6 g cm^{-3}). In both cores, peat moisture content demonstrates a gradual upcore increase from 75 % to 80–88%; however decreases at 88, 64, 48 and 29 cm are observed in core North-1, and sharp rises at 56 and 44 cm are visible in core South-1 (Figure B-1). The peat organic matter is higher in core North-1 (85–86 % on average) relative to core South-1 (80–81% on average). In North-1 organic matter is relatively stable below 40 cm except for a prominent increase up to 96% at 80 cm; above 40 cm peat has organic content of 88–89 % on average with declines at 36, 28 and 0 cm. In South-1 organic matter does not demonstrate prominent changes, except sharp decreases at 64 and 0 cm

(Figure B-1). Peat bulk density in the two core varies between 0.12 and 0.22 g cm⁻³, but core South-1 has lower average bulk density (0.17 g cm⁻³, SD=0.02) relative to core North-1 (0.19 g cm⁻³, SD=0.03) (Figure B-1). The organic matter density in the cores ranges from 0.1 to 0.19 g cm⁻³ with average of 0.17 (SD=0.02) and 0.13 g cm⁻³ (SD=0.02) for North-1 and South-1 respectively. The most prominent declines in peat bulk density and organic matter density are observed at 72, 56 and 0 cm in core North-1 while increases at 53–54, 36–40 and 21–23 cm are visible in core South-1 1 (Figure B-1).

Figure B-2. Soil electrical conductivity (a), moisture (b), water table depth (c), and temperature (d) of 40 vegetation plots along salinity gradient at Saline Fen. Plot numbers correspond to those used in Figure 4-1. Average values are shown as black rectangles, and ranges between maximal and minimal values are shown as vertical lines.



Appendix C. Spearman’s rank-order correlation coefficients between net ecosystem exchange (NEE), respiration (R), gross ecosystem productivity (GEP) and environmental variables

Table C-1. Spearman’s rank-order correlation coefficients between net ecosystem exchange (NEE), respiration (R), gross ecosystem productivity (GEP) and environmental variables (electrical conductivity (EC), water table depth (WTD), soil moisture (SM), leaf area index (LAI), soil temperature (ST), and photosynthetically active radiation (PAR)) within peatland plots during May – August (* indicates statistically significant correlation, $p < 0.05$).

	EC	WTD	SM	LAI	ST	PAR	NEE	R
Ridges								
EC								
WTD	0.19							
SM	-0.14	0.63*						
LAI	-0.51*	-0.43	-0.34					
ST	0.42	-0.06	-0.25	0.18				
PAR	0.23	0.22	0.10	-0.20	0.15			
NEE	-0.59*	-0.51*	-0.09	0.64*	-0.20	-0.02		
R	-0.59*	-0.52*	0.15	0.32	-0.39	0.01	0.77*	
GEP	-0.51*	-0.57*	-0.22	0.67*	-0.04	-0.10	0.85*	0.37
Depressions								
EC								
WTD	-0.21							
SM	-0.30	-0.63*						
LAI	-0.63*	0.30	-0.11					
ST	-0.09	0.44	-0.46	0.52*				
PAR	0.22	-0.08	0.13	-0.34	-0.20			
NEE	-0.54*	0.60*	-0.59*	0.72*	0.47	-0.35		
R	-0.59*	0.32	-0.19	0.43	0.36	-0.40	0.97*	
GEP	-0.58*	0.53*	-0.57*	0.65*	0.26	-0.27	0.85*	0.73*

Table C-2. Spearman's rank-order correlation coefficients between net ecosystem exchange (NEE), respiration (R), gross ecosystem productivity (GEP) and peat hydro-physical properties (bulk density (BD), porosity (P), specific yield (SY), soil organic matter (OM), aboveground biomass (AB), belowground biomass (BB) and increase in belowground biomass (BBI)) within peatland plots, with ridge and depression fluxes presented separately (* indicates statistically significant correlation, $p < 0.05$)

	Ridges			Depressions		
	NEE	R	GEP	NEE	R	GEP
BD	-0.34	-0.12	0.02	-0.71	-0.77	-0.77
P	0.14	0.07	-0.1	0.41	0.64	0.28
SY	0.18	0.14	-0.14	0.47	0.44	0.47
SOM	0.81*	0.74*	0.71*	0.77*	0.89*	0.71*
AB	0.81*	0.22	0.66*	0.66*	0.54	0.43
BBI	0.92*	0.48	0.89*	1.00*	0.66*	0.94*
BB	0.71*	0.07	0.64*	1.00*	0.66*	0.94*

Table C-3. Spearman's rank-order correlation coefficients between net ecosystem exchange (NEE), respiration (R), gross ecosystem productivity (GEP), electrical conductivity in July-August (EC) and nutrient availability within peatland plots during peak season (July-August) (* indicates statistically significant correlation, $p < 0.05$)

	Ridges				Depressions			
	NEE	R	GEP	EC	NEE	R	GEP	EC
Total N	-0.37	-0.12	-0.50	-0.06	-0.27	-0.23	-0.35	0.41
NO3-N	-0.31	-0.20	-0.33	-0.01	0.47	0.41	0.41	-0.23
NH4-N	-0.29	-0.08	-0.36	-0.02	-0.39	-0.36	-0.41	0.36
Ca	0.32	0.11	0.34	-0.33	0.77*	0.82*	0.73*	-0.85*
Mg	0.21	-0.04	0.33	-0.32	0.74*	0.76*	0.71*	-0.84*
K	-0.36	-0.45	-0.05	0.05	0.00	0.02	-0.07	0.49
P	-0.02	-0.04	-0.12	0.26	0.05	0.04	0.01	-0.10
Fe	-0.22	-0.20	-0.14	-0.05	0.39	0.43	0.31	-0.13
Mn	0.26	0.15	0.12	-0.59*	0.64*	0.68*	0.59*	-0.55*
Al	-0.03	-0.30	0.26	0.26	0.43	0.41	0.39	-0.06
Zn	0.21	0.58	-0.21	-0.55*	-0.46	-0.41	-0.47	0.35
B	-0.21	-0.17	-0.06	0.34	-0.01	-0.01	-0.06	-0.14
S	-0.36	-0.13	-0.41	0.32	-0.41	-0.39	-0.33	0.42

Table C-4. Spearman's rank-order correlation coefficients between net ecosystem exchange (NEE), respiration (R), gross ecosystem productivity (GEP) and environmental variables (depth (D), water temperature (WT), electrical conductivity (EC), pH, dissolved oxygen (DO), chlorophyll *a* concentration (Chl *a*), vegetation density (VD), and photosynthetically active radiation (PAR)) within pond plots during June – August (* indicates statistically significant correlation, $p < 0.05$)

	D	WT	EC	pH	DO	Chl <i>a</i>	VD	PAR	NEE	GEP
WT	-0.21									
EC	-0.17	0.58*								
pH	-0.17	0.09	-0.13							
DO	0.37	-0.06	-0.21	0.56*						
Chl <i>a</i>	-0.26	0.15	-0.19	0.20	-0.15					
VD	-0.14	0.06	0.08	0.10	-0.15	0.05				
PAR	-0.12	-0.16	-0.17	-0.17	-0.11	-0.10	-0.25			
NEE	-0.13	0.12	0.16	0.01	-0.18	0.20	0.51*	-0.35		
GEP	-0.18	0.29	0.22	0.02	-0.16	0.24	0.59*	-0.47	0.76*	
R	-0.18	0.29	0.22	0.02	-0.16	0.24	0.59*	-0.47	0.76*	1.00*

Table C-5. Spearman's rank-order correlation coefficients between net ecosystem exchange (NEE), respiration (R), gross ecosystem productivity (GEP) and major ion concentrations within pond plots in August (* indicates statistically significant correlation, $p < 0.05$)

	Cl	SO4	Na	K	Mg	Ca	NH4	NO3	PO4
NEE	0.12	0.25	0.16	0.11	0.28	0.34	-0.05	0.20	0.16
R	0.18	0.30	0.27	0.19	0.40	0.29	-0.04	0.47	0.58*
GEP	0.18	0.30	0.27	0.19	0.40	0.29	-0.04	0.47	0.58*